

Cyclopentane Hydrate for Hydrate Wetting Studies

Bashir Mohamed Hissen Abdulkader



A thesis submitted for the degree of

Master of Science (M.Sc.)

Department of Chemistry

University of Bergen

June 2013

Acknowledgements

This thesis is submitted in June 2013, for master degree in petroleum chemistry at the University of Bergen.

First of all, I would like to express my gratitude to my supervisor Professor Tanja Barth, for her unlimited supports and advices throughout the academic process of this thesis and thank you for understanding my situations.

I would also like to express my appreciations to Djurdjica Corak, who assisted me with experimental guidelines during the first production of hydrate using the same method that she had used.

Special thanks goes to Professor Tore Skodvin, for kindly answering my questions and allowing me to use his lab, and making available all the technical equipments needed for this thesis.

I am grateful to Gjertrud Skadsem Gil, for training me on how to use the GC-FID, and Terje Lygre, for his supervision in using chromeleon program. Many thanks to all my colleagues in our group (Tanja's group) petroleum and biofuel students for their kindness, support and friendship specially my friend Hailegebrel Techane Derribsa.

My deepest thanks go to my friend Mohamed Ali Alfaki, for his personal support and encouragement in reading my thesis .

My mother, father, brothers, sisters and friends deserve very special thanks for their understanding, constant support and encouragement.

Furthermore I would like to thanks my wife, for her patience and standing beside me during my study.

Abstract

Gas hydrates are often found in the systems for production of petroleum, natural gas and water systems, which is highly undesirable. In some systems the hydrates can form rapidly into large plugs and agglomerate in the transportation lines and blockage the systems, especially, in the deep sea and permafrost regions. Generally, hydrates plug agglomeration has been prevented using one of three methods, including anti-agglomeration in which surfactants are used as anti-agglomeratants.

In this thesis, experiments have been conducted to observe the behavior of cyclopentane hydrates and provide data on the morphology, kinetics and the determination of hydration numbers. Cyclopentane hydrate systems have been investigated to determine the effects of three additives used for enhancing the kinetic rate using two types of surfactants ($5 \times 10^{-3} \text{M}$ span20 and $5 \times 10^{-4} \text{M}$ tween20) and an organic compound (4 wt% tetrahydrofuran; THF) in two different ratios of water to hydrate former in order to achieve a broad experimental data set for systematic evaluation. In this systems, we have is used 3.5 wt% of saline water.

The results show that the morphology of cyclopentane hydrates during the formation depends on the type of the surfactants, while the tetrahydrofuran does not have a visual effect on the hydrate morphology. The determined hydration numbers are a function of the emulsion type (formed by the surfactants) and the contribution of the tetrahydrofuran in the hydrate cavities as a guest molecule. Water in oil emulsion causes higher hydration number, while oil in water emulsion causes lower one. The formation time measurements of cyclopentane hydrates show that the addition of THF into the cyclopentane hydrate system in presence or absent of surfactants, promotes the hydrate formation. The addition of surfactants affected the hydrate formation according to the emulsion type, in which tween20, which forms an oil in water emulsion has faster formation rate than span20, which forms a water in oil emulsion.

Table of Contents

Acknowledgements	iii
Abstract	v
Chapter 1 Introduction	1
1.1 Gas hydrates	1
1.1.1 Background	1
1.1.2 Physical properties and Crystal structure	1
1.1.3 Hydration numbers	3
1.2 Hydrate formation	5
1.2.1 Hydrate nucleation process	5
1.2.2 Hydrate growth process	6
1.3 Cyclopentane as a hydrate formation	7
1.4 THF as a hydrate formation	7
1.5 Driving forces for hydrate formation	8
1.6 Influence of temperature and pressure on hydrate formation	9
1.7 Surfactants as hydrate wettability modifiers	10
1.7.1 Span20	11
1.7.2 Tween20	13
1.8 Influence of salinity on hydrate formation	14
1.9 Aim of study	14
1.9.1 The tested systems	14
1.9.2 Measured parameters for each experiment	15
Chapter 2 Methods and experiments	17
2.1 Preparation of solutions	17
2.1.1 Preparation of the cooling liquid	18

2.2 Experimental method for hydrate production.....	18
2.2.1 Temperature logger.....	19
2.2.2 Centrifuge.....	20
2.3 Hydrate formation.....	21
2.3.1 Experimental procedure.....	21
2.4 Quantification of cyclopentane and water in the hydrate.....	25
2.4.1 Evaporation with heat.....	25
2.4.2 Evaporation with Nitrogen stream.....	26
2.4.3 Quantification by GC analysis.....	27
2.5 Prepared procedure for the preparation of the calibration curve and the standard.....	29
2.5.1 Calibration curve.....	29
2.5.2 Preparation of Stock solution.....	29
2.5.2 Preparation of work solution.....	29
2.5.3 Procedure for preparing sample for GC-FID.....	30
2.6 Output parameters.....	30
Chapter 3 Results.....	33
3.1 Observations in the hydrate system.....	33
3.1.1 Observation on the rotor of the stirring speed.....	34
3.1.2 Emulsion observations.....	34
3.1.3 Subcooling temperature.....	35
3.2 The determined hydration number.....	36
3.2.1 Quantification by Evaporation - test methods.....	36
3.2.2 Hydration numbers for N ₂ evaporation.....	38
3.3 Determining cyclopentane by GC-FID.....	39
3.3.1 Dilution and calibrations curve.....	39
3.3.2 Quantification of cyclopentane by GC-FID.....	41
3.4 The rate of the hydrate formations.....	43

Chapter 4 Discussion	49
4.1 Effects of subcooling and stirring	49
4.2 The hydrate former ratios	50
4.3 Concentration of the surfactants	50
4.4. Method developments	51
4.4.1 The quantification methods used in the experiments	51
4.4.2 Quantification of cyclopentane using GC-FID and N ₂ gas.....	51
4.5 Morphology of hydrate formation.....	52
4.6 The determined hydration number	56
4.6.1 Pure system (cyclopentane and saline water).....	56
4.6.2 Span20 and saline water.....	57
4.6.3 Cyclopentane and tween20	57
4.6.4 THF and surfactants as additives in cyclopentane hydrate system	58
4.7 The rate of formation.....	59
4.7.1 Pure system (cyclopentane and saline water).....	60
4.7.2 Cyclopentane hydrate with surfactant as additive	60
4.7.3 THF in pure system and surfactants as additives into the system	60
Chapter 5 Conclusion	63
5.1 The morphology effect of the additives to the cyclopentane hydrate system	63
5.2 The calculated hydrate number for pure cyclopentane hydrate and with additives	63
5.3 The hydrate formation kinetics	64
References	65
Appendix A.....	69
A.1 Examples of GC-FID chromatograms for each experiment	69
A.2 The solutions that used in the experiments.....	71
A.3 Recorded temperature curves.....	73
A.4 Determined hydration numbers.....	81

Chapter 1 Introduction

1.1 Gas hydrates

1.1.1 Background

In 1810 gas hydrate was defined as a crystalline solid which is formed by a combination of both gas and water at low temperature. In 1811 Sir Humphrey Davy is credited for the first hydrate discovered when he published his paper and stated that chlorine gas is more readily dissolved in frozen water than pure water. 30 years before that time, Joseph Priestley 1778 observed the freezing of SO_2 in water but that was not officially documented. Over a long period, hydrate was considered purely of academic interest, it was considered as a laboratory made substance. Most researchers were trying to identify the compound which formed hydrate, determine the ratio between the water molecules and the gas molecules, and also the physical properties of the hydrate (Sloan and Koh 2008). It was observed that natural gases and water were freezing in higher temperature and pressure than the ordinary freezing point of water, and the solid crystalline substance of gas hydrate, which resembles ordinary snow in appearance, can accumulate and compress in the transportation pipeline and plug the line. This problem has been first described by Hammersmith 1934, and since then researchers have become more interested in the gas hydrate field. In the 1960s it was recognized that hydrate can occur in both deep sea and permafrost region. This discovery makes the hydrate more interesting for researchers to investigate in potential sources of energy, gas transportation as well as potential sources of climate change and geo-hazard (Sloan and Koh 2008).

1.1.2 Physical properties and Crystal structure

A gas hydrate is a lattice structure with several interstitial cavities. The structure consists of a water molecule cage (host), which surround a gas molecule (guest). The water molecules are held together by hydrogen bonding to form a crystalline solid, which looks like ice (see Figure 1.1) above the freezing point of water (Ripmeester and Ratcliffe 1990). The hydrate types depends on the guest molecules, and there are more than 100 compounds which form clathrate hydrates with water molecules (Sloan and Koh 2008). All these guests form one of the three known hydrate structures; structure I, structure II or hexagonal structure H. The

smaller molecules and natural gases (such as methane, ethane, propane, carbon dioxide and so on) form either structure I or structure II, which is the most abundant in the nature. Some liquids (such as neohexane and cyclopentane in the presences of methane as a help gas) form structure H.

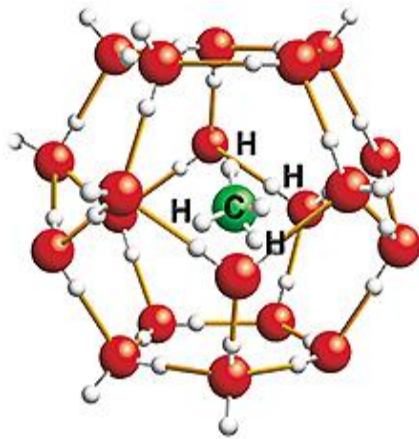


Figure 1.1: Simple illustration of a gas molecule contained inside a water molecule in a gas hydrate. The figure is adapted from the web page of Schlumberger.

The hydrate compositions and structures have been studied by using different techniques such as Raman spectroscopy, NMR and X-ray diffraction as described by Circone (2003), and several other authors including Schicks et al. (2010). An overview of the three known hydrate structures is given in Figure 1.2. As the figure shows, the nomenclature is 5^{12} for dodecahedral cavity where the 5 is the number of edges and 12 is the number of faces, which means that the structure has twelve pentagonal faces. In similar way, $5^{12}6^2$ for tetrakaidecahedral cavity has twelve pentagonal and two hexagonal faces, and $5^{12}6^4$ for hexakaidecahedral cavity has twelve pentagonal and four hexagonal.

As it shows in Figure 1.2, light gases compound such as methane, ethane, CO_2 and others can form hydrate structure I, while the heavy gas compound such as propane, butane, cyclopentane and other natural gases forms hydrate structure II. Gas hydrate structure H formed by the combination of heavy gas with light gas, in which the light gas is known as a help gas, and methane is the most common help gas in the structure.

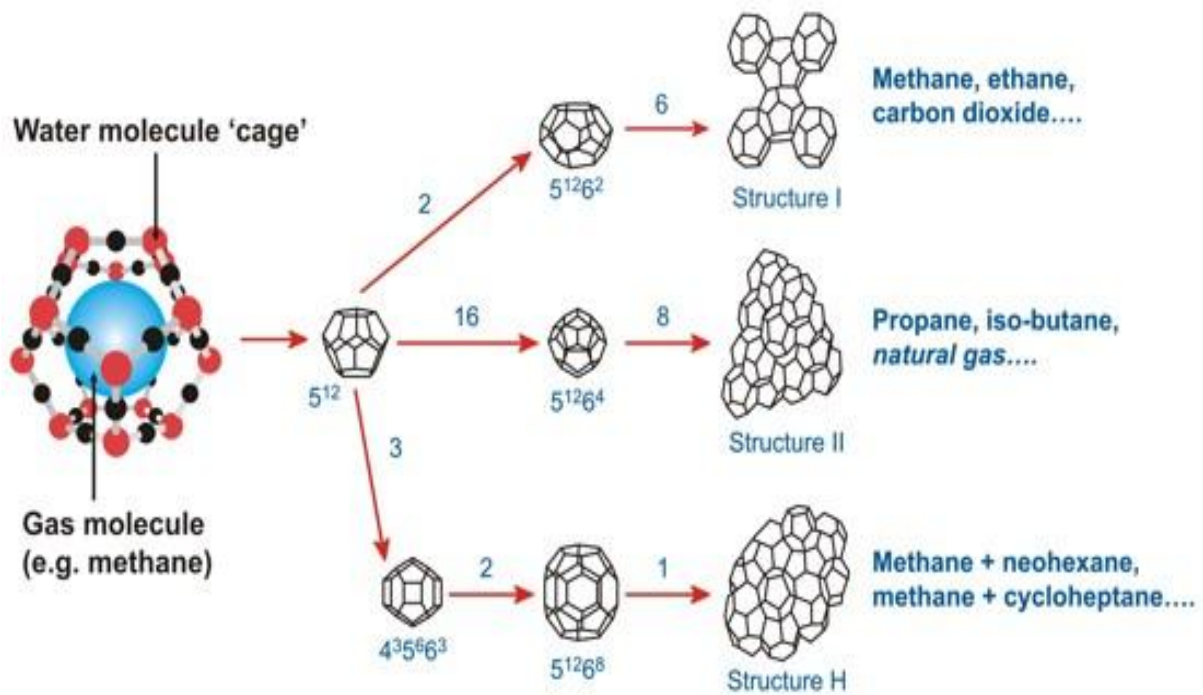


Figure 1.2: An overview of the three known hydrate structures. The figure is taken from the web page of Institute of Petroleum Engineering Heriot-Watt University: Centre for Gas Hydrate Research.

1.1.3 Hydration numbers

Scientists were very interested in the determination of hydration number in the first decade of hydrate discovery as mentioned in Section 1.1.1. In 1810, Davy reported that the chlorine hydrate contains 10 water molecules per molecule of chlorine, and Faraday confirmed this observation in 1823. Recently, by using spectroscopic methods (such as X-ray and neutron diffraction) the physical structure and the hydration number has been determined as it is shown in Table 1.1 and Figure 1.3. For example, the structure II has two types of cavities (small and large), which have different numbers of cavities per unit cell (16 for the small and 8 for the large). So the ratio between the guest molecule and the water molecule per cavity, for the larger cavity will be 8 guest molecules and 136 water molecules, which is 1 guest molecule per 17 water molecules (Sloan and Koh 2008).

Table 1.1: Hydrate cavity descriptions and number of water per unit cell.

Hydrate Crystal structure	I		II		H		
	Small	Large	Small	Large	Small	Medium	Large
Cavity	5^{12}	$5^{12}6^2$	5^{12}	$5^{12}6^4$	5^{12}	$4^35^66^3$	$5^{12}6^8$
Description	5^{12}	$5^{12}6^2$	5^{12}	$5^{12}6^4$	5^{12}	$4^35^66^3$	$5^{12}6^8$
Number of cavities per unit cell	2	6	16	8	3	2	1
Average cavity radius (Å)	3,95	4,33	3,91	4,73	3,91	4,06	5,71
Coordination number*	20	24	20	28	20	20	36
Number of water per unit cell	46		136		34		

*Number of oxygen's at the periphery of each cavity. (Sloan 2003)

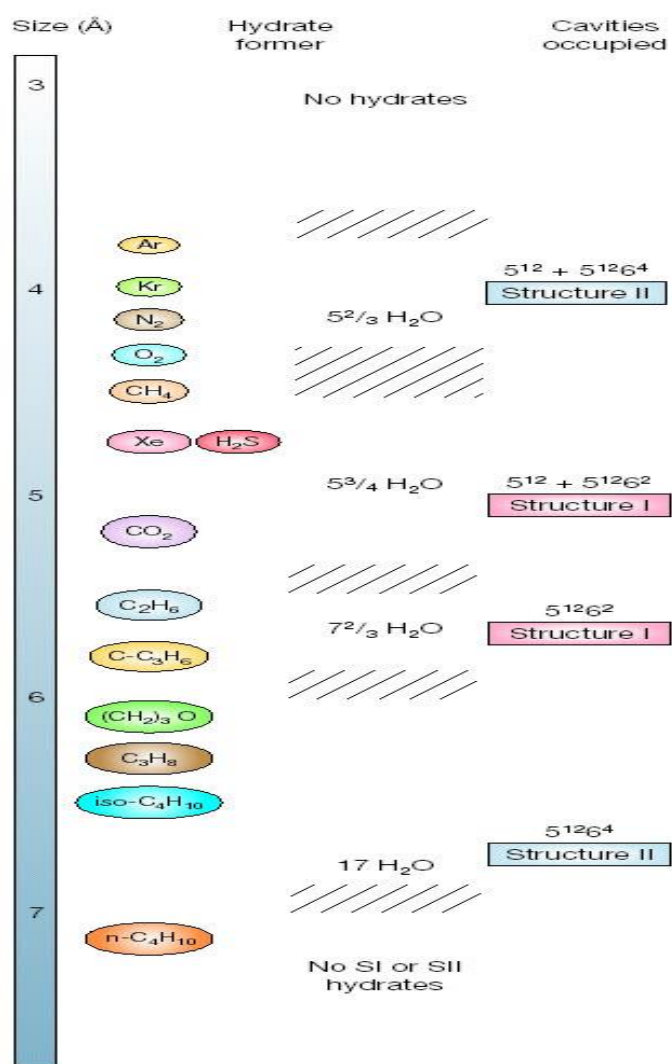


Figure 1.3: Guest molecule sizes vs. cavities occupied. The line is the size of the guest molecules in the hydrate. The figure copied from Sloan (Sloan 2003). Cyclopentane forms ($5^{12}6^4$) of structure II hydrate which means that it contains 17H₂O.

1.2 Hydrate formation

The hydrate formation occurs when the guest and the host molecules meet at low temperature and high pressure but also occur at low temperature (greater than 0C°) and at atmospheric pressure as in “cyclopentane hydrate”. The phase behavior depends in the type of the guest molecule and the purity of the water (Lundgaard and Mollerup 1991), as shown in Figure 1.4.

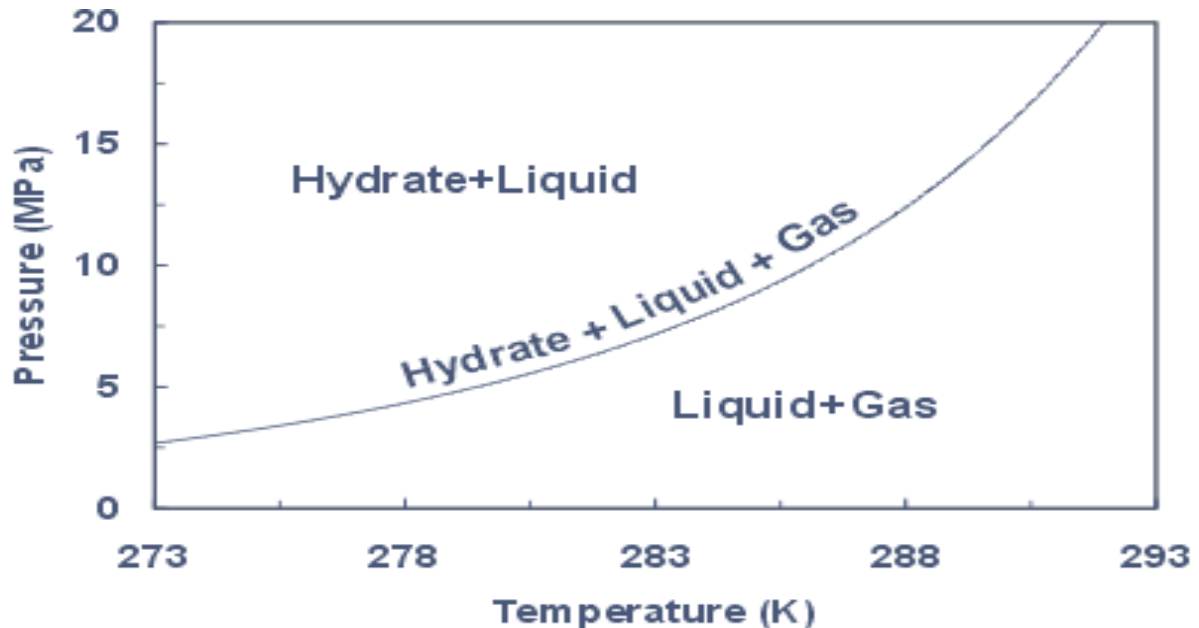


Figure 1.4: A simple illustration of gas hydrate phase diagram. The figure is taken from the web page of Institute of Petroleum Engineering Heriot-Watt University: Centre for Gas Hydrate Research.

The hydrate formation goes through two main steps:

1. Hydrate nucleation.
2. Hydrate growth.

1.2.1 Hydrate nucleation process

The hydrate nucleation process, which requires the initial formation of a concentrated zone of disordered gases, is the first step in the hydrate formation. After that the hydrate nuclei grows and disperses in order to achieve the critical size of hydrate to continue growing. (Large and Ribeiro 2008) described the nucleation theory based on kinetic and thermodynamic properties of gas hydrate nucleation. Sloan (2008) presented two hypotheses, labile cluster and local structuring. The labile cluster hypothesis indicates that there are many labile rings formed by water under certain temperature and pressure, and the water molecules will form a labile

cluster around the gas molecules during the gas dissolution. These clusters will agglomerate until reaching the critical size of the cluster. The local structuring hypothesis is the result of molecular dynamic simulation methods and by using this method one can predict favorable nucleation mechanisms by calculating the formation free energy.

The nucleation step is critical because it can take time to initiate hydrate growth. In order to accelerate the induction time, which is the time the first hydrate is observed, hydrate seeds can be added to the hydration system when the formation temperature achieved and stabilized. Small pieces of ice, clay, chalk and etc. can be used as a hydrate seeds.

1.2.2 Hydrate growth process

After the hydrate nuclei have stabilized and formed a critical size of nuclei in a supersaturated solution, the hydrate growth rate becomes straightforward and the nuclei starts to build up until it becomes stable hydrate. Selim and Sloan (1987) suggested a molecular mechanism for the hydrate growth of hydrate of methane in a liquid film surrounding a saturated gas- liquid interface (found in Sloan and Koh 2007 and mentioned that it is unpublished work), as it is shown in the Figure 1.5.

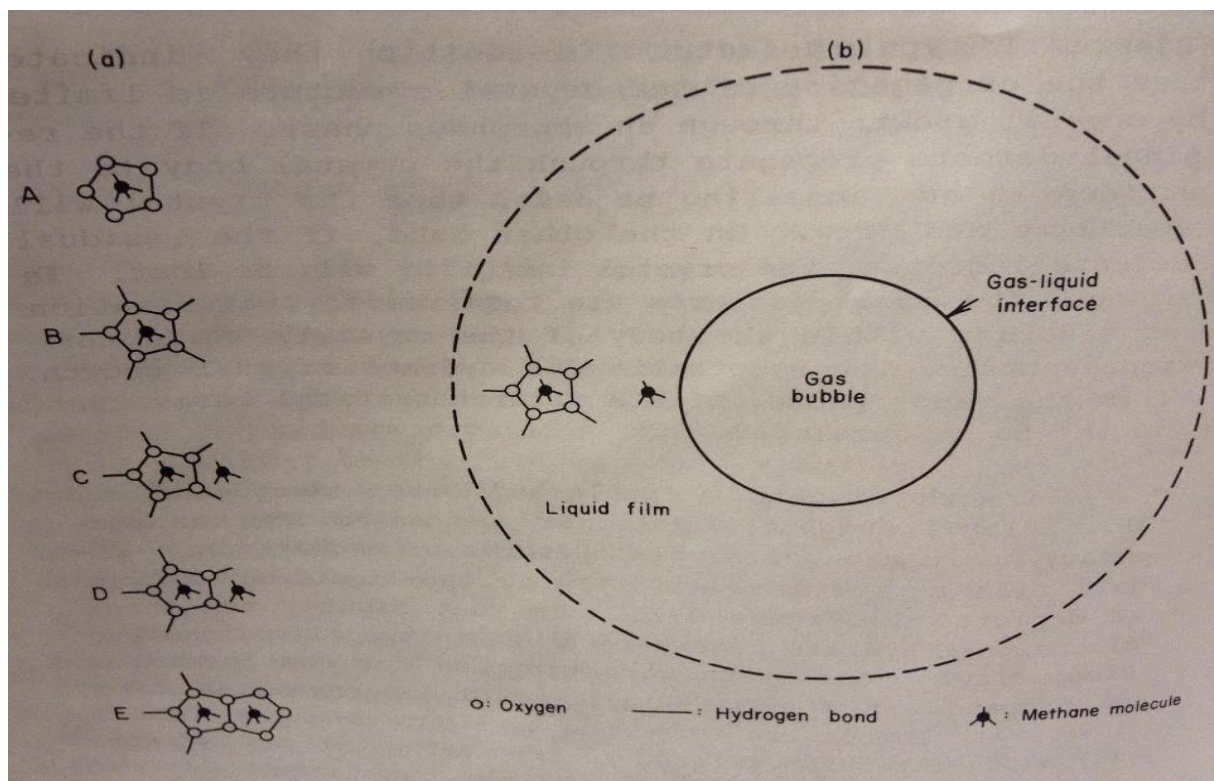


Figure 1.5: A mechanism for the molecular growth of hydrate crystals. The figure is taken from Sloan and Koh (2007).

Here, nucleus A absorbs water into the initial cage and forms B, the methane is absorbed into the partial cage structure B to form C, the water bond partially cages the methane and the water molecules diffuse to the partially cage and completely cages the methane by hydrogen bonding to form E, which is similar to nucleus A and continues to forms until it reaches the critical size of hydrate (Sloan and Koh 2007).

1.3 Cyclopentane as a hydrate formation

Cyclopentane (CP) is a nearly water immiscible compound that forms structure SII hydrate at atmospheric pressure with and without help gas (Mohammadi and Richon 2009). The equilibrium temperature for cyclopentane hydrate at atmospheric pressure has been tested by several groups and the results were in between 7 C° to 7.9 °C. Dirdal and his co works found that the cyclopentane hydrate can be kept in a fridge below 7.7 C° to stop it decomposing (Dirdal et al. 2012), which is above the ice point. This is useful to ensure that there is no ice present in the hydrate system. Corak (2011) reported that there are different kinetic of cyclopentane hydrate formation at different degrees of subcooling, and she shows that the kinetics of cyclopentane hydrate formation in subcooling of 5.6 C° is significantly faster than the kinetic of subcooling of 3.6 C°. The chemical formula of cyclopentane hydrate for the ideal hydration is given as CP/17H₂O as is shown in Figure 1.3. And the illustration of the chemical structure of cyclopentane is shown in figure 1.6.

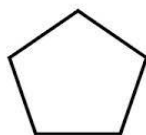


Figure 1.6: Cyclopentane structure.

1.4 THF as a hydrate formation

Tetrahydrofuran (THF) is water miscible organic liquid, which forms structure-II hydrate with water at atmospheric pressure or with moderated low pressure. Figure 1.7 illustrate the chemical structure of THF. It has chemical formula for the ideal hydration number THF/17H₂O. Adding of THF in the hydrate forming systems reduces the equilibrium pressure for the hydrate formation by coexisting with other hydrate systems (Makinol et al. 2005). Florusse et al.(2004) and Lee et al.(2005) mentioned that the stability of THF hydrate as a

second guest can stabilize the hydrogen cluster and makes it possible to store hydrogen molecules within the clathrate at low pressure and ambient temperature. Recently, Torre (2012) found that THF can be used as additive to speed up the hydrate formation and promotes the formation of the single CO₂ hydrate by mixing CO₂+ THF. In this work, THF has been tested as additive to cyclopentane hydrate system to enhance the kinetics.



Figure 1.7: Tetrahydrofuran structure.

1.5 Driving forces for hydrate formation

In order to define and study the driving forces for gas hydrate formation, Kashchiev (2002) suggested a detail picture based on three phases system at fixed temperature and pressure as it shown in Figure 1.8. The system consists of one gas component, aqueous solution of the gas and the resulting hydrate of the gas.

(P,T) = const.	
Gas	μ_{gg}
Solution	$\mu_{hs} = \mu_{gs} + n_w \mu_w$
Hydrate	μ_h

Figure 1.8: Three-phase system of one-component gas, aqueous solution of the gas and gas hydrate at constant temperature. This figure is taken and modified from Kashchiev (2002).

In the presence of one gas molecule (G) with n_w water molecules of the solution forms one building unit of Gn_wH_2O .



Where μ_{gs} , μ_w and μ_{hs} are the chemical potential for the gas, the water molecules and the hydrate building unit in the solution, respectively (see Figure 1.8).

According to thermodynamic phase, the driving force for a new phase formation defined as “the difference between the chemical potentials for the old and the new phases” Kashchiev and Firoozabadi (2002). So the difference between μ_{hs} and the hydrate phase, μ_h , is called supersaturation.

$$\Delta\mu = \mu_{hs} - \mu_h = \mu_{gs} + n_w\mu_w - \mu_h \quad (2)$$

The nucleation and the growth of hydrate formation require a supersaturated solution to take place. In this situation, the value of $\Delta\mu$ must be greater than zero, which means that the chemical potential of the old phase is greater than the new phase. When $\Delta\mu$ is equal to zero that means, the system is in phase equilibrium and the solution is saturated, i.e. both phases can coexist. However, when the $\Delta\mu$ is less than zero the solution will be undersaturated and the formation will not happen, therefore the value of $\Delta\mu$ will be minus ($-\Delta\mu$), which means that is the driving force of hydrate dissolution (Kashchiev and Firoozabadi 2002).

1.6 Influence of temperature and pressure on hydrate formation

From the experimental works and thermodynamic theory the temperature and pressure are considered the most important factors in hydrate formation (Lederhos et al. 1996). A pressure-temperature plot of hydrate formation and dissolution is shown in this Figure 1.9.

At the beginning, the system (point 1) is cooled until it reaches suitable temperature and pressure to where the first hydrate formed (point 2). When the onset hydrate is formed the temperature is held constant while the pressure drops very fast due to the formation of hydrate and consuming of the gas phase, so that hydrate formation occurs between point 2 and point 3. Heating the system at point 3 leads to the hydrate dissociation at constant pressure until it reaches point 4. Because of the dissociation releases the gas phase, the pressure will increase quickly and the temperature increases slowly until it achieves equilibrium at point 5 (Lederhos et al. 1996).

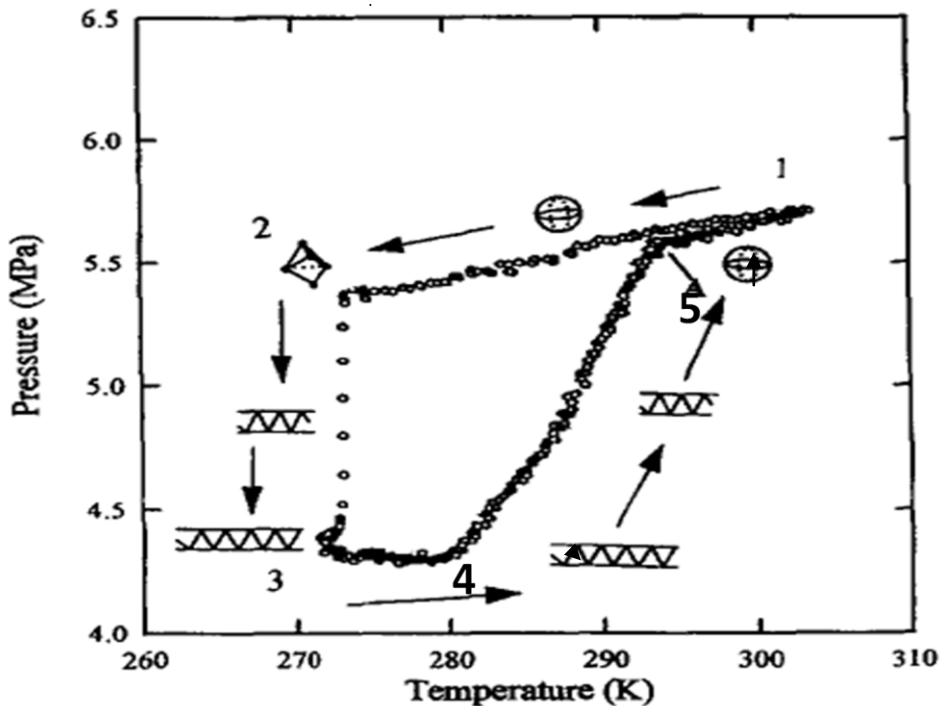


Figure 1.9: Influence of temperature and pressure on hydrate formation and dissociation. The figure is taken from Lederhos et al. (1996).

1.7 Surfactants as hydrate wettability modifiers

Recently, the gas and oil industry faces a challenge to prevent petroleum and gas transportation lines from the formation of hydrate plugs, especially in the deep water and permafrost regions, where the temperature and pressure are suitable for forming a hydrate phase. In order to prevent the hydrate blockage, three methods have been developed. The first method is thermodynamic inhibitors, which prevents the hydrate formation by changing the temperature and pressure equilibrium by adding thermodynamic inhibitors solutions. This method achieves good results but it has high economical costs. The second method is kinetic inhibitors, which does not prevented the hydrate formation but delays the hydrate formation so that the plug takes long period to form in the presence of kinetic inhibitors. This method does not suit well at pipeline shut in conditions or at high subcooling. The third method is anti-agglomeration, which is applied by adding surface active components (such as surfactants) to the hydrate system to prevent the accumulation of hydrate by reducing the strong attractive hydrogen-bonding between the hydrate particles. It also makes the hydrate particles disperse as small masses in the continuous liquid phase in the transportation lines. The last method gives good results at high subcooling and shut in conditions (Huo et al. 2001) and (Høiland et al. 2005). Due to the amphiphilic property of the surfactants, which means

that the surfactants consists of both hydrophilic and hydrophobic groups (see Figure 1.10), can cause very stable emulsions in the oil-in-water (o/w) and the water in-oil (w/o) type, according to the affinity of the surfactants toward the water or the oil phase (Binks and Lumsdon 2000). Emulsions determined by particles wettability by measuring the contact angle of the particles on the oil-water interface (Binks and Lumsdon 2000).

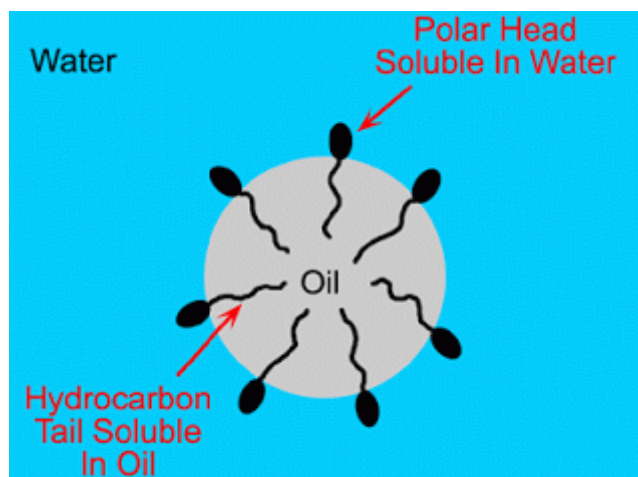


Figure 1.10: A simple illustration of surfactant. Figure taken from web page of Textile learner.

In this study, the effects of two surfactants in cyclopentane hydrate system have been determined. The surfactants were selected to represent different CMC and HLB values, which is the CMC “Critical Micelle Concentration” defined as the minimum concentration of the surfactants to make them associate in aqueous solution (Priev et al. 2001), and HLB “Hydrophilic-Lipophilic Balance” is the measurement of size and strength of the hydrophilic and lipophilic groups in emulsifiers (Griffin 1949).

1.7.1 Span20

Span20 (sorbitan monolaurate) is an ester sorbitan which is a nonproteic emulsifiers with stronger hydrophobic than hydrophilic character (Márquez et al. 2007). It is a liquid at room temperature. Table 1.2 shows some properties of span20, and Figure 1.11 shows its chemical structure.

Table 1.2: The properties of span20.

Name	sorbitan monolaurate
Formula	C ₁₈ H ₃₄ O ₆
Molecular mass	346.46 g/mol
Physical condition in room temperature	Yellow liquid
Solubility in water	Very low solubility
Solubility in oil	Soluble
CMC in water	6.13×10 ⁻⁵ M
CMC in oil	~10 ⁻³ M
HLB- value	8.6

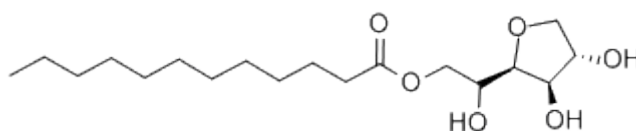


Figure 1.11: Simple illustration of Span20.

As it is shown in Figure 1.11, span20 contains of 12 carbon atoms and tow oxygen atoms at the tail of the component, which makes the span20 more hydrophobic than hydrophilic. At the head, span20 has six carbon atoms and four oxygen atoms, which gives the sorbitan ester hydrophilic proprieties. So the head part which is more polarized will be soluble at the water phase, and the tail part will be soluble in the oil phase (Peltonen and Yliruusi 2000).

Márquez (2007) mentioned that span20 can be used in preparation of water in oil emulsion at low water contents, between 10 and 15 % water, and at higher than 20% content of water can prepare w/o/w emulsion. Other studies indicate that span20 can be used to prepare oil in water emulsions, which makes the affinity of the water phase more complex factor (Opawale and Burgess 1998).

1.7.2 Tween20

Tween20 (polyoxyethylene sorbitan monolaurate) is an ester sorbitan which has hydrophilic character, and is liquid at room temperature. Table 1.3 shows some properties of tween20, and Figure 1.12 shows its chemical structure.

As Figure 1.12 shows, tween20 has a hydrophobic tail, which consists of 12 hydrocarbon units. Also it has hydrophilic part, which is the biggest part in the molecule composed of three hydroxyl groups that have in total 20 ethylene oxides.

Due to high HLB value, 16.7, tween20 is classified as water soluble and forms oil in water emulsion (Velev et al. 1994). Tween20 has ability to participate in self organizing processes on the surface to give more molecules and make a denser adsorbed phase in the surface as it is illustrated in Figure 1.13(Shen et al. 2011).

Table 1.3: Properties of tween20.

Name	Polyoksyetylen sorbitan monolaurate
Formula	$C_{58} H_{114} O_{25}$
Molecular mass	1227,54 g/mol
Physical condition in room temperature	Yellow liquid
Solubility in water	Soluble
Solubility in oil	slightly soluble
CMC in water	$8,04 \times 10^{-5}$ M
HLB- value	16,7

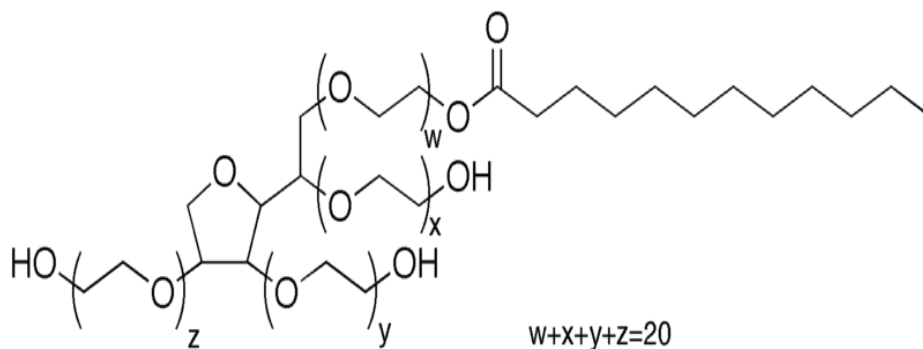


Figure 1.12: Chemical structure of Tween20.

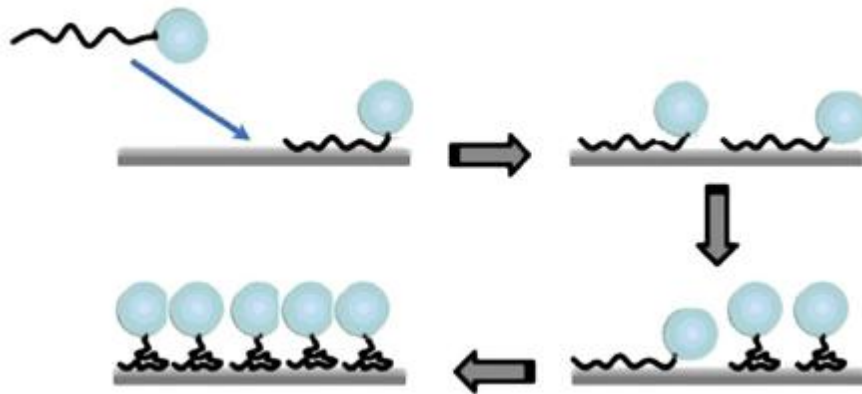


Figure 1.13: Illustrations of the adsorption of tween20 on a hydrophobic surface. Black color represents the alkyl tail and light blue is the hydrophilic head group.

1.8 Influence of salinity on hydrate formation

Salt have a thermodynamic inhibitors property in hydrate formation (Sloan 2008) and (Hui et al. 2007). Several hydrate formers has been investigated using salt in the hydrate formatting water phase (Duan et al. 2006).

The clusters bounded by strong Columbic bonds that made by interacting the salt ions and the water molecules dipole will decrease the water molecules that would be available for the hydrate former, and the solubility of the hydrate former will decrease due to the clustering of the water and salt molecules in which called “salting-out”. So the hydrate formation system that used saline water required lower subcooling (Corak 2011).

1.9 Aim of study

To test that the cyclopentane hydrate system is suitable for studies of hydrate morphology and wetting as a function of additives, and to investigate the effect of two surfactants and a promoter in the system.

1.9.1 The tested systems

The systems contain 3.5% of NaCl in water. The proportion of cyclopentane to water in one of the systems is 1:5, while the proportion in the other system is 1:3 of volumes. The subcooling temperature in all of the systems is configured to be 1.5 °C.

Pure system + systems with $5 \cdot 10^{-3}$ M surfactant added to the phase that it is soluble in.

1. Cyclopentane and saline water.
2. Span20 solved in cyclopentane and saline water.
3. Tween20 solved in saline water and cyclopentane.
4. The three system above by adding (4wt %) THF in each.

1.9.2 Measured parameters for each experiment

Temperature curve to show the time before the hydrate formation, the rate of crystallisation and the heat generated during the formation.

Hydration number: How much water per cyclopentane molecule in the formed hydrates.

Morphology of the hydrates: “Lumps” or “snow” – using pictures for documentation.

Chapter 2 Methods and experiments

In this chapter the description of methods and experiments has described briefly. All experiments have been done at the Department of Chemistry, UiB using the equipments available in the laboratories at the department. The chemicals used in this project are listed in Table A.2.

2.1 Preparation of solutions

For preparation of the samples used mainly pipettes from “EM Techcolor Volumetric Pipettes”, for μL pipetting the “Thermo Scientific pipette” used, for details about the weight used weight “Mettler Toledo AX205 Delta Range”, and “KERN EW620-3N” used to weight the chemicals.

The concentration have been calculated by using

$$C(\text{g/L}) = \frac{w(\text{g})}{M_w \times V(\text{L})} \quad (1)$$

$$C_a \left(\frac{\text{g}}{\text{L}} \right) V_a(\text{L}) = C_b \left(\frac{\text{g}}{\text{L}} \right) V_b(\text{L}) \quad (2)$$

Which is C in (g/L) is the concentration, w (g) is the weight, M_w is molecular mass and V (L) is the volume. C_a and V_a is the concentration and the volume of sample a and C_b and V_b is the concentration and volume of sample b.

Table 2.1: Description of solution preparations in the experiments

Solution number	Solution Name	Solvent	NaCl (weight%)	Span20 (M)	Tween20 (M)	THF%
1	Saline water	Water	3.5	-	-	-
2	Span20	Cyclopentane	-	0.005	-	-
3	Tween20	Saline water	-	-	0.0005	-
4	THF in Saline water	Saline water	-	-	-	4
5	THF in Tween20 solution	Tween20 solution	-	-	-	4

2.1.1 Preparation of the cooling liquid

Glycol has strong thermodynamic property which has the ability to stabilize the temperature in the cooling bath, and the cooling liquids are prepared by mixing glycol with water as it is shown in Table 2.2.

Table2.2: amount of glycol and distilled water used for preparation the cooling liquid.

Solution	Glycol	Distilled water
Amount (L)	5	20

2.2 Experimental method for hydrate production

A simple experimental setup used, adopted from Corak et al. (2011) as its shown in Figure 2.1. There was metal stand placed beside the cooling bath to hold the reactor (a round-bottomed three necks flask 500ml), the whole flask inserted in the cooling liquid, except the necks. The reactor fitted with a paddle stirrer, connected to an Ultra Turrax stirrer. Two temperature sensors inserted into the necks number 1 and 3, to control the temperature inside the reactor during the hydrate formation. The cooling bath was set at 1.5 C° in order to achieve stable subcooling temperature in the reactor and in the cooling liquid. The cooling bath "Thermo Scientific V26" which is supported by a thermometer and a stirrer has been used (see Figure 2.2).

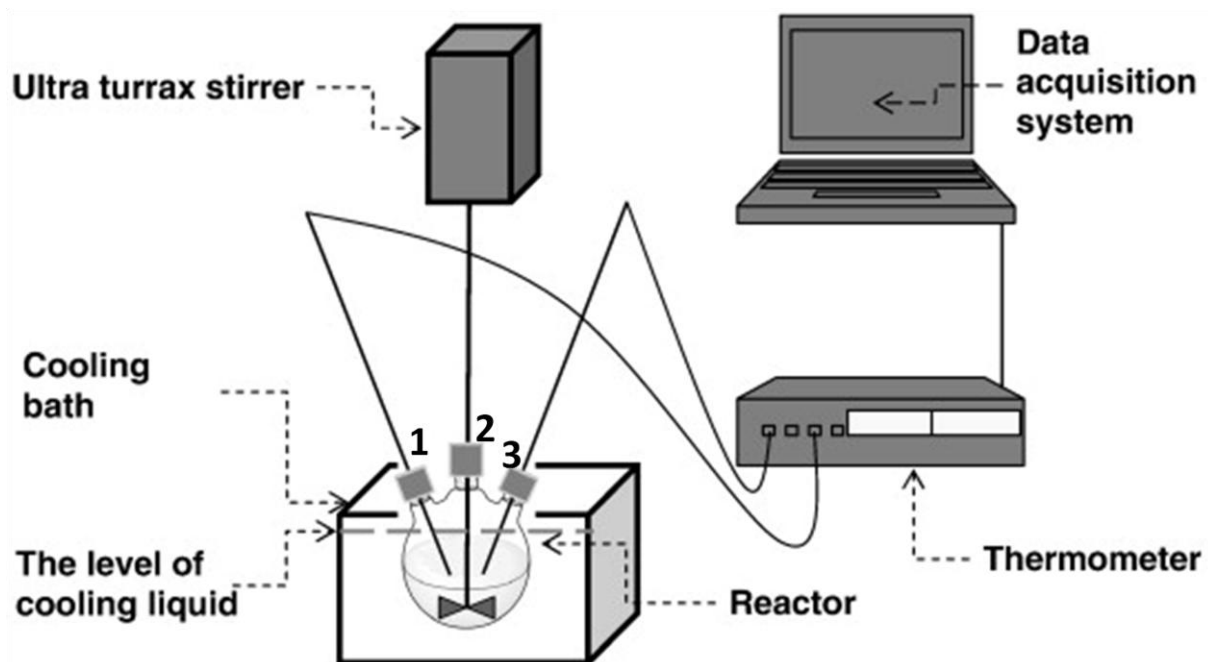


Figure 2.1 Schematic diagram of the experimental setup (figure taken from D. Corak 2011) with added numbers.



Figure 2.2: The experimental setup used for hydrate investigation.

2.2.1 Temperature logger

The Testo logger (Testo 176t2) is used in this work as a thermometer, which is supported by two temperature sensors to record the temperature (see Figure 2.3), and send it to the computer, in order to make sure that the temperature inside the reactor kept within the stable hydrate region (as shown in Section 1.6).



Figure 2.3: The Testo logger (Testo 176t2) with the sensor, used to control the temperature in the hydrate system.

2.2.2 Centrifuge

The centrifuge is used to remove the excess saline water on the hydrate samples (some of the excess saline water has been already removed by the vacuum suction and the hydrate has been transferred into tubes). After that the samples will be transferred to sample glasses in order to be quantified. We have used the Universal 320 centrifuge (Figure 2.4) by configuring the rotor speed as it is shown in Table 2.3, temperature and time to desirable numerical values that achieve good separation results, as described in Corak (2011).



Figure 2.4: Universal 320 centrifuge use to separate the excess water.

Table 2.3: The centrifuge configurations.

Rotation RPM	9000
Time min	5
Temperature C°	-5

2.3 Hydrate formation

The diagram below describes the experiment steps.

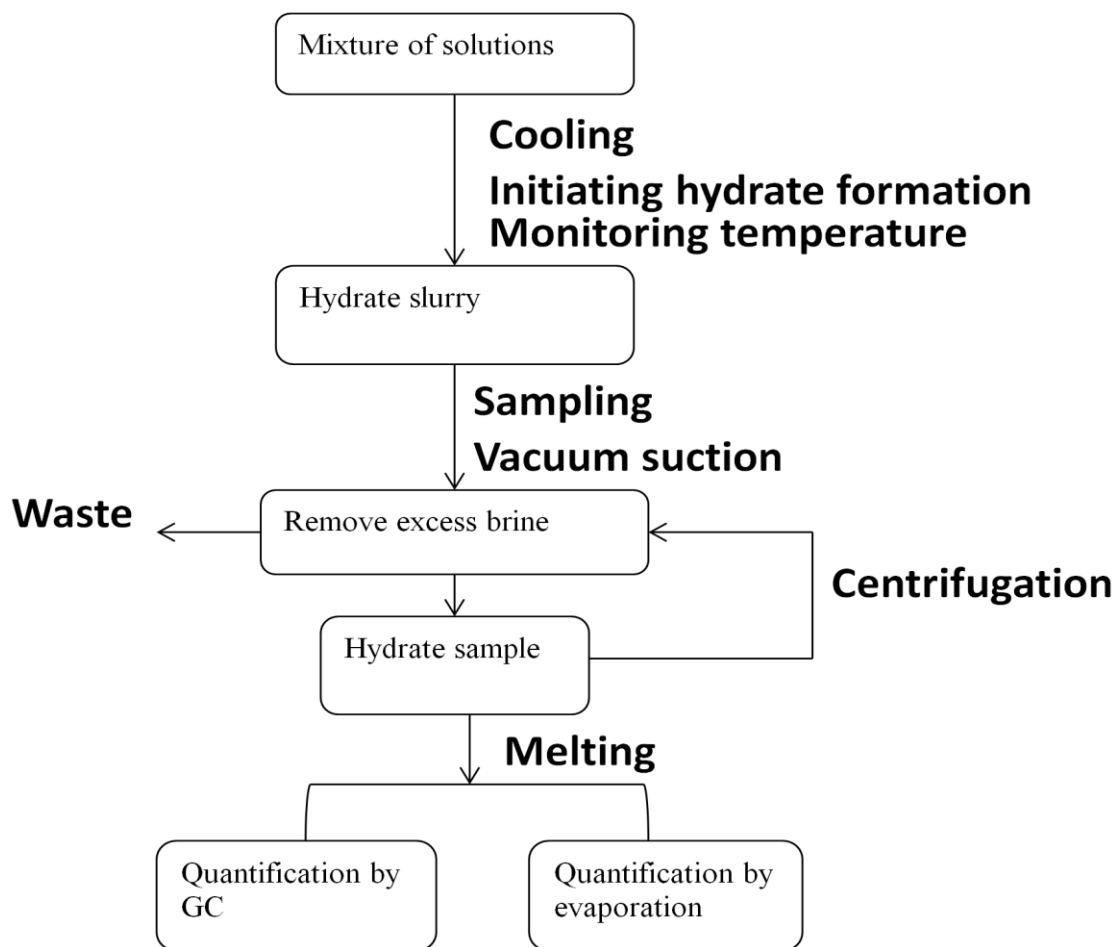


Figure 2.6: The flow diagram of the experimental steps.

2.3.1 Experimental procedure

In this work, cyclopentane hydrate system has been tested in four experimental systems as mentioned in Section 1.9.1.

The solutions (see Table 2.1) are transferred to the reactor in different ratios as it described in Table 2.4, and mixed in specified ratios at 500 RPM, by putting a rotor, which is connected to

a metal stand beside it, over the reactor. Then the solutions cooled down during the continuous stirring to the specified temperature. The temperature should be within in the stable hydrate region (see Section 1.3).

Two temperature sensors are inserted into the reactor (necks 1 and 3). Before starting the Ultra Turrax stirrer, we check the system if all is well (the cooling temperature, the stirrer and the rotation speed of the Ultra Turrax stirrer). Because if there is any contact of the stirrer with the flask, it can change the rotation speed, as it explains in Section 3.1.1, and can occur corrosion on either the stirrer or the flask. All must be linked tightly in order to prevent from any change in the different experiments).

Then we started the paddle stirrer, connect the temperature sensors to the computer and set the Testo program in the computer.

Table 2.4: Amount of solution used to form the hydrate:

Ratio	Saline water(ml)	Cyclopentane (ml)	Span20(ml)	Tween20 (ml)	THF in water (ml)	THF in Tween20 (ml)
1:3	270	90	-	-	-	-
1:5	250	50	-	-	-	-
1:3	270	-	90	-	-	-
1:5	250	-	50	-	-	-
1:3	-	90	-	270	-	-
1:5	-	50	-	250	-	-
1:5	-	50	-	-	250	-
1:5	-	-	50	-	250	-
1:5	-	50	-	-	-	250

When the temperature inside the reactor becomes stable (about 1.27C°), a small piece of ice is added to the reactor to initiate the hydrate formation. After few minutes of the induction time the hydrates will start forming. We let the formation continue until the temperature passes a

maximum and returns to stable temperature as it shown in Figure 2.7 which shows an example of the recorded temperature of cyclopentane hydrates formation.

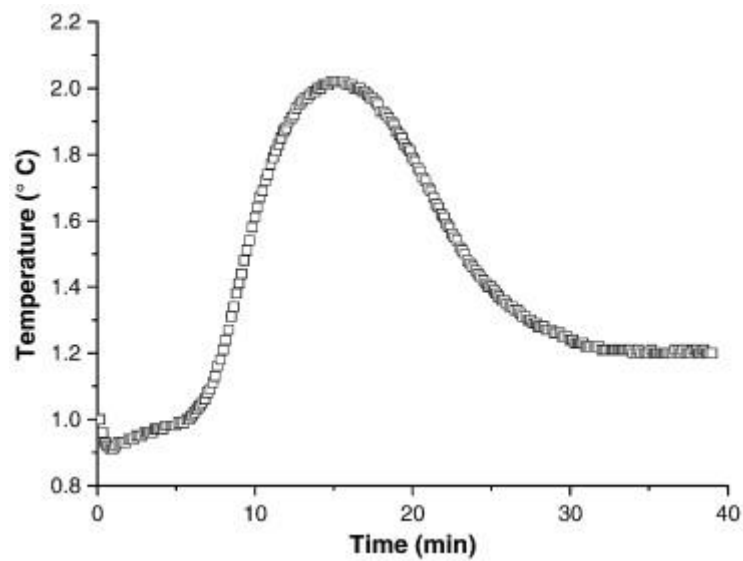


Fig. 2.7: An example of recorded temperature date of cyclopentane hydrate formation (Corak 2011).

While the hydrate is forming, we bring 12 plastic tubes, and fill each with either 7 small compresses or 2 medium and one small compresses (see Figure 2.8) and put it in ice.



Figure 2.8: The tube and Compresses used in the Experiment.

Two of 20ml and four of 5ml volume glasses have been weighted and put in ice. After the temperature has been stable, paddle stirrer is stopped, the reactor is taken out as it is shown in figure 2.9, and the hydrate transferred to the vacuum suction. We let it there for about 5 to 10 minutes to dry from the excess water.



Figure 2.9: Illustrate the reactor (Three necks glass) with hydrate after forming.

We fill the 12 plastic tubes with hydrate from the vacuum filter, cover the tubes and put it back on the ice.



Figure 2.10: The hydrate in tube before it transferred to the Centrifuge.

We put three pars of plastic tubes in the centrifuge, which is configured as it shown in Table 2.3. After that, we transfer the dry hydrate from the plastic tubes to the 20ml weighted glasses and we take small amount from one of the plastic tubes to one of 2ml glasses. We weight the

glasses with the hydrate. The cyclopentane and water in the 20 ml glasses will be quantified using nitrogen gas and the 2ml glasses will be analyzed using the GC-FID (see Figure 2.11).

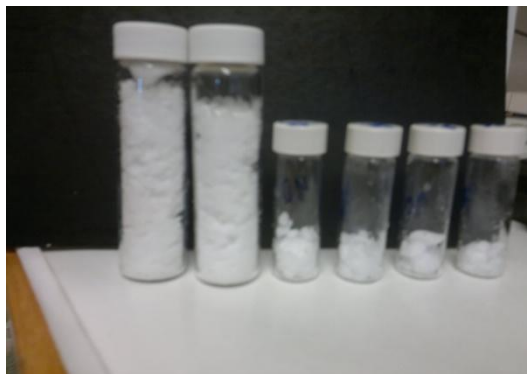


Figure 2.11: The hydrate sample collected in a glass to analyse.

We let the hydrate melt (it is better to put it in a fridge at about 6C° to reduce the effect of the emulsion).

2.4 Quantification of cyclopentane and water in the hydrate

In order to determine the ratio between water and cyclopentane in the hydrate sample, we did quantification using three methods: evaporation with heat, evaporation in a stream of nitrogen gas, and gas chromatography-flame ionisation detector.

2.4.1 Evaporation with heat

Heating the solutions, which consist of more than one component, above the boiling point of the target compound will transfer all the components that have a lower boiling point to a vapour phase. This procedure can achieve separation of the target compound from the solutions. In this work, we have evaporated the cyclopentane from the solution, which consists of water and cyclopentane (and small amount of THF and/or surfactant, either Span20 or Tween20, in some cases). The boiling point of cyclopentane is 40 C°, which is the lowest boiling point in the solution, so at 50 C° the cyclopentane will be released.

The samples were heated for two hours with checking every 15 minutes to make sure that all the cyclopentane evaporated. By weighing the remained water, we quantify the ratio between the cyclopentane and the water.

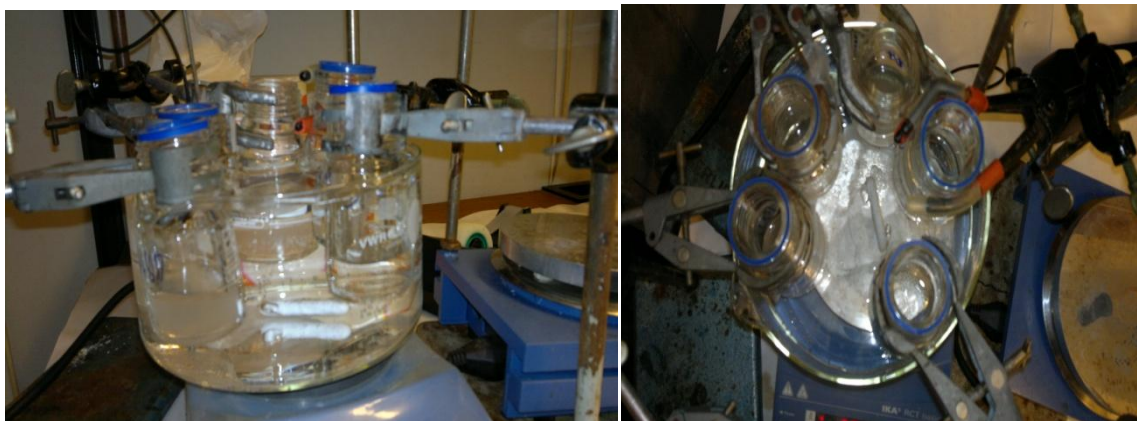


Figure 2.12: Illustration of the heating system.

2.4.2 Evaporation with Nitrogen stream

By directing a nitrogen gas stream directly toward the top of the liquid, which contains a volatile oil phase, will cause effective evaporation of the oil phase. To achieve maximum efficiency, the nitrogen stream must be positioned accurately and its velocity must be capable of precise adjustment (Komarek 1964).

In this work, a nitrogen stream has used to remove the cyclopentane from the sample, after the dissociation of hydrate. The procedure consists of directing the nitrogen stream into the top of the tube to evaporate the cyclopentane (as it is shown in Figure2.13) , until the visual oil phase could not be observed, and weighing the remaining water to evaluate the ratio between the cyclopentane and water.

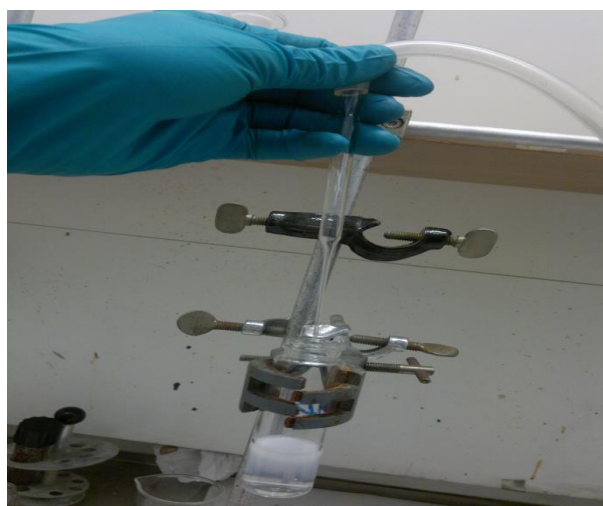


Figure 2.13 Illustration of the evaporation by nitrogen stream.

2.4.3 Quantification by GC analysis

2.4.3.1 Gas chromatography

Gas chromatography (GC) is an analytical separation procedure based on principle that the compounds separated according to their boiling point, polarity or molecular masses, that means the compounds will distributed in two phases, one of them will moves carrying the sample (mobile phase), and the another stands in the column (stationary phase), Helium, hydrogen and nitrogen are the most popular carrier gases, and helium has been used as a carrier in this experiment. The stationary phase is often high boiling liquid or polymer which is placed in the column (Miller 2009). Modern gas chromatography often uses open capillary columns. The column is placed in an oven to convert the sample to vapor phase. There are different detectors used in gas chromatography among which is the flame ionization detector (FID) that has been used here.

In this experiment, we used a Thermo Finnigan TRACE GC Ultra with FID detector. Data processing controlled by a Dionex Chrome Leon v6.0 software system. The specific dilution introduced by manual injection for a non polar Agilent Ultra 2 - column. The column is substituted by 5% phenyl, also known as DB-5 column. Table 2.5 shows the temperature program used for these analyzes.

The program:

Injection Form: Manual

Injection volume: 0.5uL

Split ratio: 1:20

Temperature split injector: 300 ° C

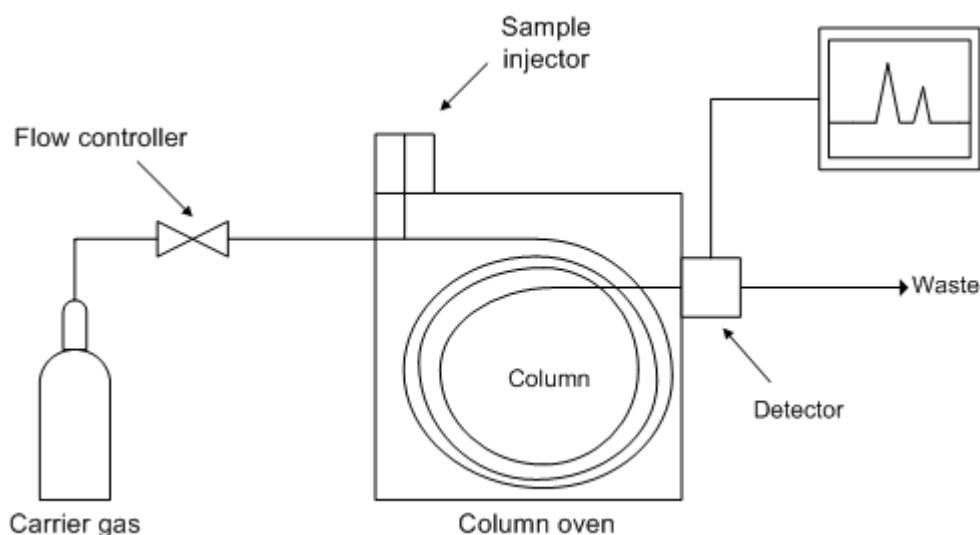


Figure 2.5: Scheme of Gas chromatography. Taken from the web page of Faculty of Health and Wellbeing , Biosciences Division, On-Line Learning

Table 2.5: The temperature program in GC-FID oven.

	Temperature °C	Time min	Rate °C/min
Start	30	5	
Ramp 1	60	00	7
Ramp 2	320	2	40

2.4.3.2 Flame Ionization Detector (FID)

Flame Ionization Detector (FID) is hydrogen-oxygen flame, producing a small current of ions by burning the sample, the current is collected and amplified before it sent to a data system. FID used for organic analyses because of its high sensitivity to the organic compounds, due to that and to the property has FID concedes as a good quantification detector with gas chromatography (Miller 2009).

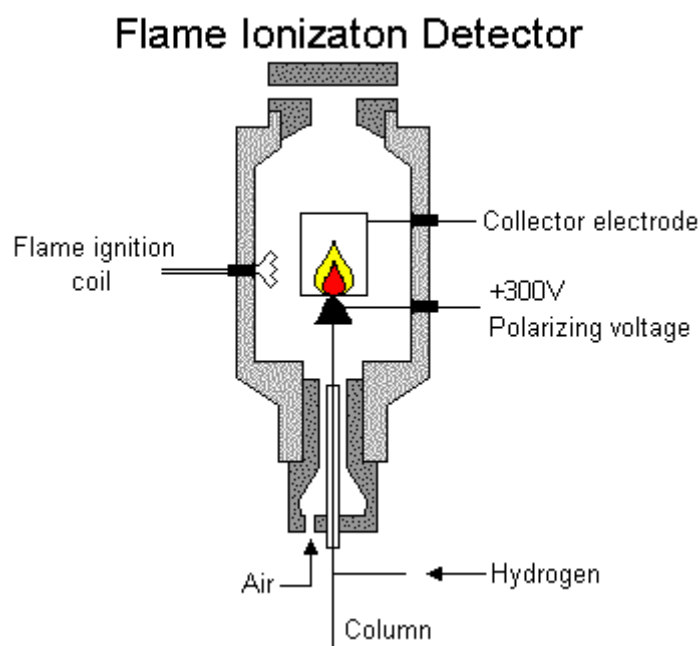


Figure 2.6: Flame Ionization Detector. Taken from the web page of Faculty of Health and Wellbeing , Biosciences Division, On-Line Learning

2.5 Prepared procedure for the preparation of the calibration curve and the standard

2.5.1 Calibration curve

The calibration curve is the method of determining the concentration of a substance in a sample. This method works by comparing the sample with known concentration standard solution to calibrate the instrument and the analyst. The calibration curve is a line or a curve that has been fitted to the data and the resulting equation is used to convert readings of the unknown samples into concentration. The line or the curve achieved by preparing and measuring a serial of standard solutions, as shown in Figure 3.6.

2.5.2 Preparation of Stock solution

We take 100 μ l Cyclopentane to a known weight, 5ml volumetric flask, and weigh it. Then we add isooctane until it reaches to the mark and weigh it again.

2.5.2 Preparation of work solution

We weigh 250ml volumetric flask and take exactly amount of hexadecane to the volumetric flask and weigh it. We add isooctane until it reaches to the mark and weigh it. After that we take 3ml from the work solution to 7 known weight of 5ml volumetric flasks, and weigh the

samples including the volumetric flasks to know the exact weight of work solution. By adding 10 μ l, 25 μ l, 50 μ l, 75 μ l, 100 μ l, 125 μ l and 150 μ l from the stock solution to each flask, respectively, and weigh again the new amount in each flask. Each flask should be filled by isooctane up to the mark of 5ml, and weigh it. Finally, we mix the solution in each flask carefully and analyze it in the GC-FID.

Table2.6: Amount of solution used for work and stock solutions.

	Cyclopentane(g)	Amount of isooctane ml	Weight of Hexadecane (g)
Work solution	-	250	0.130
Stock solution	0.0685	4.840	-

The density of isooctane =0.692 g/ml

The concentration of the stock solution = 0.0139 g/ml

The concentration of internal standard hexadecane the work solution = 0.000052 g/ml.

2.5.3 Procedure for preparing sample for GC-FID

After the hydrate in the glasses has been melted, we add a known amount of isooctane (2ml) and weigh it. So we transfer carefully 10 μ l from the organic phase (the upper phase) from each of the glasses to a new glass (glass A). We should make sure that no water has been taken with it. Finally, we add 1ml isooctane to glass A and analyze the solution in glass A with the GC-FID.

2.6 Output parameters

The hydration number known as the number of the water molecules in the hydrate divided by the number of the guest molecules in the same hydrate as it defined in Section 1.1.3. The guest molecule in this case is cyclopentane. The determined hydration number can be expressed by the following equation:

$$N_H = \frac{n_{H_2O}}{n_{Cp}}, \quad (3)$$

where n_{H_2O} and n_{Cp} are moles of water and cyclopentane, respectively. The determined hydration numbers are based on the experimental results, given as:

$$N_H^{\text{cal}} = \frac{n_{\text{H}_2\text{O}}^{\text{exp}}}{n_{\text{cp}}^{\text{exp}}}, \quad (4)$$

where the experimentally estimated moles of water are given in the nominator and cyclopentane is given in the dominator are both included. Then the outcome will be the hydration number which represents the water per hydrate former molecular ratio in the hydrate structure at the given experimental conditions. The computed hydration number experimentally is given by the following formula:

$$N_H^{\text{cal}} = \frac{m_{\text{hw}}^{\text{exp}} \times \text{Mw}_{\text{cp}}}{m_{\text{cp}}^{\text{exp}} \times \text{Mw}_{\text{H}_2\text{O}}}, \quad (5)$$

where $m_{\text{hw}}^{\text{exp}}$ is the mass of the purified hydrate water in the test sample, Mw_{cp} and $\text{Mw}_{\text{H}_2\text{O}}$ are molecular masses of cyclopentane and water, respectively, and $m_{\text{cp}}^{\text{exp}}$ is the mass of cyclopentane in the test sample. The mass of cyclopentane is calculated by:

$$m_{\text{cp}}^{\text{exp}} = m_{\text{hydrate}}^{\text{exp}} - m_{\text{H}_2\text{O}}^{\text{exp}} \quad (6)$$

where is $m_{\text{hydrate}}^{\text{exp}}$ the mass of the hydrate test sample. Loss of hydrates by melting during the work-up procedure is assumed not to systematically influence the values of the experimental hydration numbers, since both water and cyclopentane will be removed as fluids. (Corak, 2011)

Chapter 3 Results

This chapter presents the results from the quantification and the hydrate formation rate, as well as the observations in the hydrate system during and after the formation of the hydrate.

3.1 Observations in the hydrate system

After the hydrate formation ended, observations were recorded to describe the physical form (morphology) of the produced hydrate. Table 3.1 shows the observations from the first experiments series.

Table 3.1: Observations for the first experiments series

Experiment no.	Ratio	Observations
1	1:3 Cyclopentane to water	After the hydrate formation ended, free water remained (separate from the hydrate). The morphology of the hydrates during filtering is similar to snow, and it has more lumps after separating the excess water in the centrifuge.
2	1:5 Cyclopentane to water	After the hydrate formation ended, free water remained (separate from the hydrate) which is more than the water in experiment no. 1. The morphology of the hydrates during filtering is similar to snow, and it has more lumps after separating the excess water in the centrifuge.
3	1:3 or 1:5 Span20 to water	Here it is easier to get out the produce hydrate from the reactor, and it looks softer than the hydrates in experiment no. 1 and 2. After the hydrate formation ended there is not so much water and the morphology of the hydrates during filtering is more like powder.
4	1:3 or 1:5 Tween20 to cyclopentane	In this experiment, it is easier to get out produce hydrate from the reactor, looks softer than the hydrate in experiment no. 1 and 2. After the hydrate formation, ended free water remained, and the morphology of the hydrates

		during filtering is lumps but softer than the one for cyclopentane and water.
5	1:5 THF to cyclopentane	Similar to the result in experiment no. 2.
6	1:5 Span20 THF to	Similar to the result in experiment no. 3.
9	1:5 THF in tween20 to cyclopentane	Similar to the result in experiment no. 4.

3.1.1 Observation on the rotor of the stirring speed

The change of the stirring speed to mix the solutions, while the hydrates are forming can be seen clearly at the temperature curve which is shown in Figure 3.1. The rotation speed changes down from 500RPM to 450RPM which gives big difference in the maximum temperature (about 2.2°C) from the results which we get at 500RPM. In less than 500RPM, the maximum temperature curve is low, we neglected that result.

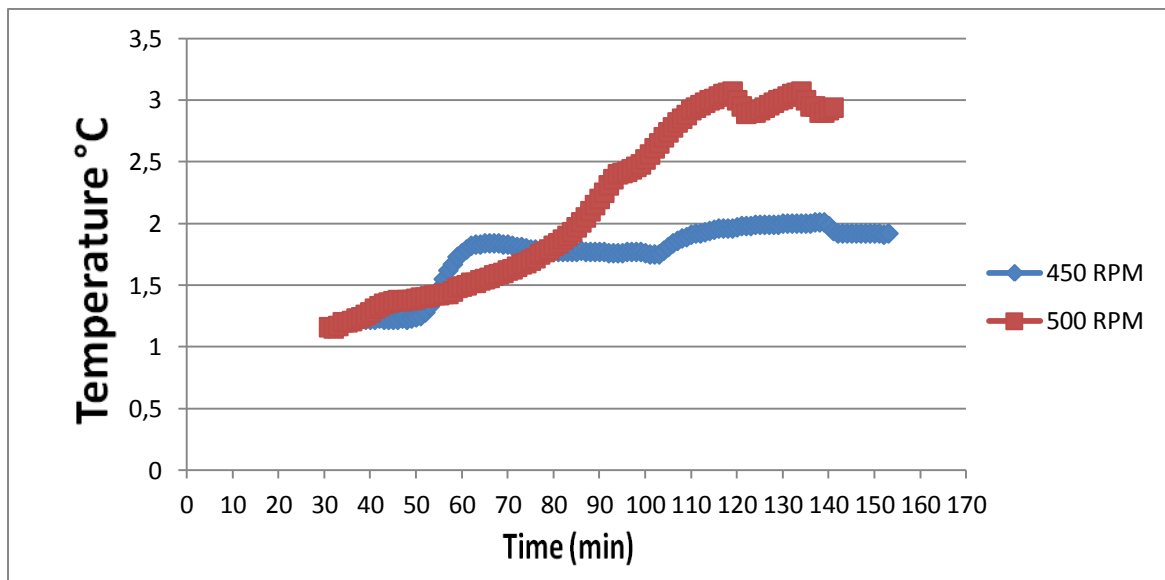


Figure 3.1: Kinetic of hydrate formation in low stirring speed

3.1.2 Emulsion observations

The cyclopentane hydrate system has been tested by adding surfactants and THF as it is discussed in Section 1.9.1. The dissociation of the hydrate that contains cyclopentane and

saline water has not observed an emulsion. On the other hand, the dissociation of the hydrate that contains cyclopentane, saline water and surfactant observed an emulsion in between the aqueous phase and the oil phase. While the THF did not have any emulsion effect as it is shown in Figure 3.2.

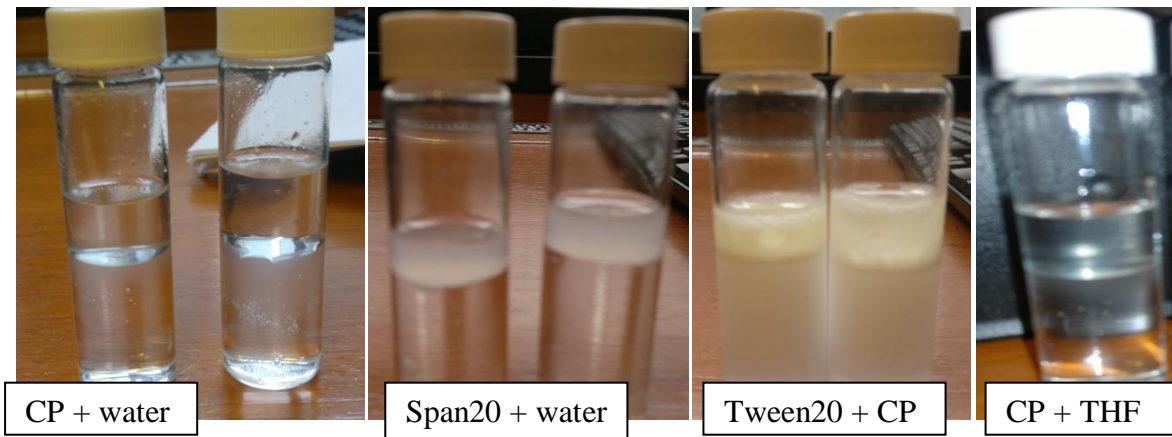


Figure 3.2: The appearances of hydrate dissociations solutions

3.1.3 Subcooling temperature

The cooling bath configured at 1.5 °C as mentioned at Section 2.2. A thermometer placed in the cooling bath to record the temperature around the reactor during the formation, Figure3.3 shows three examples of recorded temperature.

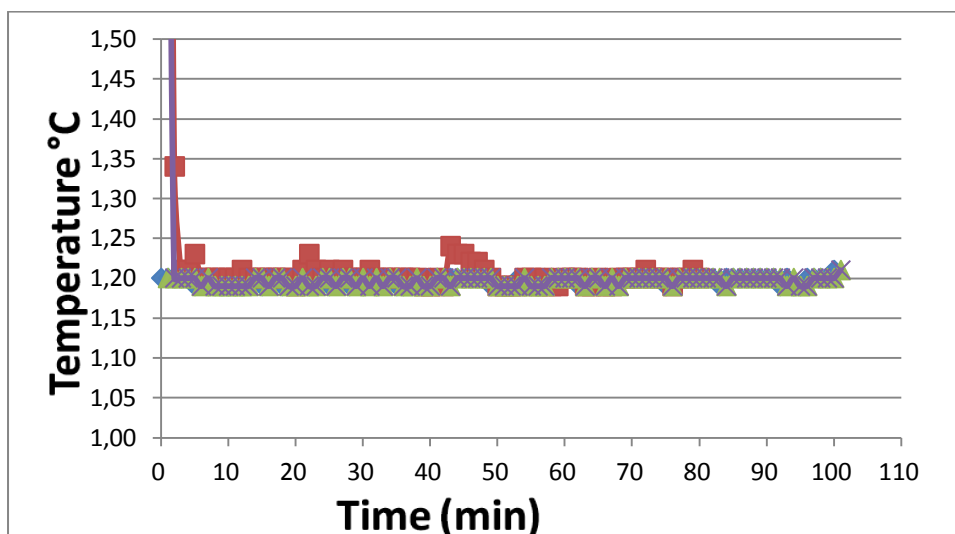


Figure 3.3: The subcooling around the reactor during the formation.

3.2 The determined hydration number

The hydration number has been determined as the ratio between the water and the guest molecules (cyclopentane) in the hydrate framework. This calculation is based on quantification of cyclopentane and water in a hydrate sample. Several methods for quantification have been tested.

3.2.1 Quantification by Evaporation - test methods

In the beginning, we make a series of tests to determine the precision in determining amount of water that is removed with the cyclopentane during the evaporation of the cyclopentane.

3.2.1.1 Evaporation by heat- test methods

Table 3.2 and Figure 3.4 shows the total loss of cyclopentane and water in a solution that consists of known amount of cyclopentane and water after two hours of heating at 50°C,

Table 3.2: The evaporated amount of cyclopentane by heating known amount of water and cyclopentane.

Solutions	Water(g)	w. cp(g)	Initial amounts	Weight after +0.5 hour(g)	Weight after +1 hour(g)	Weight after +1.5 hour(g)	Weight after +2 hour(g)	Total loss of water(g)
Water + CP	30.021	2.981	33.002	32.945	29.786	29.556	29.34	0.681
Pure water	30.015	-	30.015	29.969	29.091	28.575	28.323	1.692

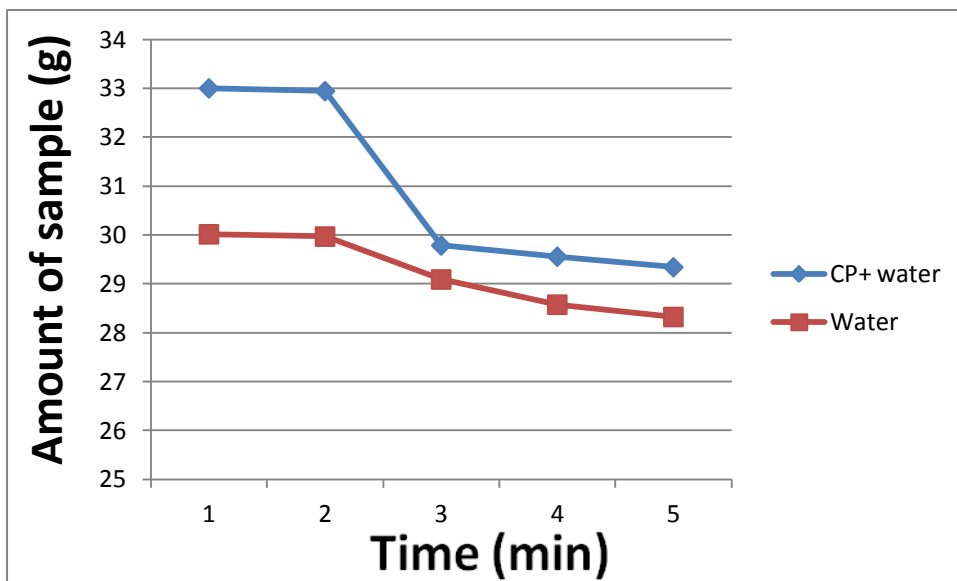


Figure 3.4: Quantification of water that is lost during heating to evaporate Cyclopentane

3.2.1.2 Evaporation by N₂ gas stream

Table 3.3 and Figure 3.5 shows the total loss of cyclopentane and water in a solution that consists of known amount of water and cyclopentane, after observing that the whole oil phase has removed by using nitrogen gas stream.

Table 3.3: The evaporated amount of cyclopentane by using nitrogen gas stream in known amount of water and cyclopentane.

Parallels	Water (g)	CP	Remain after ~one minute (g)	Remain after ~1.5 minutes (g)	The remain water	The total loss of water
1	8.708	3.187	8.612	8.52	8.454	0.254
2	9.938	2.97	9.916	9.899	9.825	0.113
3	8.991	3.305	9.594	9.001	8.819	0.172
4	9.701	3.428	10.602	9.951	9.559	0.142
5	8.886	3.674	10.12	9.145	8.864	0.022
6	14.294		14.249	14.209	14.113	0.181

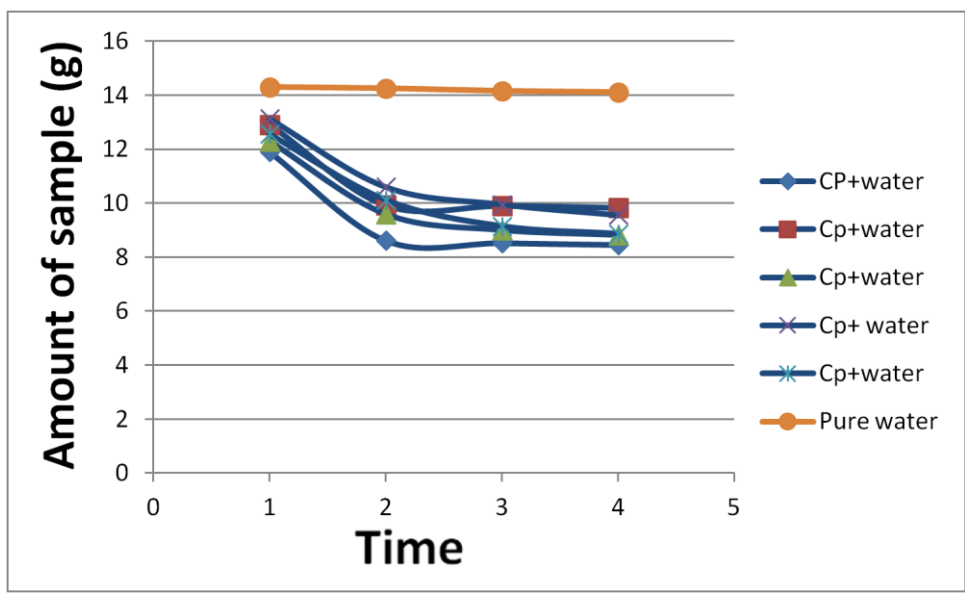


Figure 3.5: Quantification of water losses during the evaporation of cyclopentane using nitrogen gas stream for six parallel tests.

Based on these results, an evaporation loss of 0.2 g water was assumed to be the average, and this amount is added to the weight in the final experiments.

3.2.2 Hydration numbers for N₂ evaporation

The cyclopentane has been evaporated from the sample after the dissociation of the hydrate phase using nitrogen gas steam. Table 3.5 illustrates the average of the water content per one molecular cyclopentane, which is calculated using formula (4). Figure 3.6 shows the determined hydration numbers for all experiments using nitrogen gas evaporation

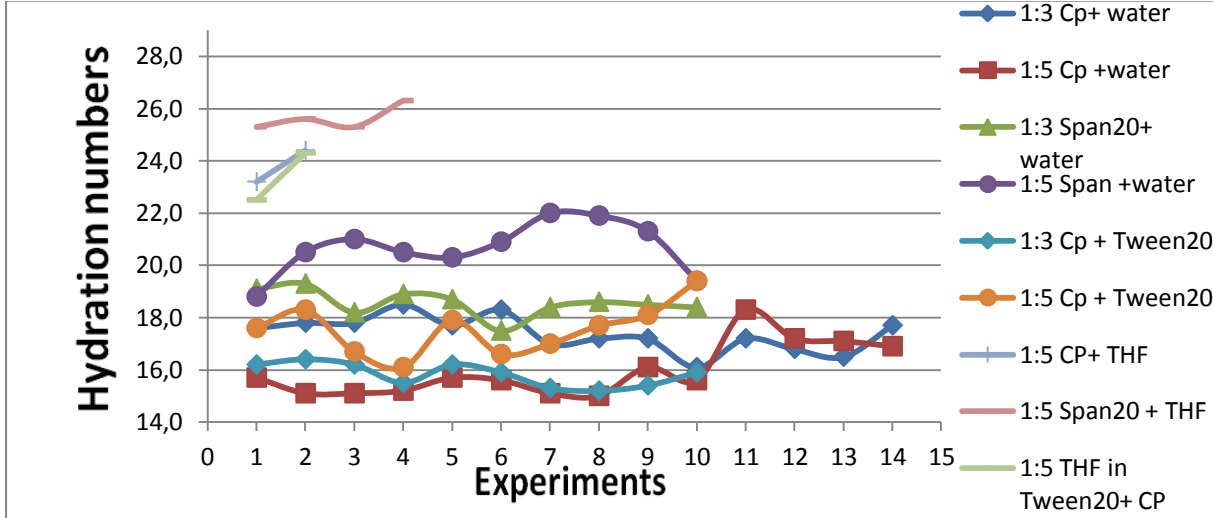


Figure 3.6: The determined hydration numbers using nitrogen gas evaporation

Table 3.4: The average content of water per molecular hydrate former (Evaporated by nitrogen gas stream).

No	Ratio	Solutions	No of experiment	Average of water content per cyclopentane molecular	Standard deviation
1	1:3	Cp to water	14	17.2	±0.66
2	1:5	Cp to water	14	15.8	±1.01
3	1:3	Span20 to water	10	18.6	±0.50
4	1:5	Span20 to water	10	20.6	±1.01
5	1:3	Cp to tween20	10	16.0	±0.44
6	1:5	Cp to tween20.	10	17.2	±0.97
7	1:5	Cp to THF	2	23.8	±0.85
8	1:5	Span20 to THF	4	25.5	±0.47
9	1:5	THF in tween20 to Cp	2	23.4	±1.27

3.3 Determining cyclopentane by GC-FID

As mentioned in Section 2.4.3.1, GC-FID analysis with a external calibration curve has used in this work, in order to determine the quantification of cyclopentane in hydrate sample.

3.3.1 Dilution and calibrations curve

The standard solutions, which we have described their preparations in Section 2.5, have injected to a GC-FID in order to achieve a calibration curve that can be used to calculate the concentration of the solution that is unknown concentration by comparing it with known concentration standard solutions. Table 3.5 illustrates the concentration of the cyclopentane in the standard solutions and the resulted areas. The standard solutions also helped to determining the retention time of the component as it is shown at Table 3.6.

Table 3.5: The concentration and area of the standard solutions.

No,	Stock solution (μl)	Concentration (g/ml)	Area
1	10	0.000027	0.1951
2	25	0.000060	0.437
3	50	0.000133	0.9306
4	75	0.000198	1.3813
5	100	0.000272	1.9331
6	125	0.000337	2.4064
7	175	0.000485	3.4332

By applying, the areas that resulted from the standard solutions using GC-FID, in excel program, the linear regression and the coefficient of determination (R^2) has given as it is shown at the calibration curve below in Figure 3.7.

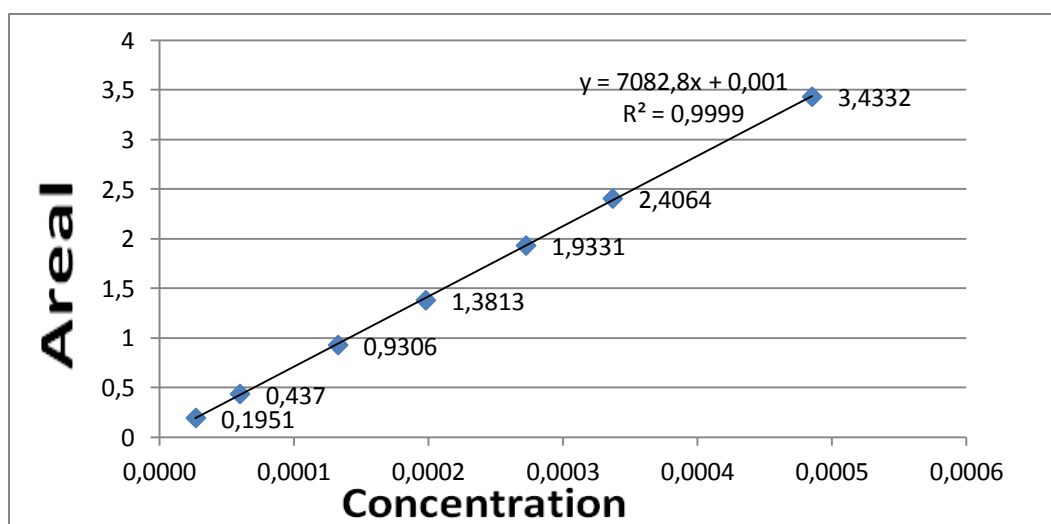


Figure 3.7: Calibration curve of cyclopentane.

Table 3.6: Determination of the retention times in GC-FID

Standard	Retention times (min)							
	10µl	25 µl	50 µl	75 µl	100 µl	125 µl	175 µl	Average
Cyclopentane	1.104	1.097	1.097	1.096	1.105	1.101	1.100	1.100
Isooctane	2.444	2.444	2.502	2.478	2.418	2.520	2.516	2.475
Hexadecane	13.427	13.428	13.428	13.428	13.428	13.429	13.431	13.428
THF	1.447	1.457	1.449	1.451	1.445	1.448	1.449	1.449

THF was not efficiently extracted.

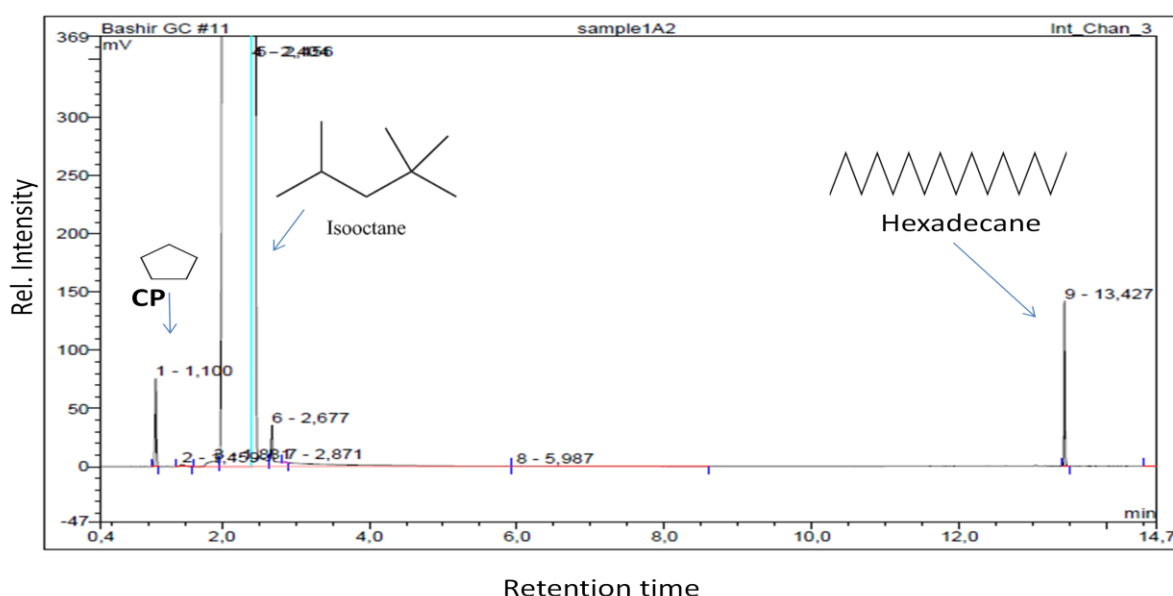


Figure 3.7: An example of GC chromatogram for the standard solution.

3.3.2 Quantification of cyclopentane by GC-FID

The hydrate melted and was diluted as it mentioned in Section 2.5.3, and glass A analysed by GC-FID. We injected 0.5µl from the sample in glass A into the GC-FID, from the chromatogram in the computer it reads the areas according to the retention time of the component, after that the cyclopentane to water ratio in the hydrate framework will be calculated. There is a series of experiments that has been performed, and examples are shown in Figure 3.7, and 3.9, for the other results see Appendix A.1., Table 3.7 shows the average content of the water in the hydrate framework per one cyclopentane molecule. Figure 3.8 shows the determined hydration numbers for all the experiments using GC-FID

Table 3.7: The average content of water per one cyclopentane molecule (analysed by GC).

NO.	Experiments	n	Average of water content per cyclopentane molecular	Standard deviation
1	1:3 Cp to water	4	18.8	±2.4
2	1:5 Cp to water	4	19.01	±4.8
3	1:3 Span20 to water	4	23.7	±0.9
4	1:5 Span20 to water	3	21.4	±1.2
5	1:3 Tween20 to Cp	4	15.81	±1.6
6	1:5 Tween20 to Cp	4	17.2	±0.1
7	1:5 Cp to THF	4	43.12	±8.5
8	1:5 Span20 to THF	3	30.4	±10.9
9	1:5 THF in tween20 to CP	4	25.2	±4.8

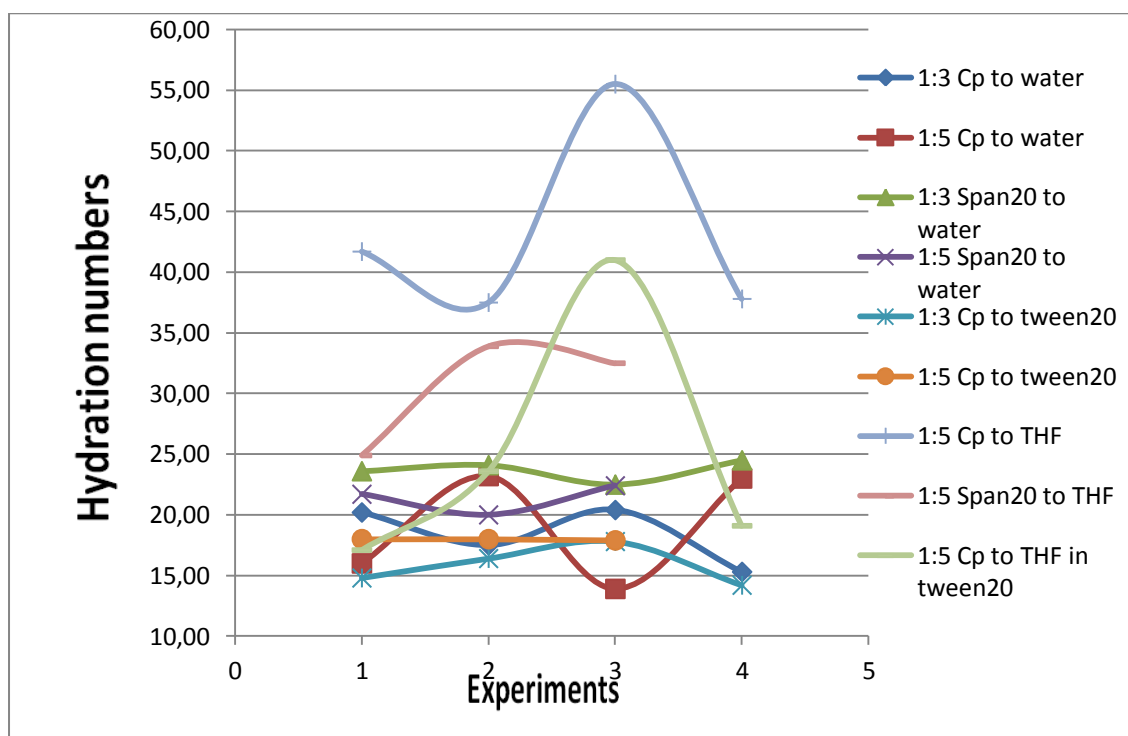


Figure 3.8: The determined hydration numbers using GC-FID.

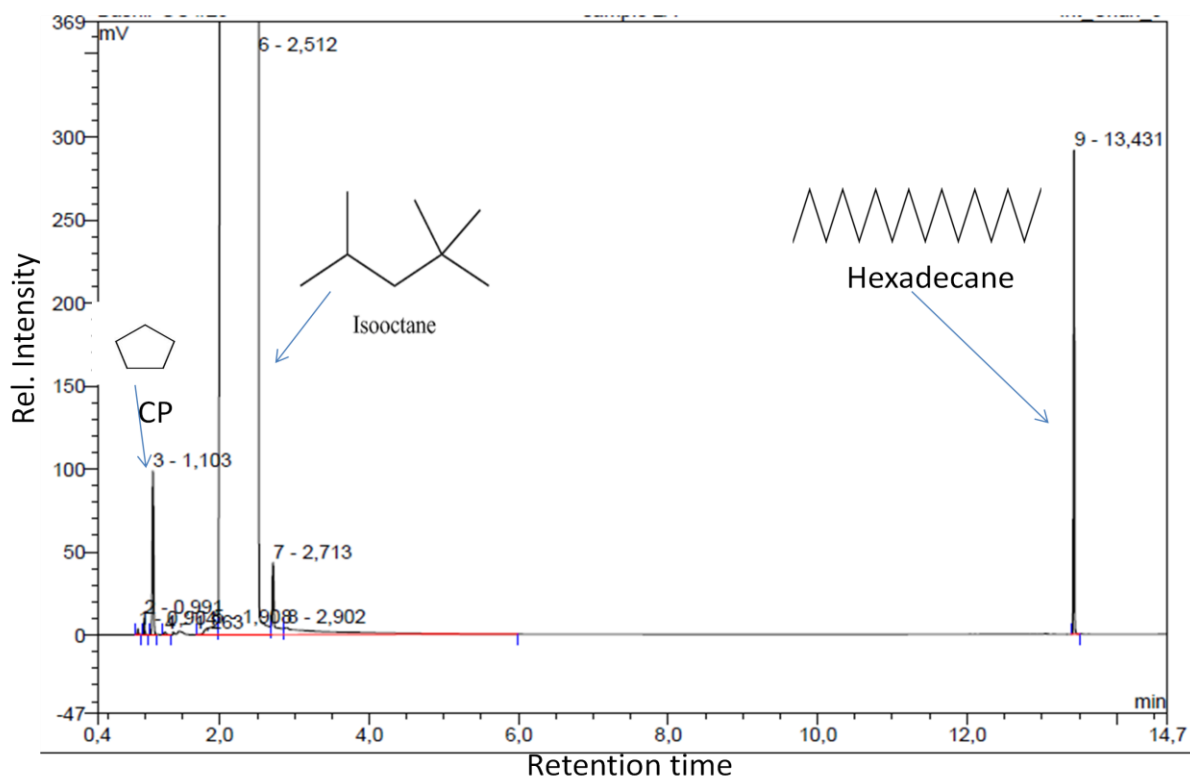


Figure 3.9: An example GC-FID chromatogram for (CP: water hydrate)

3.4 The rate of the hydrate formations

During the hydrate formation, the Testo logger recorded the formation temperature of the hydrate system. The logger connected to the reactor immediately after adding the solution that forms hydrate. So it starts to record during the cooling of the sample until it reaches stable temperature, which is the temperature that we add the piece of ice to initiate the reaction, and it continues to record to the maximum temperature of the formation. The most interesting data is the time between the induction time and the maximum temperature. Table 3.8 and Figures from 3.10 to 3.19 and A.3 illustrate the time that used to form the hydrate, the slope line shows the recordation in every one minutes, while the hill line shows the recordation in every 10 minutes.

Table3.8: results from the curves.

	1:3 CP :water	Induction time(min)	No	Average of formation time (min)	Induction temperature (C°)	Maximum temperature (C°)
1	1:3 CP :water	1	6	97	1.15	3.07
2	1:5 Cp :water	1	6	100	1.18	3.25
3	1:3 Span20: water	1	5	136	1.17	3.32
4	1:5span20:water	1	5	138	1.22	3.31
5	1:3 CP:tween20	1	5	75	1.24	3.3
6	1:5 Cp:tween20	1	5	69	1.18	3.21
7	1:5 CP : THF	1	2	30	1.21	2.37
8	1:5 Span20: THF	1	2	42	1.21	2.57
9	1:5 CP: THF in tween20	1	2	35	1.17	

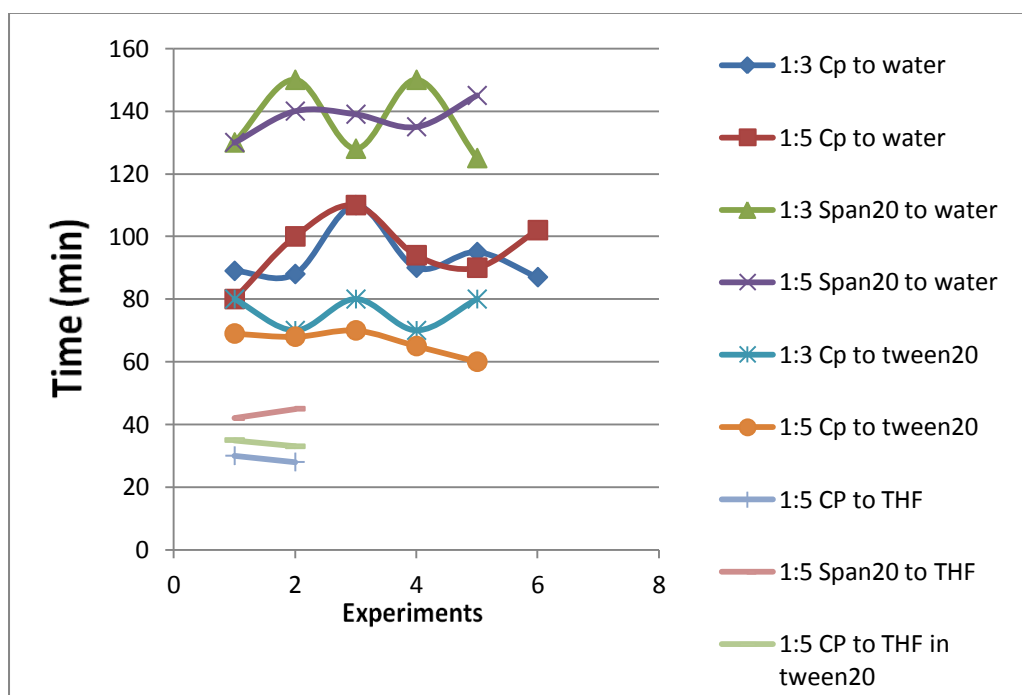


Figure 3.10: The time used to form the hydrate.

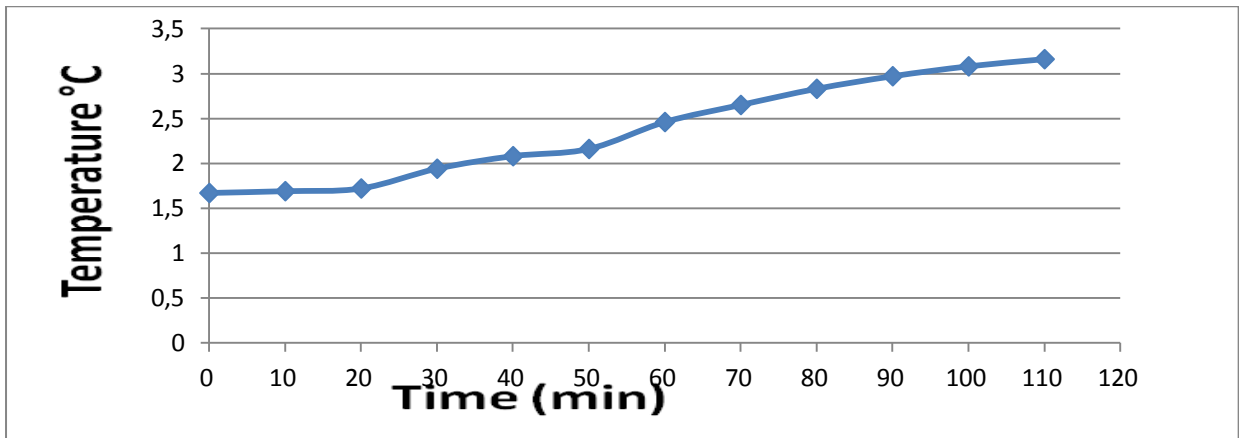
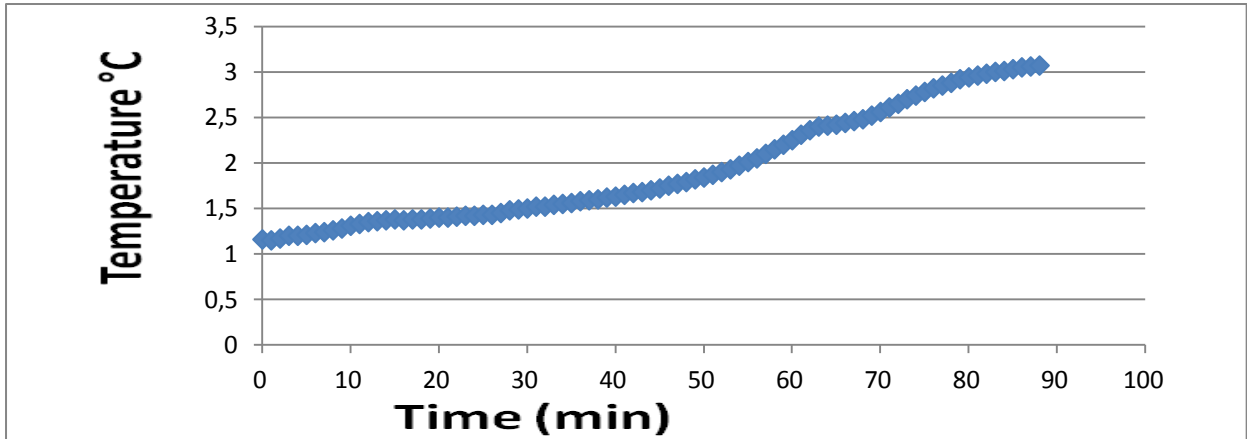
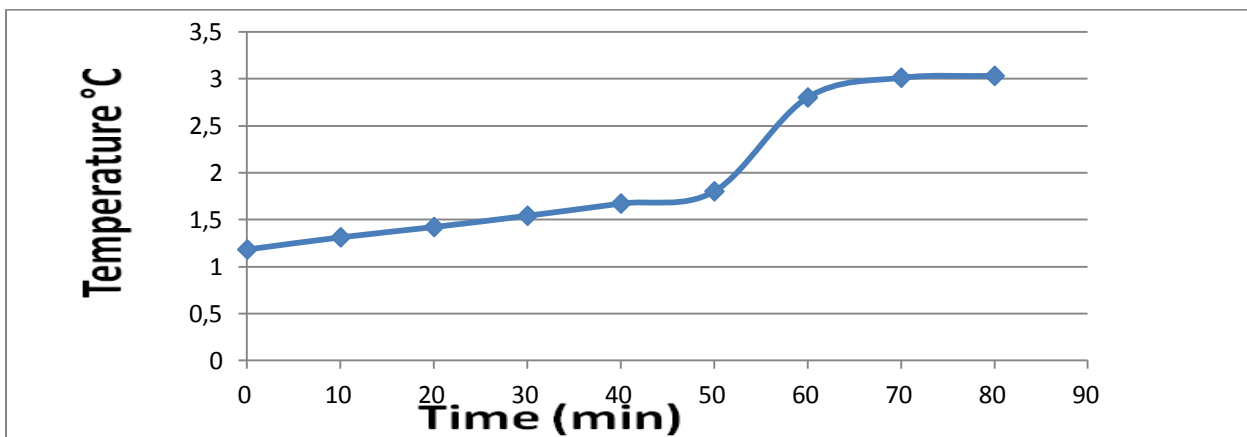


Figure 3.11: Recorded temperatures for 1:3 CP: water hydrate formation, recorded every 1 minutes.



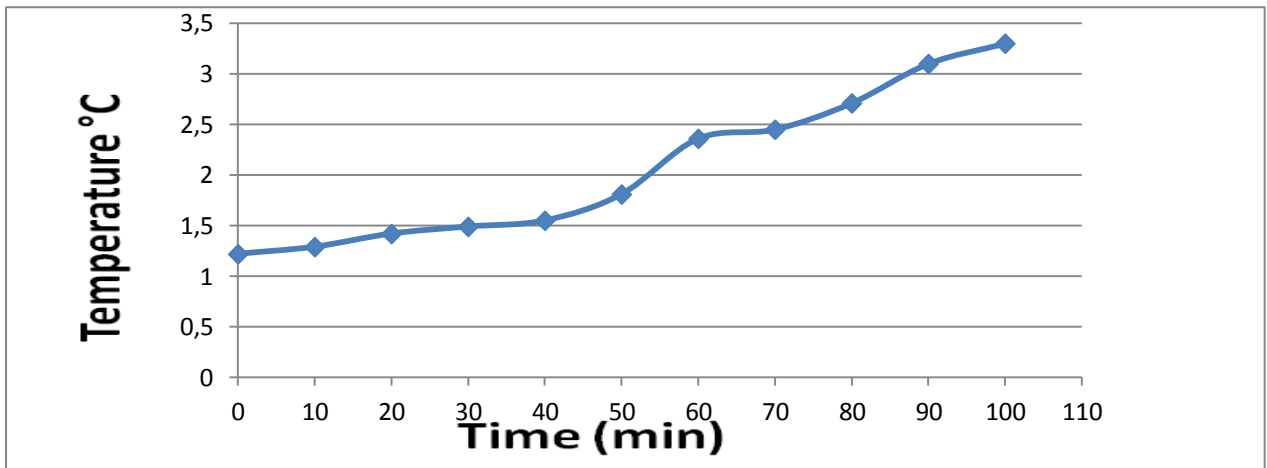


Figure 3.12: Recorded temperatures for 1:5 CP: water hydrate formation, recorded every 10 minutes.

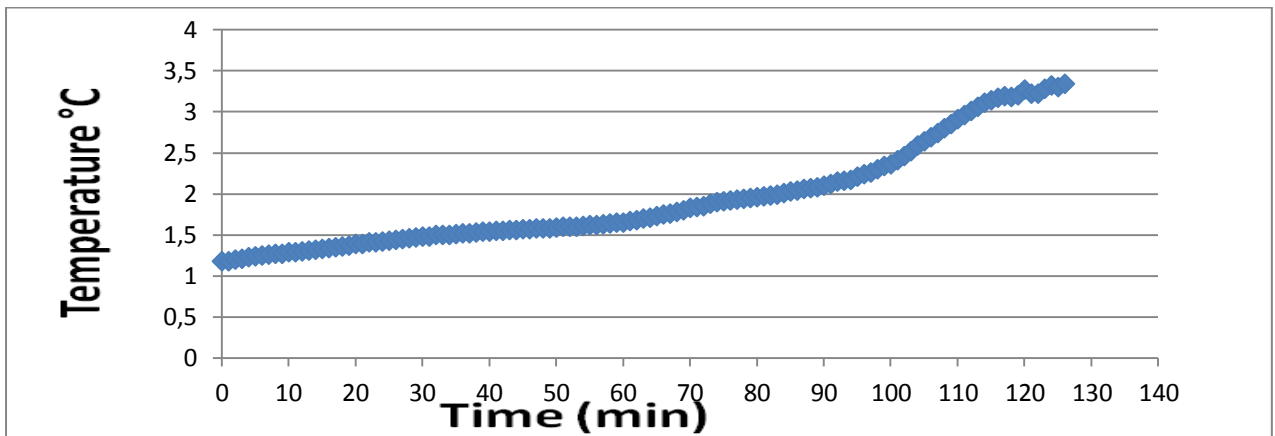


Figure 3.13: Recorded temperatures for 1:3 span20: water hydrate formation.

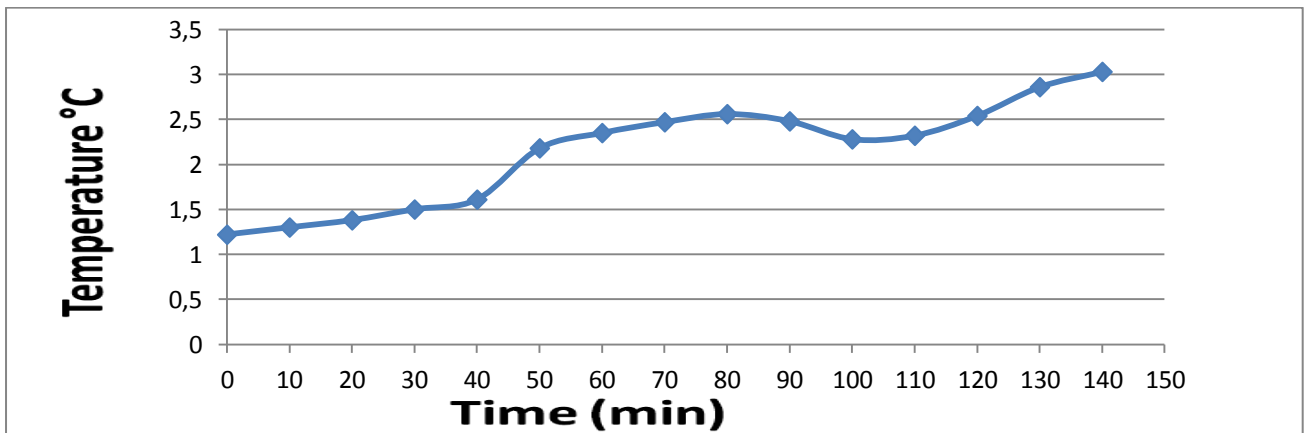


Figure 3.14: Recorded temperatures for 1:5 span20: water hydrate formation

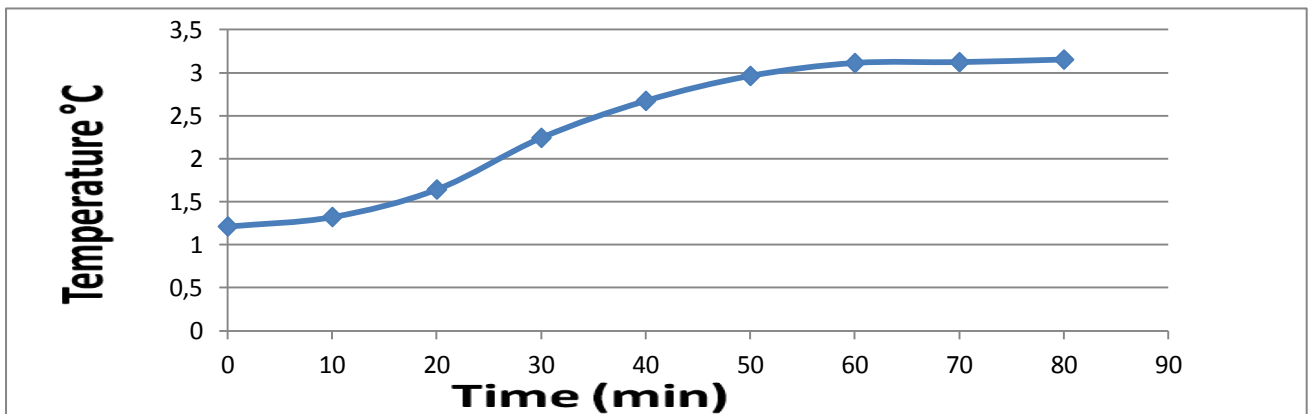
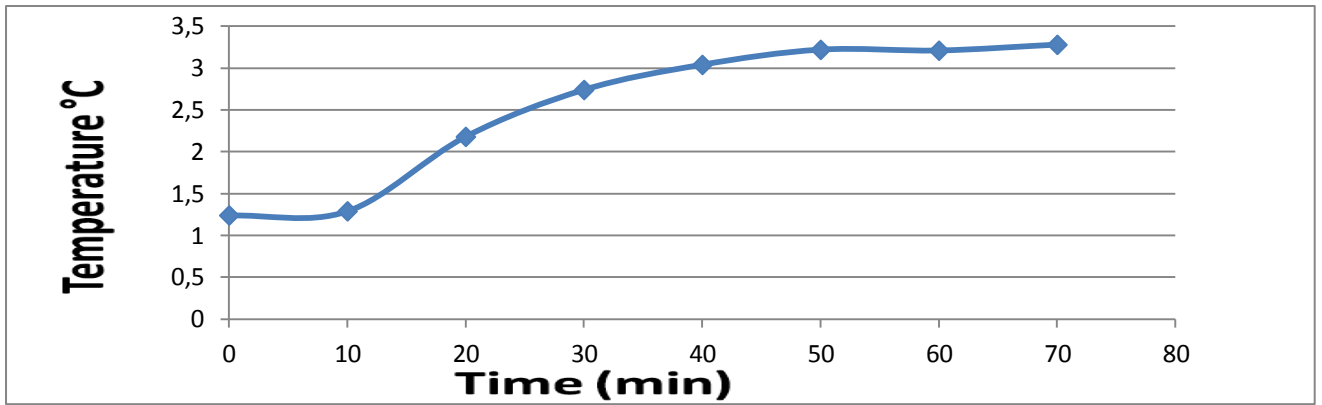
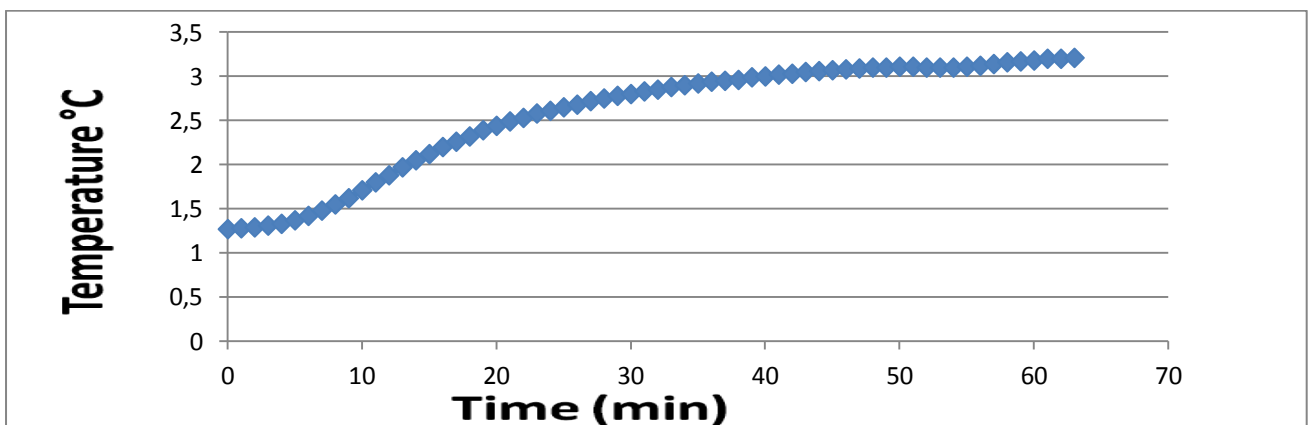


Figure 3.15: Recorded temperatures for 1:3 CP: tween20 hydrate formation



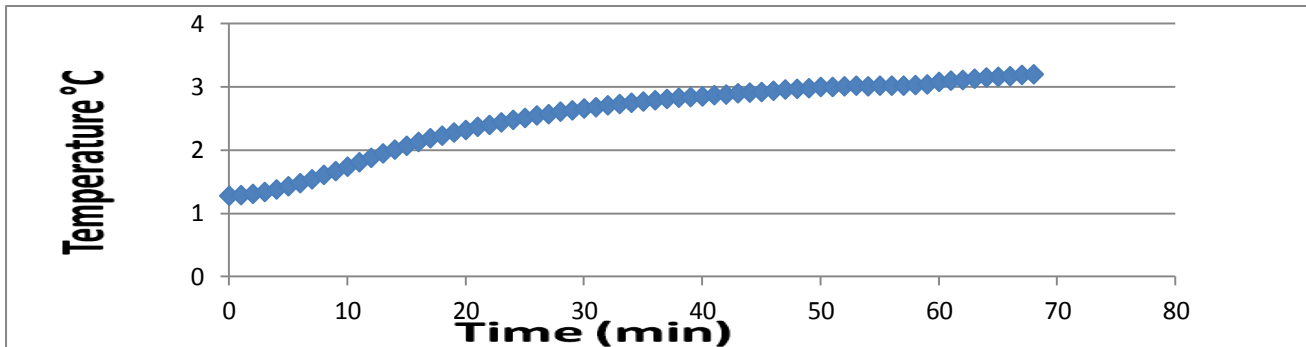


Figure 3.16: Recorded temperatures for 1:5 CP: tween20 hydrate formation.

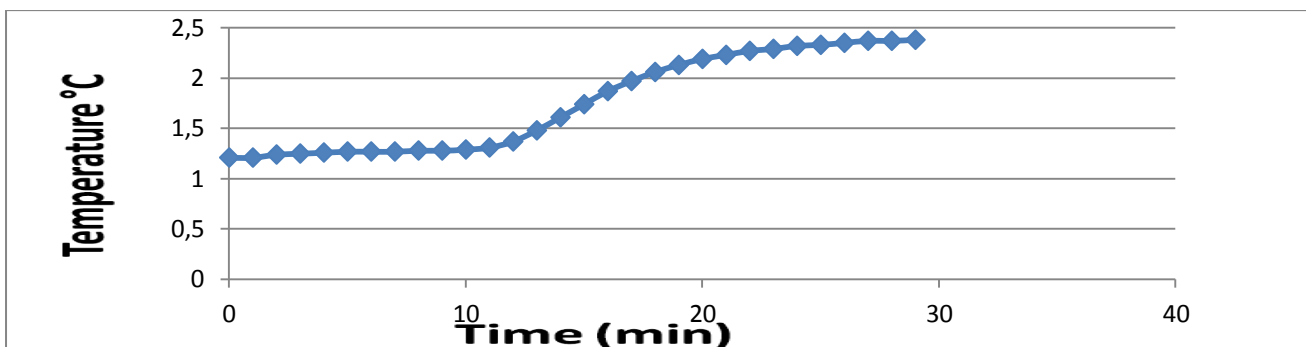


Figure 3.17: Recorded temperature for 1:5 CP: THF hydrate formation

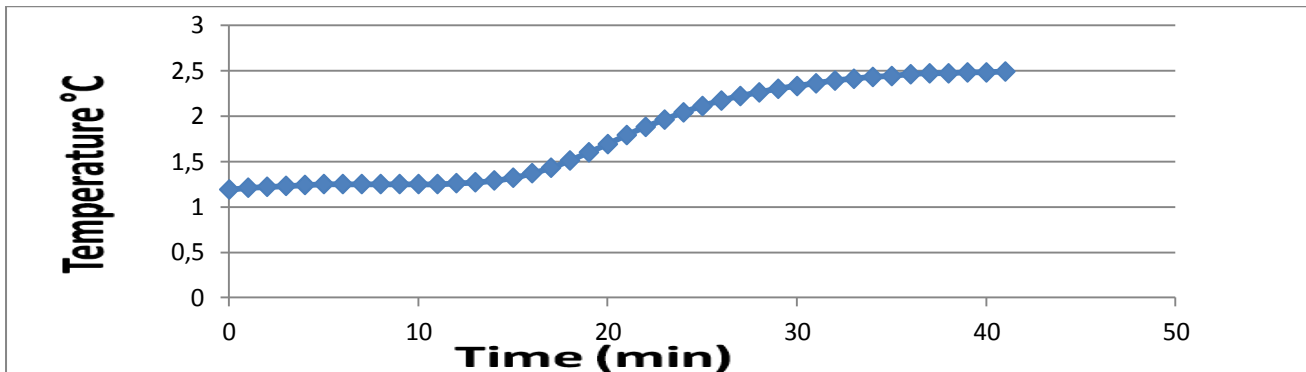


Figure 3.18: Recorded temperatures for 1:5 span20: THF hydrate formation

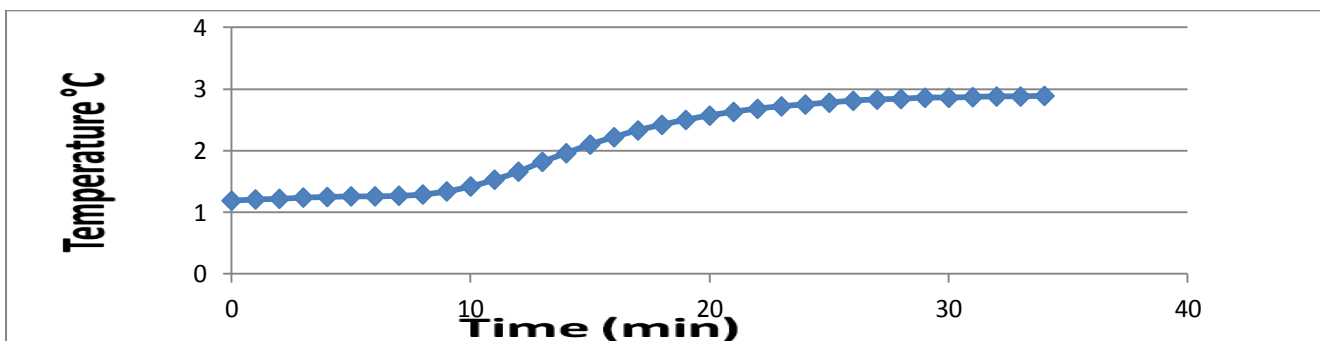


Figure 3.19: Recorded temperatures for 1:5 CP: THF in tween20 hydrate formation

Chapter 4 Discussion

This thesis discussed the following topics:

1. Methods development for the hydrate formation
2. Effects of subcooling and stirring
3. The ratio between the solutions that forms the hydrate
4. The quantification methods that used in the experiments
5. The quantification of the hydration numbers
6. Morphology of the hydrate formation
7. The kinetic of hydrate formation

4.1 Effects of subcooling and stirring

The methods used in the experiments have been tested by Corak (2011), who concluded that the hydration number of cyclopentane hydrates at low subcooling gives values closer to the theoretical values than the high subcooling. According to the suggestion of Kashichiev et al. (2002) as it shown in equation (7), the driving force for an isobaric regime of hydrate formation as a function of subcooling indicates that lower subcooling causes stronger driving force. Higher subcooling gives faster kinetic formation as mentioned in Section 1.3. According to that we have chosen the low subcooling at 1.5 °C in this work.

$$\Delta\mu = \Delta S_e \Delta T \quad (7)$$

Where $\Delta\mu$ is the driving force, ΔS_e is the hydrate dissociation entropy per hydrate building unit at equilibrium temperature, ΔT is the subcooling.

The stirring speed for mixing the solution during the formation of pure cyclopentane hydrate and cyclopentane with surfactants gives strong and stable driving force at 500 RPM as shown in section 3.1.1, while at less stirring speed the driving force was weaker, therefore we choose it to be 500 RPM in our work.

4.2 The hydrate former ratios

In this work, we have tested two proportions between the oil and aqueous phases, 1:3 and 1:5 by volume, which are equal to 1:15.6 and 1:26.2 atomic mole ratios, respectively, as hydrate formers. The main aim for these proportions is to be close to the theoretical ratio in the first case, and to have an excess of water around the hydrate phase in the reactor during the formation of hydrate at the second set of conditions. The theoretical hydrate proportion in cyclopentane hydrate is 1:17 atomic mole ratio cyclopentane to water, as it is discussed in Section 1.3. In the beginning we tested 1:1 (by volume) cyclopentane to water and we observed that all the water was used and there was a lot of free cyclopentane remaining in the system.

4.3 Concentration of the surfactants

Two surfactants (span20 and tween20) were used as additives in the hydrate system, at a concentration of the surfactants of $5 \times 10^{-3} \text{ M}$ dissolved in suitable phases. Span20 dissolved in cyclopentane and tween20 dissolved in the aqueous phase. This concentration is suitable for span20, but for tween20 it forms a high amount of foam that must be removed from the hydrate phase in the vacuum suction (see Figure 4.1). However, the removal takes a long time, which contributed to the loss of a high amount of cyclopentane due to the dissociation of the hydrate as it is explained in Section 1.6. To reduce the amount of foam we reduced the concentration of the tween20 to $5 \times 10^{-4} \text{ M}$.

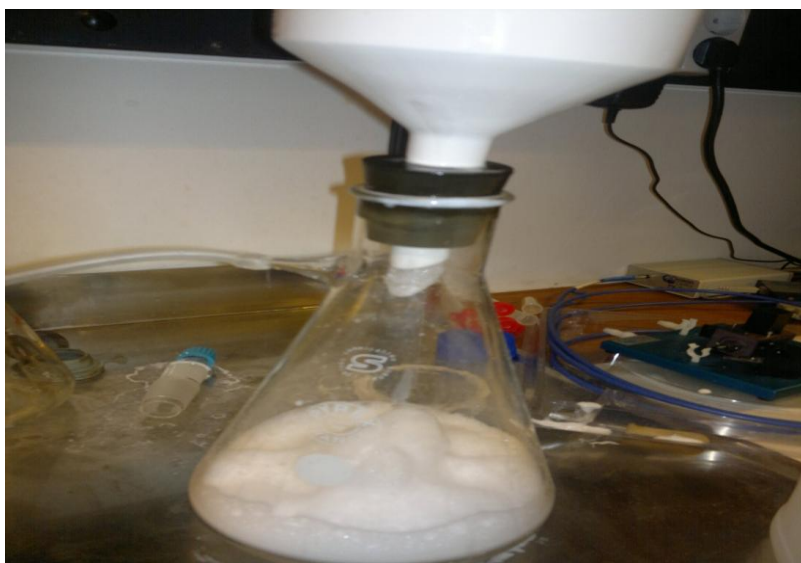


Figure 4.1: The separation of the foam from the hydrate slurry with high concentration ($5 \times 10^{-3} \text{ M}$) of tween20.

4.4. Method developments

4.4.1 The quantification methods used in the experiments

There are three methods has been used as quantification methods for cyclopentane in the hydrate. Two of them used the evaporation of the cyclopentane from the sample which is produced from the hydrate dissociation, and the third one analyzed the recovered cyclopentane using gas chromatography with external calibration curve as it is shown in Section 3.3. The two evaporation methods were tested in order to choose the efficient evaporation of cyclopentane with less loss of water as it is shown in Section 3.2.1.

Evaporation with heat shows more water loss, which has been tested using pure water and water with cyclopentane. The pure water shows loss of high amount of water gradually from the initial amount, but in the experiment with water and cyclopentane most of the cyclopentane evaporated in the first hour and there was a small amount of the oil phase visible in the sample. After two hour, all the cyclopentane had evaporated, together with some water. As shown in Figure 3.4, using heat evaporation the water loss is too large, and the method cannot be used. When a nitrogen gas stream was directed into the tubes that contain water and cyclopentane until the cyclopentane disappeared visually from the sample, there was smaller amount of water evaporated with the cyclopentane compared to the loss of water in the evaporation using heat. When nitrogen gas stream is directed into a tube that contains pure water for two minutes (which is the estimated average time of evaporating the cyclopentane), the loss of water that observed was lower compare to the evaporation by the heat, as it is illustrated in Figure 4.2. So the evaporation of cyclopentane using nitrogen gas has shown better precision and for this reason we used it in this work. The average loss of water during the evaporation using nitrogen gas is determined as 0.2g, and this amount is added to the determined hydration number of the experiment that uses the nitrogen gas evaporation method.

4.4.2 Quantification of cyclopentane using GC-FID and N₂ gas

In this work, we have investigated two methods in order to quantify the cyclopentane in the hydrate. The results show that the quantification of cyclopentane in the hydrate by evaporation using the nitrogen gas stream method is the most reliable, because it has the best

reproducibility between parallel experiments as it is shown in Table A.3.2. On the other hand, the quantification using GC-FID gives less precision.

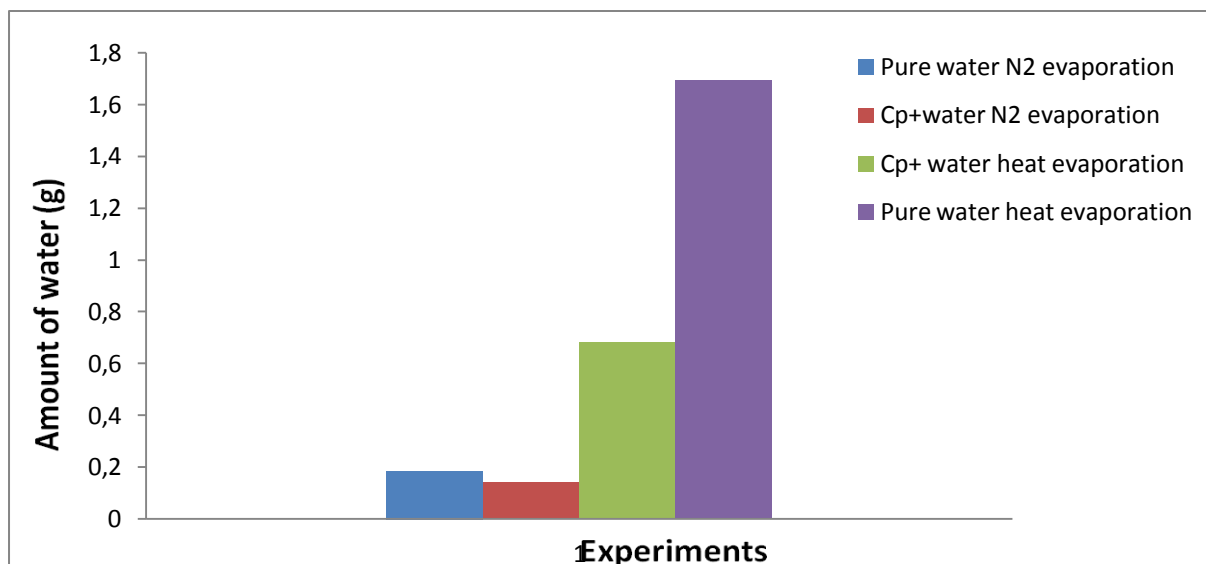


Figure 4.2: An example of the water loss in the hydrate using nitrogen gas.

4.5 Morphology of hydrate formation

The morphology of hydrate in the pure cyclopentane hydrate and cyclopentane hydrate with additives in the reactor, during the hydrate formation system, has been observed through a visual window in this work. Some of the pictures that are taken from the system are shown in Figures 4.3, 4.4 and 4.5 for pure cyclopentane system, cyclopentane with span20 and tween20 as additives, respectively. Several pictures have been taken in every 10 to 15 minutes for each of the hydrate systems.

As shown in Figure 4.3A, the snapshot taken before the stirring is started to mix the cyclopentane and the saline water. Visually, we see two stable phases (oil and water phases). Snapshot 4.3B shows the aspect of the solution during the cooling stage: The liquid is transparent, and a vortex deformed the liquid free surface due to the vigorous stirring. The cooling stage continues until the temperature of the solution in the reactor becomes stable according to the subcooling temperature, at that time we add the ice. At stage C (snapshot C), the snapshot has been taken after the ice is added and the solution temperature starts to rise by several degrees. It has been observed that an important quantity of small crystals of a hydrate slurry is produced that is quasi instantaneously over the whole solution, which is the first

crystallization of hydrate (the first hydrate formation). In stage D, the temperature of the solution in the reactor increases rapidly which means that the formation rate of the hydrate increases strongly, interestingly the same phenomenon can be observed very distinctly in stages C and E as well. Several pictures have been taken, but we choose the pictures that look differently. The temperature rises continuously until it reaches the maximum temperature and starts to stabilize and then to decrease again, which means that all the free cyclopentane in the solution have consumed, and the hydrate formation has finished by forming a snow solid-like crystals floating in the excess water as it is show in stage F.

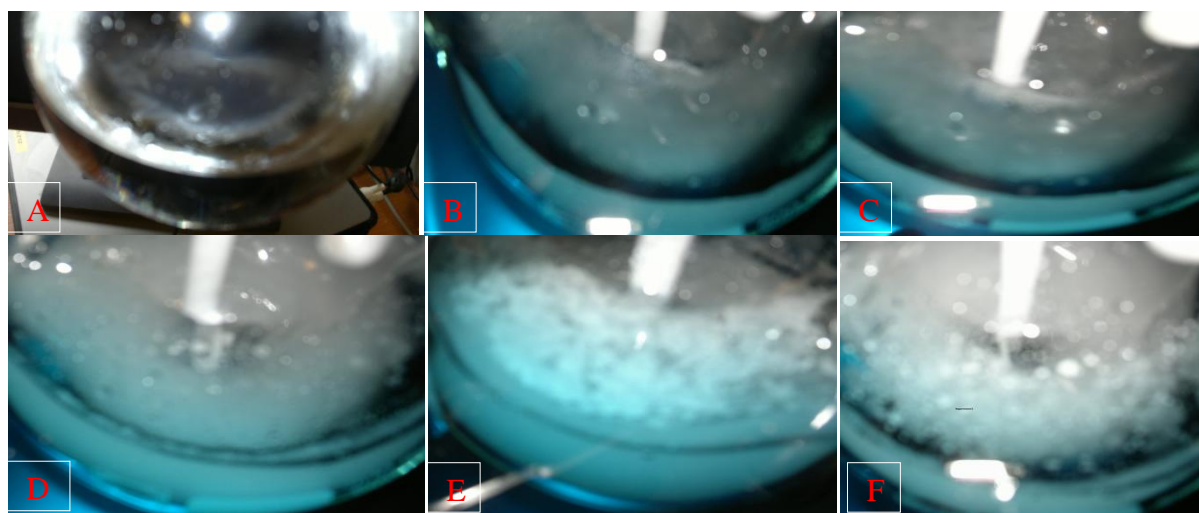


Figure 4.3: The pictures have been taken from 1:5 cyclopentane to water hydrate system during the formation in different stages and times. A : The sample before placing in the cooling bath, B: at the cooling stage, C: at the induction time, D: after the first hydrate formation observed, E: 20 to 30 minutes after first hydrate formation and F: at the end of the Formation.

Figures 4.4 and 4.5 show the pictures that have been taken during the formation of cyclopentane hydrate with surfactants as additive in different stages and times. In Figure 4.4, snapshot A shows the solution that is transferred into the reactor, the surfactant span20 dissolved in the oil phase, which is a separate phase from the aqueous phase in the reactor. Stage B has been taken during the cooling stage. Due to the vigorous stirring, the solution changed completely from colorless. When the solution is cooled and the temperature is stabilized, foams covered the whole surface of the solution as it is shown in stage C. A small piece of ice was added to the system and the temperature was carefully monitored until the first hydrate slurry is observed in stage D. At the same time the temperature increases, which is referred to the first hydrate formation. The formation rate increases strongly and the

temperature rises in stage E. In snapshot F, a solid-like layer grows up onto the reactor windows, that were used to take the snapshots, while the temperature continues to increase. In cyclopentane hydrate with span20 as additive, there are two observations that are not observed in other hydrate systems. The first observation: The formation time is longer than other hydrate systems, there are several pictures between stages D and F, we choose snapshot E. The second observation: The whole water phase was consumed with both ratios that have been tested (see Section 1.9.1) and the hydrate was almost dry. This is due to the water in oil emulsion which is formed by span20. Snapshot G shows the hydrate in the reactor after the formation is ended. In Figure 4.5, snapshot A shows the solution that is prepared in order to form the hydrate system by adding tween20 to the cyclopentane hydrate system. Snapshot B shows that the solution color is changed due to the emulsion, and a vortex is formed due to the stirring in the cooling stage. After the stabilization of the solution temperature, small pieces of ice are added to initiate the hydrate formation. After few minutes, some hydrate slurry appears in the reactor as it is shown in stage C. The hydrate grows and the temperature increases through stages D and E. After that the temperature starts to decrease. The hydrate slurry in cyclopentane with tween20 system is spread in the excess water in the reactor. In contrary, in pure cyclopentane system the hydrate slurries accumulate on the top of the solution in the reactor during the hydrate formation.

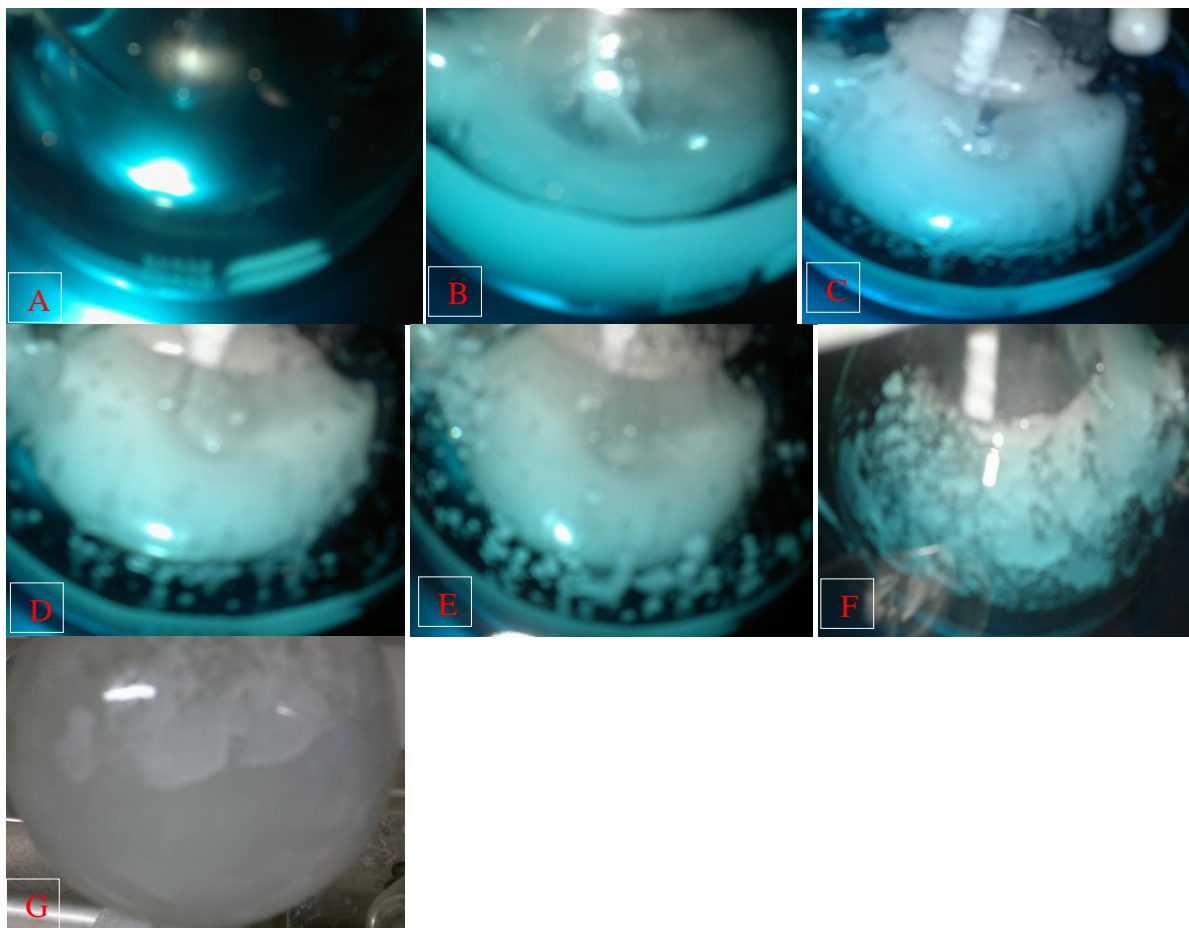


Figure 4.4: The pictures that have been taken from 1:5 cyclopentane to span20 hydrate system during the formation in different stages and times. A: The sample before placing in the cooling bath, B: at the cooling stage, C: at the induction time, D: after the first hydrate formation observed, E: 20 to 30 minutes after first hydrate formation, F: at the end of the Formation and snapshot G: Taken after the reactor has taken out from the subcooling and the produced hydrate will transfer to vacuum suction.

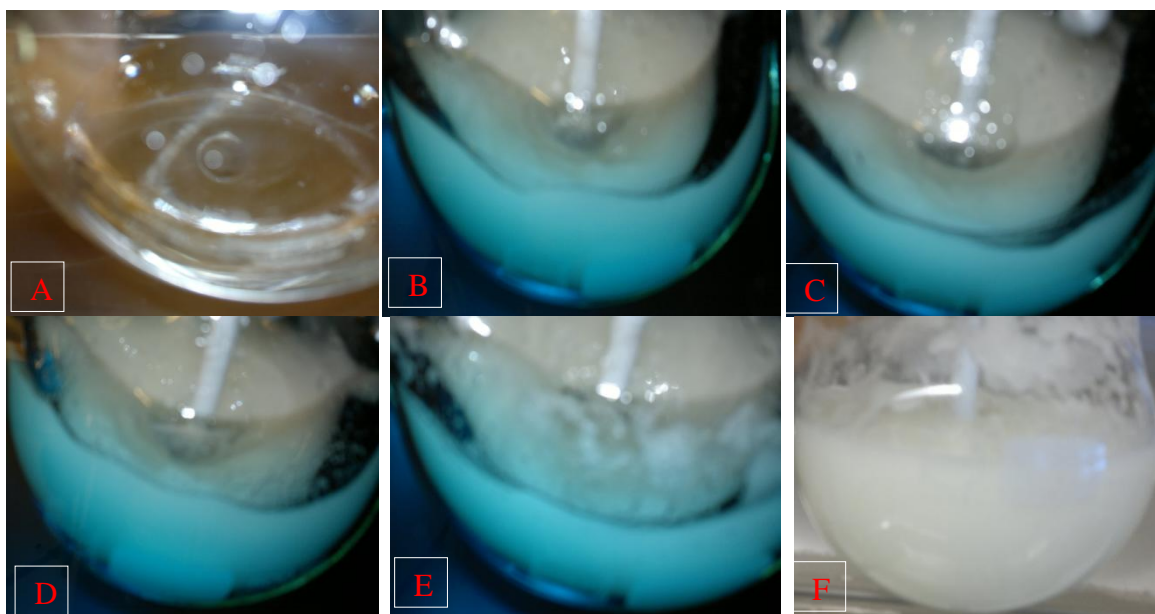


Figure 4.5: The pictures that have been taken from 1:5 cyclopentane to tween20 hydrate system during the formation in different stages and times. A: The sample before placing in the cooling bath, B: at the cooling stage, C: at the induction time, D: after the first hydrate formation observed, E: 20 to 30 minutes after first hydrate formation and F: formation has ended, the reactor taken out from the cooling water and the produced hydrate will transfer into the vacuum suction.

4.6 The determined hydration number

The variation of the determined hydration number of cyclopentane hydrate as a function of different additives (surfactants and THF) in different ratios are illustrated in Figure 4.6, which shows the hydration numbers that have been determined by evaporation using nitrogen gas, Figure 4.7 which shows the hydration numbers that determined by analysis with GC-FID. The determined hydration numbers seem to be affected by the differential of the ratio and the type of the additives. Theoretical hydration number for pure cyclopentane hydrate system is 17 (Sloan and Koh 2008).

4.6.1 Pure system (cyclopentane and saline water)

The determined hydration numbers for the pure system of cyclopentane hydrate are given in Table 3.4, 3.7, A.4.1 and A.4.2, show more deviation in high ratios of water to cyclopentane, the mean value of determined numbers are 17.2 and 15.8 for the ratios 1:3 and 1:5 cyclopentane to water, respectively. The mean value of 17.2 is approximately close to the theoretical value, the 0.2 deviation means there is less cyclopentane in the hydrate structures

than the ideal number and this is because of some of the cavities are not filled with guests. The mean value of 15.8 shows 1.2 less water compared to the theoretical value of the hydration number, which means that there is more cyclopentane in the hydrate structures than the theoretical number, which can be explained as there are more than cyclopentane presences in a cavity that form the hydrate structure such as in nitrogen and argon hydrate (Sloan 2003). This is perhaps less probable with cyclopentane, as the cyclopentane is large molecule. There can be free cyclopentane in the system that encapsulated either inside pores of hydrate sample or in hydrate shells formed around cyclopentane droplets due to the subcooling (Corak 2011). The determined hydration number that is found using GC-FID analyses shows larger deviations than the one that found by nitrogen evaporation; 18.8 and 19.0 for 1:3 and 1:5 cyclopentane to water, respectively, which may be due to loss of cyclopentane during the dilution of the sample.

4.6.2 Span20 and saline water

In cyclopentane hydrate with span20 as additive, the determined hydration numbers have been found to be larger than the ideal hydration number for pure cyclopentane hydrates with the mean values of 18.6 and 20.6 for 1:3 and 1:5, span20 ratios, respectively using nitrogen gas evaporation, and the mean values of 23.7 and 21.4 for the same ratios and solutions that are mentioned above using GC-FID analyses. These results are shown Figure 4.6 and 4.7. The additive span20 creates water in oil emulsions, which give droplets that are can be incorporated in the hydrate crystal formations, and then in the frameworks. In addition some of the cavities in the structure can be without a guest molecule.

4.6.3 Cyclopentane and tween20

The determined hydration numbers of cyclopentane hydrate system in the presence of tween20 as additive does not show large deviation from the ideal hydration number of the pure cyclopentane hydrate, especially in higher ratios of tween20 to cyclopentane, where the mean values of 16 and 17.2 for 1:3 and 1:5 cyclopentane to tween20 solved in saline water, respectively, when quantified using nitrogen gas. The mean values of 15.8 and 17.2 for 1:3 and 1:5 are found using GC-FID analyses, which is a good correspondence. Tween20 formed an oil in water emulsion into the cyclopentane hydrate system that can be the reason for the excess cyclopentane in the system, because there may be free cyclopentane in between and around the cavities. There could also be some cavities that have more than one guest in the hydrate framework, but this is less probably as it discussed in Section 4.6.1

4.6.4 THF and surfactants as additives in cyclopentane hydrate system

The three cyclopentane hydrate systems that have been tested with the addition of THF are quantified using evaporation by nitrogen gas and GC-FID analyses to determine the cyclopentane hydration numbers. The systems show larger deviation from the theoretical cyclopentane hydration number, and this is because of THF has contributed as a guest in the hydrate framework. It has the same theoretical hydration number as cyclopentane hydrate does and both of them form cyclopentane hydrate and THF hydrate in the system.

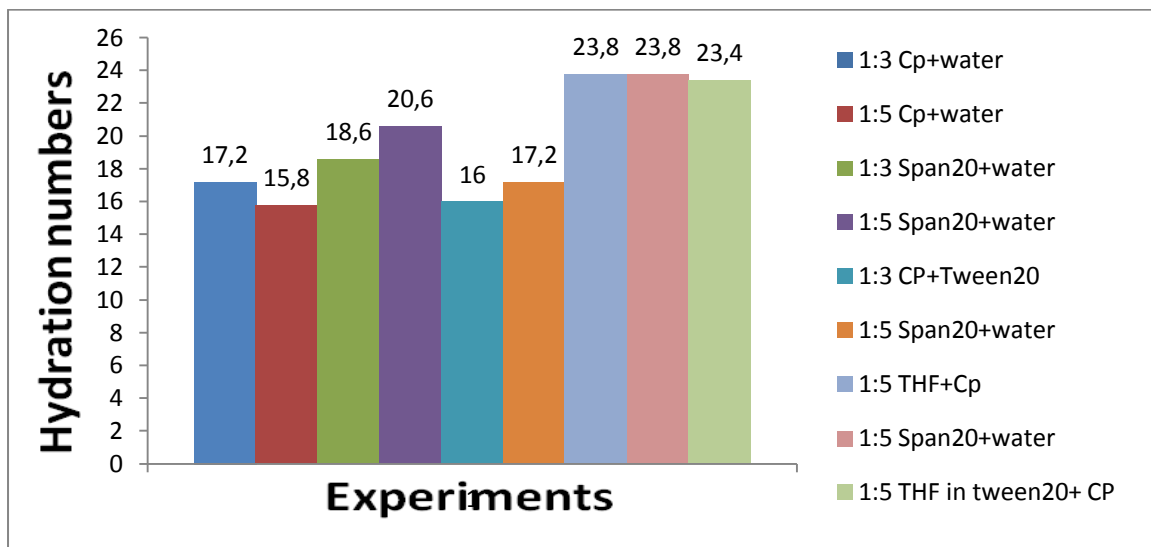


Figure 4.6: The mean values of determined hydration numbers that found using N₂ gas evaporation.

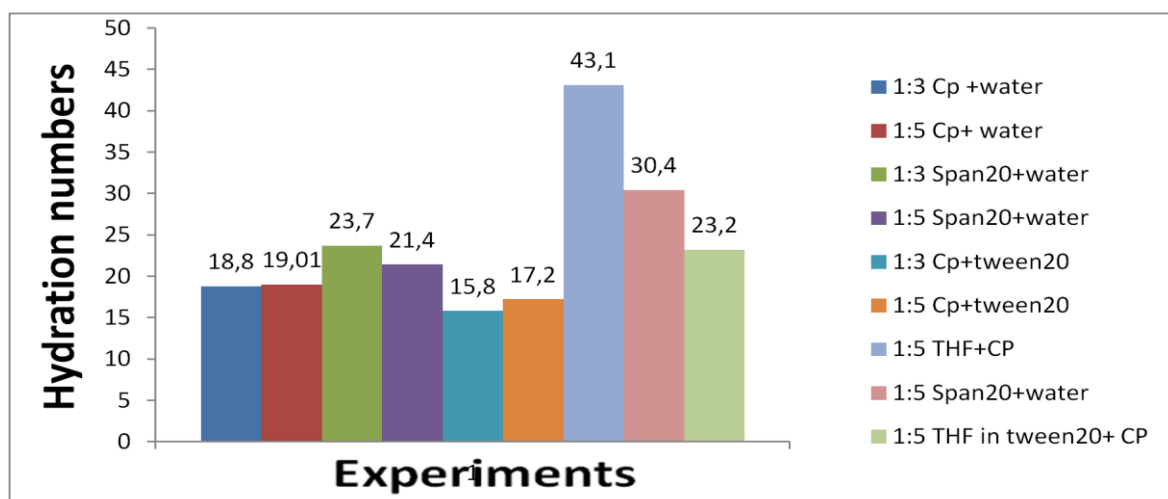


Figure 4.7: The mean values of the determined hydration numbers that found using GC-FID analyses.

4.7 The rate of formation

The variations of the formation time of cyclopentane hydrate system with surfactants and THF as additives in the system is illustrated in Figure 4.8, 4.9 and 4.10. The Figures show the recorded time of hydrate formation using the Testo logger. The recorded hydrate formation times have shown variations according to the additives, even in surfactants as additive show variations according to the type of emulsions formed, which will be discussed in the following sections.

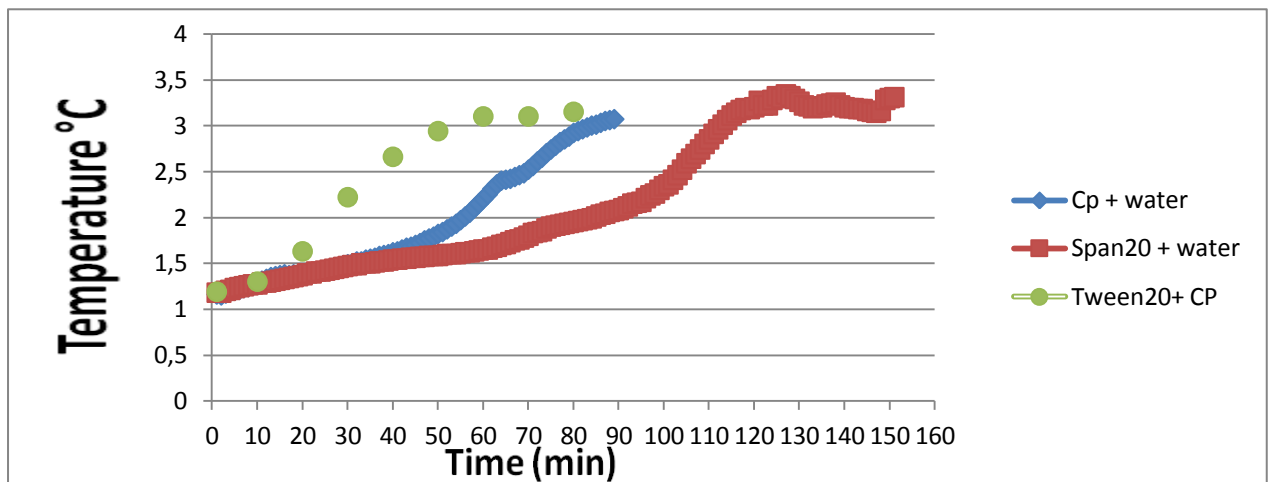


Figure 4.8: The formation rates for the pure cyclopentane hydrate and cyclopentane with surfactants. In 1:3 volumetric ratio.

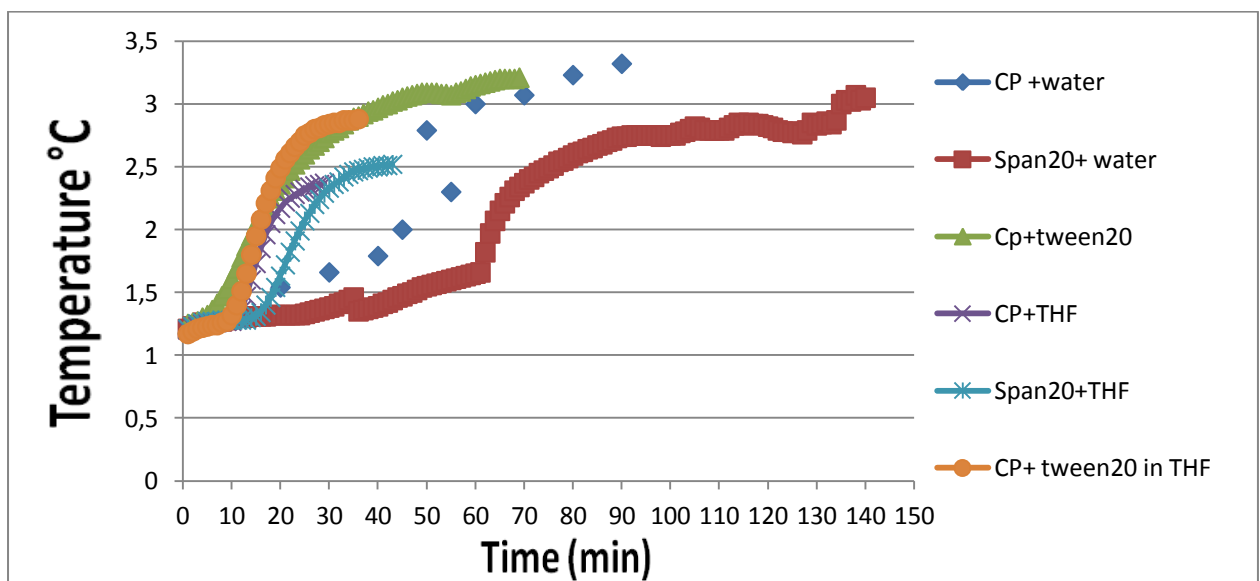


Figure 4.9: The formation rates for the pure cyclopentane hydrate and cyclopentane with additives. In 1:5 volumetric ratio.

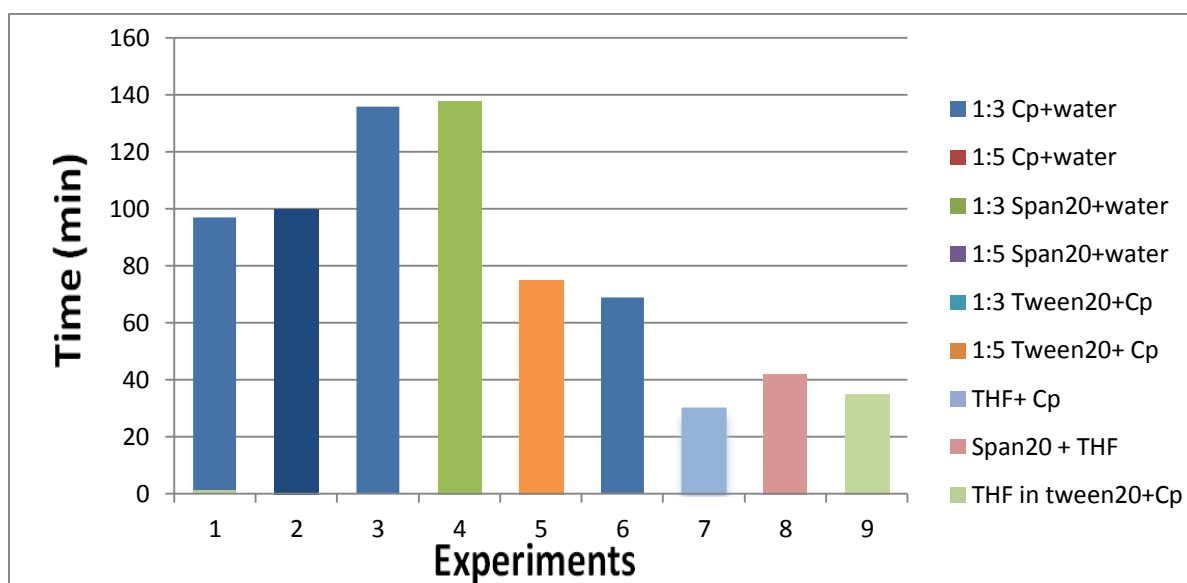


Figure 4.10: The formation times for the pure cyclopentane hydrate and cyclopentane with additives, given as the time from addition of ice to the maximum temperature.

4.7.1 Pure system (cyclopentane and saline water)

The pure cyclopentane hydrate in 1:3 and 1:5 ratios have shown the mean formation rates of 97 and 100 minutes, respectively. The different ratios do not give a large variation in the formation times. The formation rate of the pure system has been taken as a standard in order to study the effect of the additives into the cyclopentane hydrate system.

4.7.2 Cyclopentane hydrate with surfactant as additive

Adding surfactants to the cyclopentane hydrate system influences the hydrate formation rate according to the emulsion types (water in oil, or oil in water) as it is shown in Figure 4.8. For span20, we have recorded longer time of formation, around 136 and 138 minutes, for both ratios (1:3 and 1:5 span20 solved in cyclopentane to saline water), which means that the emulsion of water in oil that is formed by span20 delays the formation of hydrates. Tween20 as an addition recorded mean formation rates of 75 and 69 minutes for both ratios, and this reduced the time due to the oil in water emulsion that formed is by tween20 in the hydrate system.

4.7.3 THF in pure system and surfactants as additives into the system

The presence of THF in cyclopentane hydrate system, either in pure system or with addition of surfactants, has improved the rate in the kinetic hydrate formation, as it is shown in Figure

4.8. The addition of THF into the cyclopentane hydrate system accelerates the hydrate formation more than the surfactants additives. In presence of THF and one of the surfactants in the cyclopentane hydrate system, the span20 in cyclopentane + THF system will takes longer times than the cyclopentane + THF in tween20 system, which the last system takes approximately the same time as cyclopentane + THF system do.

Chapter 5 Conclusion

We have determined experimentally the equilibrium curve for both of the pure cyclopentane hydrate and the mixed cyclopentane + THF hydrate (4% wt THF in water) in the presence and absence of surfactants (5×10^{-3} span20 in cyclopentane and 5×10^{-4} tween20 in water).

5.1 The morphology effect of the additives to the cyclopentane hydrate system

The morphology of the pure cyclopentane hydrate during the hydrate formation resembles snow. The hydrate accumulates at the top of the solution in the reactor, while the addition of span20 surfactant into the cyclopentane hydrate system gave a foam and emulsion in the hydrate system and reduced the accumulation of the hydrate in the top of the reactor as well as consuming more water than the pure system does. In the case of tween20 surfactant as additive, the hydrate particles were distributed in the solution and there is no accumulation of large hydrate lumps in the system.

After the formation has ended, and the excess water removed, the result hydrate for pure cyclopentane looks like snow and sticks strongly together, and has a white color, while the span20 the cyclopentane hydrates look like new snow with white color and some colorless lump particles. While with tween20, the cyclopentane hydrates lumped together and has a white color.

Adding THF to cyclopentane hydrate did not shows a visual change or difference to the cyclopentane hydrate morphology.

5.2 The calculated hydrate number for pure cyclopentane hydrate and with additives

We have found that the determined hydration number of cyclopentane hydrate is affected by the addition surfactants (span20 and tween20) according to the type of emulsion that forms. The determined hydration numbers of the pure cyclopentane hydrate system in high ratio of cyclopentane is close to the theoretical hydration number and in low ratio there is about 1.2

less water from the ideal number. While in addition of span20 the determined hydration numbers of cyclopentane is lower cyclopentane than the theoretical hydration number due to the water in oil emulsion, and the additive tween20 to the cyclopentane hydrate system gives higher cyclopentane in the determined values form the ideal hydration value due to the oil in water emulsions.

The cyclopentane hydrate with THF as additive forms cyclopentane and THF hydrates, since both of these molecules will enter in the framework as guest, the determined hydration number gives lower levels of cyclopentane compared to the theoretical hydration number of cyclopentane hydrate due to the contribution of THF.

5.3 The hydrate formation kinetics

It is confirmed that, in presence of THF, the mixed cyclopentane + THF hydrate forms rapidly in comparison to pure cyclopentane hydrates. The surfactant influence on the formation rate of pure cyclopentane hydrate or the mixed cyclopentane + THF hydrate is due to the emulsion type . Tween20 forms oil in water emulsion and gives hydrate formation more rapidly than the span20 which forms water in oil emulsions. Span20 shows slowest formation rate in cyclopentane hydrate formation in both the pure cyclopentane hydrate and the mixed cyclopentane + THF hydrate. Literature suggests that adding the surfactants into the hydrate system leads to the result that the obstructing hydrate film (which reduce the kinetics) does not build up (Roger et al. 2007). Watanabe (2005) has reported that the solubility of the surfactants represents a crucial factor which affects the behavior of the hydrate formation. Surfactant that is soluble in water (as tween20) enhances the kinetic of hydrate growth.

References

- Binks, B. P., & Lumsdon, S. O. (2000). Influence of particle wettability on the type and stability of surfactant-free emulsions. *Langmuir*, 16(23), 8622-8631.
- Circone, S., Stern, L. A., Kirby, S. H., Durham, W. B., Chakoumakos, B. C., Rawn, C. J., ... & Ishii, Y. (2003). CO₂ hydrate: synthesis, composition, structure, dissociation behavior, and a comparison to structure I CH₄ hydrate. *The Journal of Physical Chemistry B*, 107(23), 5529-5539.
- Corak, D., Barth, T., Høiland, S., Skodvin, T., Larsen, R., & Skjetne, T. (2011). Effect of subcooling and amount of hydrate former on formation of cyclopentane hydrates in brine. *Desalination*, 278(1), 268-274.
- Dirdal, E. G., Arulanantham, C., Sefidroodi, H., & Kelland, M. A. (2012). Can cyclopentane hydrate formation be used to rank the performance of kinetic hydrate inhibitors?. *Chemical Engineering Science*.
- Duan, Z., & Sun, R. (2006). A model to predict phase equilibrium of CH₄ and CO₂ clathrate hydrate in aqueous electrolyte solutions. *American Mineralogist*, 91(8-9), 1346-1354.
- E.D. Sloan and C.A. Koh. (2007). *Clathrate Hydrates of Natural Gases*. Taylor & Francis Group, CRC, New York, USA, second edition.
- E.D. Sloan and C.A. Koh. (2008) .*Clathrate Hydrates of Natural Gases*. CRC Press, Taylor & Francis Group, New York, USA, third edition.
- Florusse, L. J., Peters, C. J., Schoonman, J., Hester, K. C., Koh, C. A., Dec, S. F., ... & Sloan, E. D. (2004). Stable low-pressure hydrogen clusters stored in a binary clathrate hydrate. *Science*, 306(5695), 469-471.
- Griffin, W.C., 1949. Classification of surface-active agents by HLB. *J. Soc. Cosmet. Chem.* 1, 311–326
- Hammerschmidt, E. G. (1934). Formation of gas hydrates in natural gas transmission lines. *Industrial & Engineering Chemistry*, 26(8), 851-855.

- Huo, Z., Freer, E., Lamar, M., Sannigrahi, B., Knauss, D. M., & Sloan, E. D. (2001). Hydrate plug prevention by anti-agglomeration. *Chemical Engineering Science*, 56(17), 4979-4991.
- Høiland, S., Askvik, K. M., Fotland, P., Alagic, E., Barth, T., & Fadnes, F. (2005). Wettability of Freon hydrates in crude oil/brine emulsions. *Journal of Colloid and Interface Science*, 287(1), 217-225.
- Kashchiev, D., & Firoozabadi, A. (2002). Driving force for crystallization of gas hydrates. *Journal of crystal growth*, 241(1), 220-230.
- Komarek, R. J.³ R. G. Jensen, and B- w- Pickett. (1964). *J. Lipid Res.* 5: 268.
- Lederhos, J. P., Long, J. P., Sum, A., Christiansen, R. L., & Sloan, E. D. (1996). Effective kinetic inhibitors for natural gas hydrates. *Chemical Engineering Science*, 51(8), 1221-1229.
- Lee, H., Lee, J. W., Do Youn Kim, J. P., Seo, Y. T., Zeng, H., Moudrakovski, I. L., ... & Ripmeester, J. A. (2005). Tuning clathrate hydrates for hydrogen storage. *Nature*, 434(7034), 743-746.
- Rogers, R., Zhang, G., Dearman, J., & Woods, C. (2007). Investigations into surfactant/gas hydrate relationship. *Journal of Petroleum Science and Engineering*, 56(1), 82-88.
- Lundgaard, L., & Mollerup, J. M. (1991). The influence of gas phase fugacity and solubility on correlation of gas-hydrate formation pressure. *Fluid phase equilibria*, 70(2-3), 199-213.
- Makino, T., Sugahara, T., & Ohgaki, K. (2005). Stability boundaries of tetrahydrofuran+ water system. *Journal of Chemical & Engineering Data*, 50(6), 2058-2060.
- Márquez, A. L., Palazolo, G. G., & Wagner, J. R. (2007). Water in oil (w/o) and double (w/o/w) emulsions prepared with spans: microstructure, stability, and rheology. *Colloid and Polymer Science*, 285(10), 1119-1128.
- Miller, G. T. & Spoolman, S. E. (2009) *Living in the Environment: concepts, connections and solutions*. Belmont, Cal., Brooks/Cole.
- Mohammadi, A. H., & Richon, D. (2009). Phase equilibria of clathrate hydrates of cyclopentane+ hydrogen sulfide and cyclopentane+ methane. *Industrial & Engineering Chemistry Research*, 48(19), 9045-9048.

- Opawale, F. O., & Burgess, D. J. (1998). Influence of interfacial properties of lipophilic surfactants on water-in-oil emulsion stability. *Journal of colloid and interface science*, 197(1), 142-150.
- Peltonen, L. J., & Yliruusi, J. (2000). Surface pressure, hysteresis, interfacial tension, and CMC of four sorbitan monoesters at water–air, water–hexane, and hexane–air interfaces. *Journal of colloid and interface science*, 227(1), 1-6.
- Priev, A., Zalipsky, S., Cohen, R., & Barenholz, Y. (2002). Determination of critical micelle concentration of lipopolymers and other amphiphiles: comparison of sound velocity and fluorescent measurements. *Langmuir*, 18(3), 612-617.
- Ribeiro Jr, C. P., & Lage, P. L. (2008). Modelling of hydrate formation kinetics: State-of-the-art and future directions. *Chemical Engineering Science*, 63(8), 2007-2034.
- Ripmeester, J. A., & Ratcliffe, C. I. (1990). Xenon-129 NMR studies of clathrate hydrates: new guests for structure II and structure H. *Journal of Physical Chemistry*, 94(25), 8773-8776.
- Schicks, J. M., Ziemann, M. A., Lu, H., & Ripmeester, J. A. (2010). Raman spectroscopic investigations on natural samples from the Integrated Ocean Drilling Program (IODP) Expedition 311: Indications for heterogeneous compositions in hydrate crystals. *Spectrochimica Acta Part A: Molecular and Biomolecular Spectroscopy*, 77(5), 973-977.
- Shen, L., Guo, A., & Zhu, X. (2011). Tween surfactants: Adsorption, self-organization, and protein resistance. *Surface Science*, 605(5), 494-499.
- Sloan, E. D. (2003). Fundamental principles and applications of natural gas hydrates. *Nature*, 426(6964), 353-363.
- Torré, J. P., Ricaurte, M., Dicharry, C., & Broseta, D. (2012). CO₂ Enclathration in the Presence of Water-Soluble Hydrate Promoters: Hydrate Phase Equilibria and Kinetic Studies in Quiescent Conditions. *Chemical Engineering Science* 82, 1-13.
- Velev, O. D., Gurkov, T. D., Chakarova, S. K., Dimitrova, B. I., Ivanov, I. B., & Borwankar, R. P. (1994). Experimental investigations on model emulsion systems stabilized with non-ionic surfactant blends. *Colloids and Surfaces A: Physicochemical and Engineering Aspects*, 83(1), 43-55.

Watanabe, K., Imai, S., & Mori, Y. H. (2005). Surfactant effects on hydrate formation in an unstirred gas/liquid system: An experimental study using HFC-32 and sodium dodecyl sulfate. *Chemical engineering science*, 60(17), 4846-4857.

Yang, D., & Xu, W. (2007). Effects of salinity on methane gas hydrate system. *Science in China Series D: Earth Sciences*, 50(11), 1733-1745.

Web page of Institute of Petroleum Engineering- Heriot Watt University: Centre for Gas Hydrate Research. (last visited Mars 2013).

http://www.pet.hw.ac.uk/research/hydrate/hydrates_what.cfm

Web page of Institute of Petroleum Engineering- Heriot Watt University: Centre for Gas Hydrate Research. (last visited June 2013).

http://www.pet.hw.ac.uk/research/hydrate/hydrates_where.cfm

Web Page of Schlumberger. (last visited Mars 2013).

http://www.slb.com/news/inside_news/2010/2010_0719_gas_hydrates.aspx.

Web Page of Textile learner. (last visited May 2013).

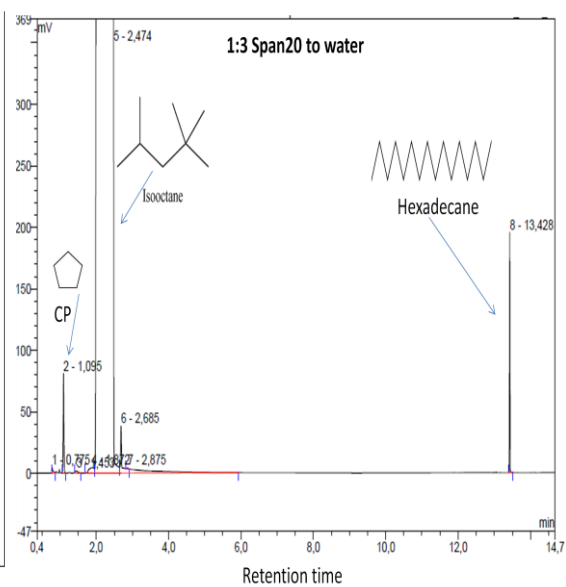
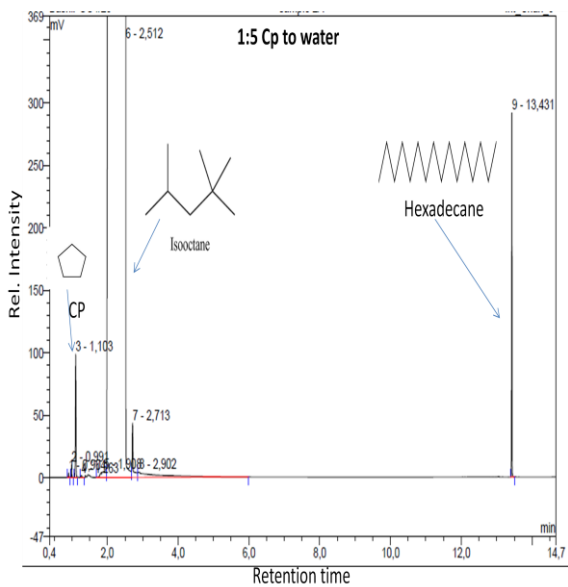
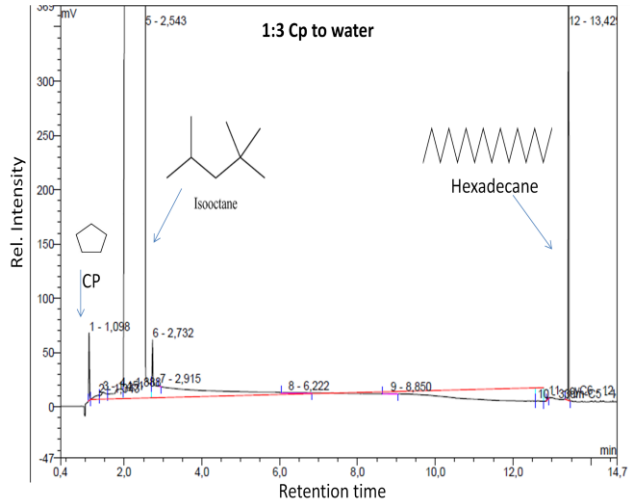
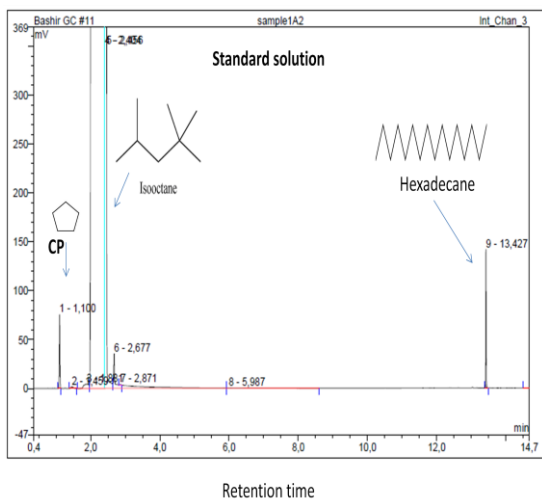
<http://textilelearner.blogspot.no/2012/12/surfactants-in-textile-processing.html>.

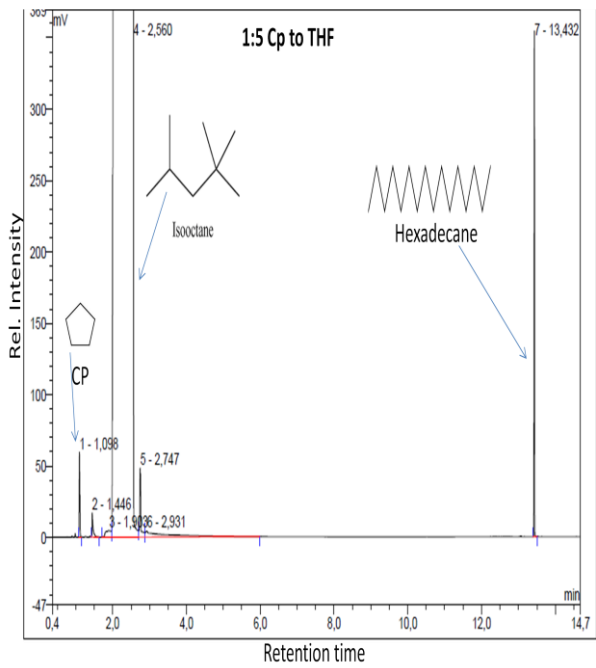
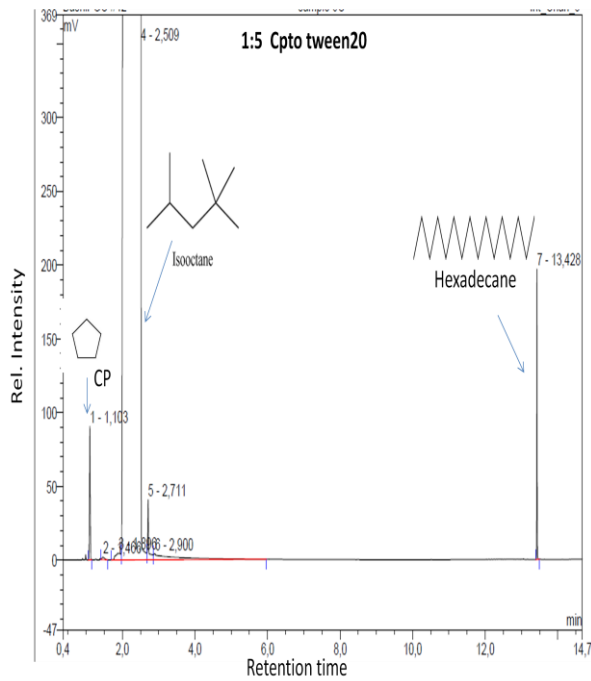
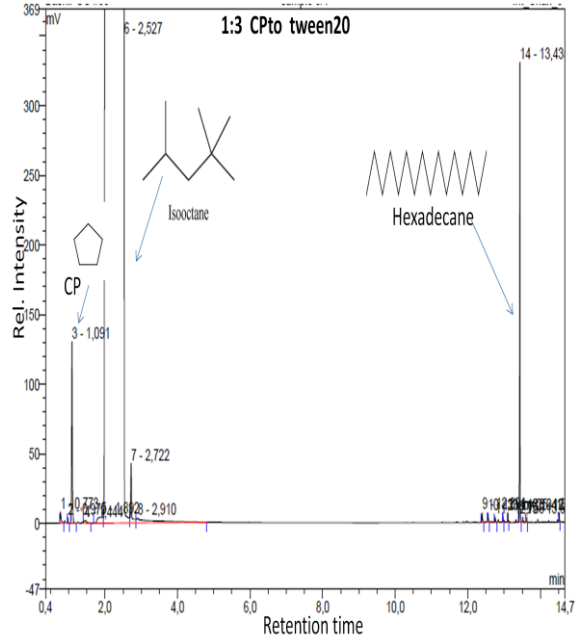
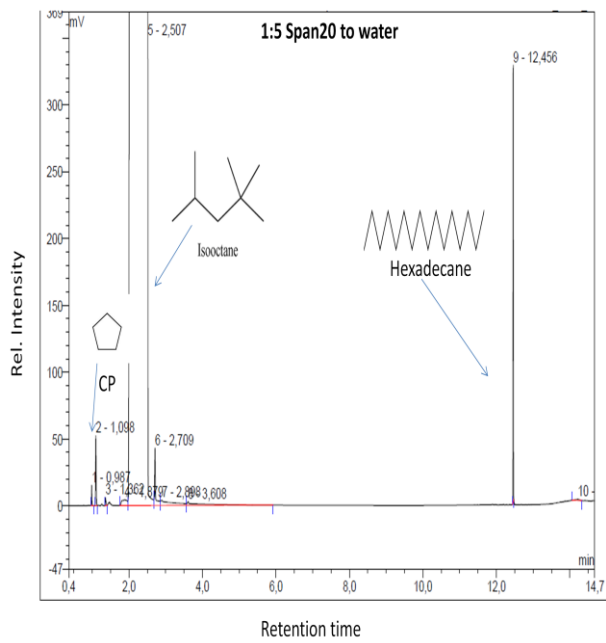
Web page of Faculty of Health and Wellbeing , Biosciences Division, On-Line Learning. (last visited May 2013).

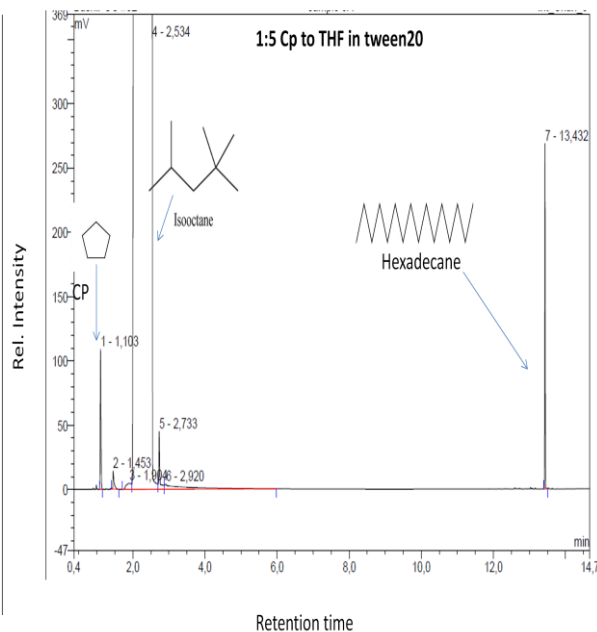
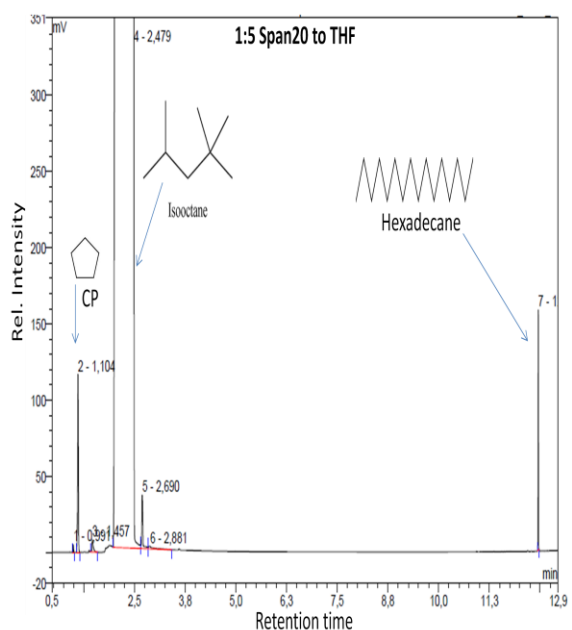
<http://teaching.shu.ac.uk/hwb/chemistry/tutorials/chrom/gaschrn.htm>

Appendix A

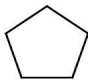
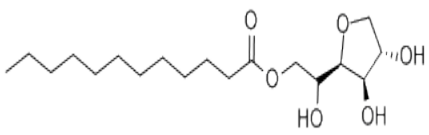
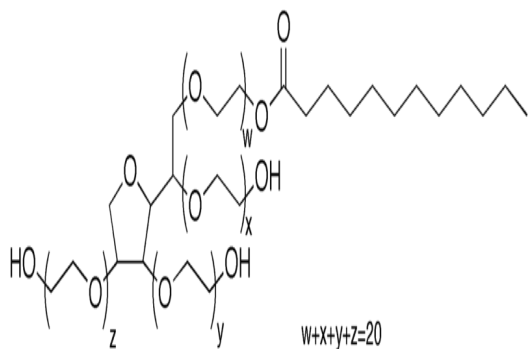
A.1 Examples of GC-FID chromatograms for each experiment


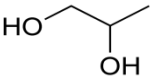
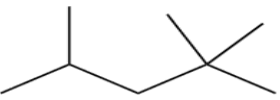





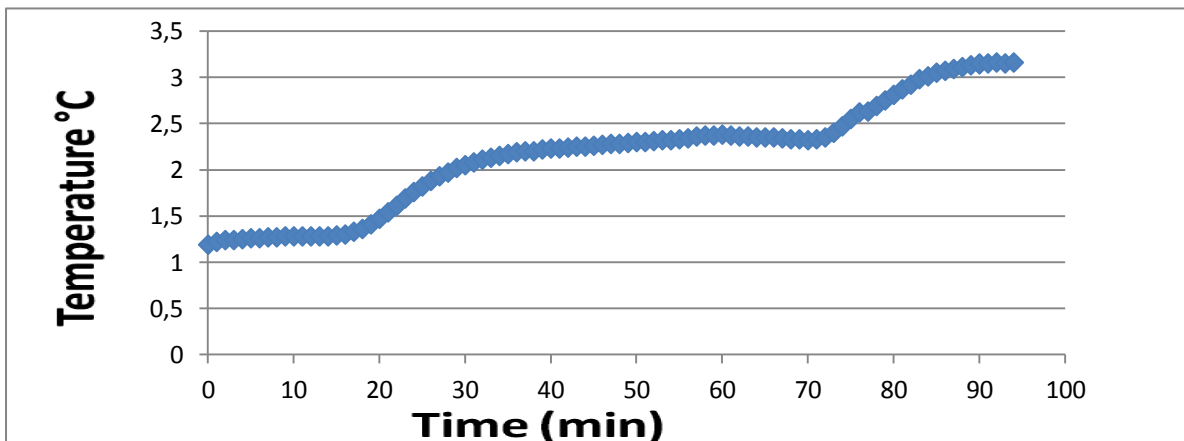
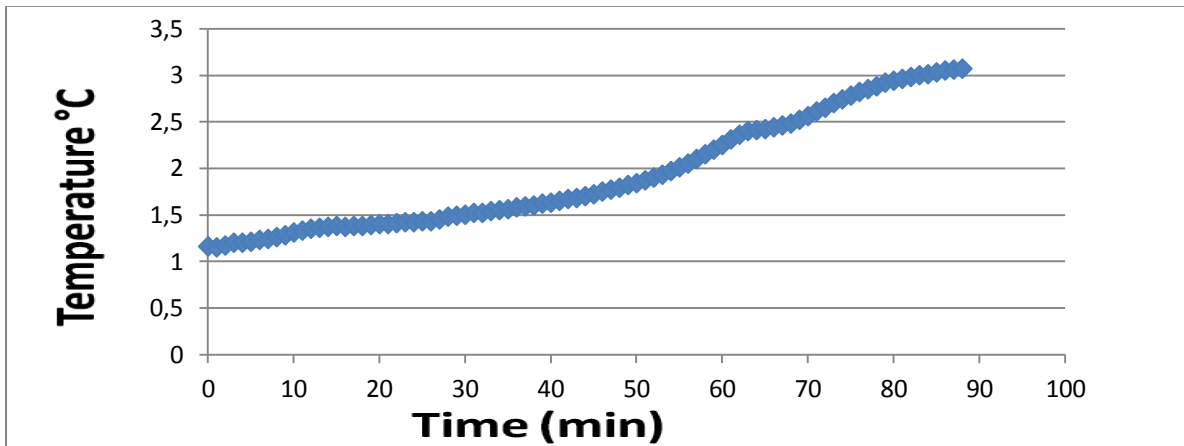
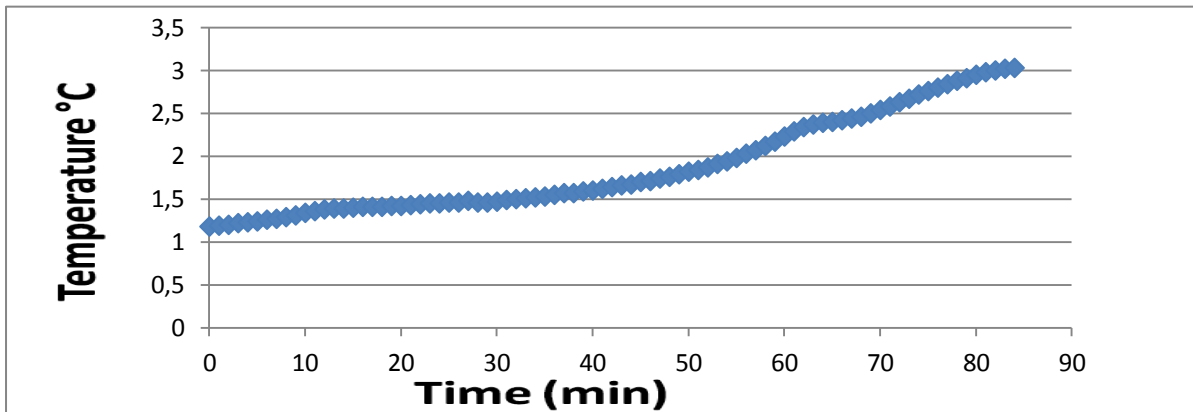
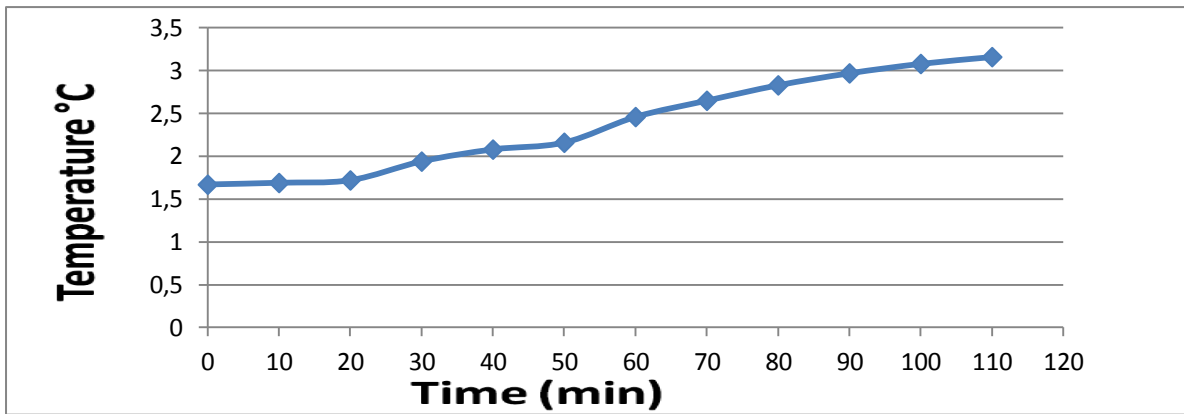


A.2 The solutions that used in the experiments

No.	Name	Company	Quality	Molar mass	Boiling point
1	Cyclopentane 	Sigma - Aldrich	99.5%	70.1 g/mol	49.2 °C
2	NaCl	Sigma - Aldrich	99.8%	58.44 g/mol	1413 °C
3	Span20 	Sigma-Aldrich		346.46 g/mol	516.1°C at 760mmHg
4	Tween20 	Sigma-Aldrich		1227.54 g/mol	> 100 °C

5	THF 	Sigma - Aldrich	≥99.8%	72.11 g/mol	66 °C
6	Distillate water	UIB	~98 %	18 g/mol	100°C
7	Glycol 	Sigma- Aldrich		76.09 g/mol	188.2 °C
8	Isooctane  Isooctane	Sigma- Aldrich	≥ 99%	114.23 g/mol	99 °C
9	Hexadecane 	Sigma- Aldrich	99%	226.44 g/mol	287 °C

A.3 Recorded temperature curves



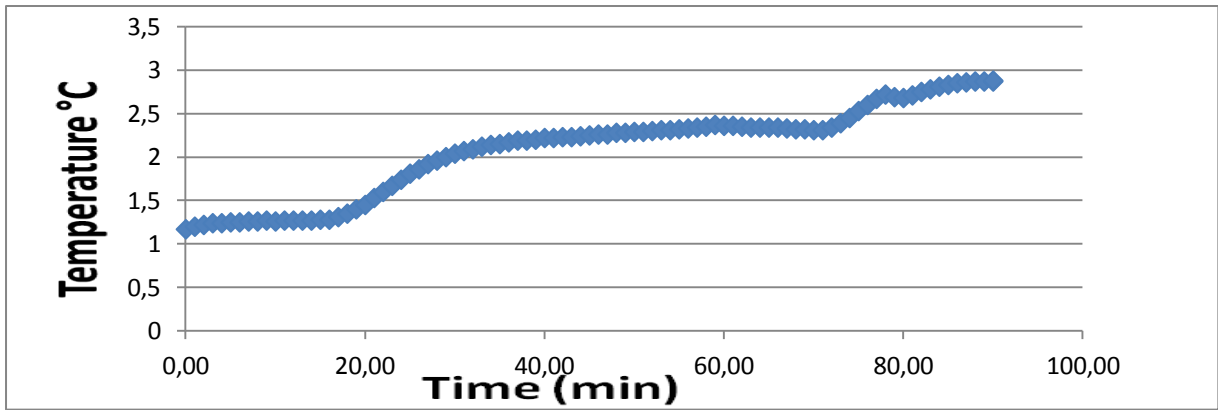


Figure A.3.1: For 1:3 Cyclopentane to water ratio.

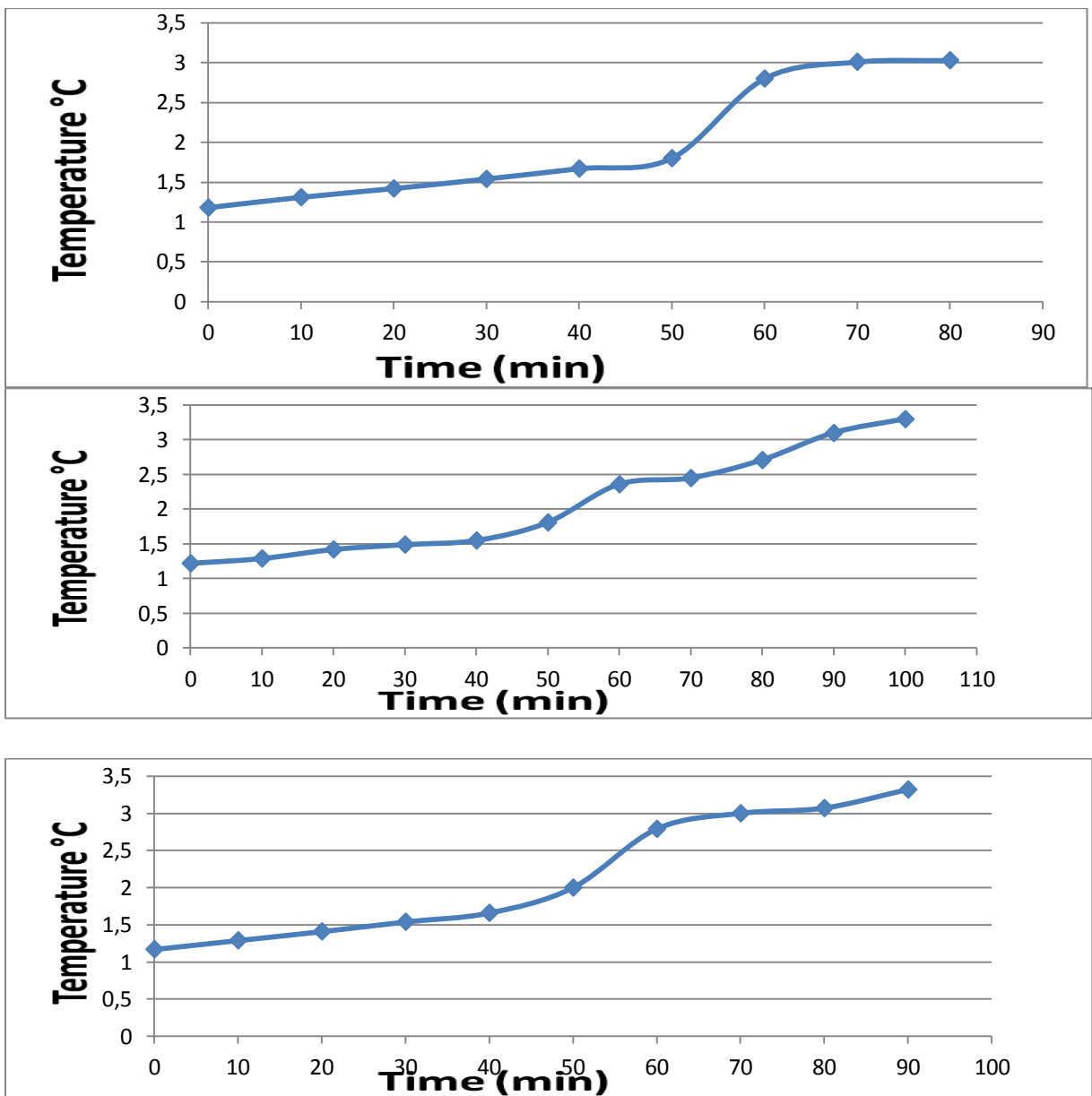
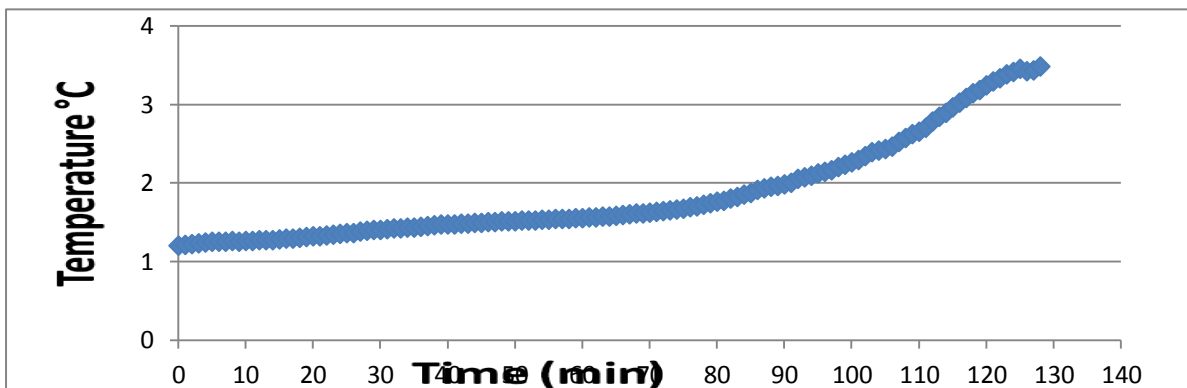
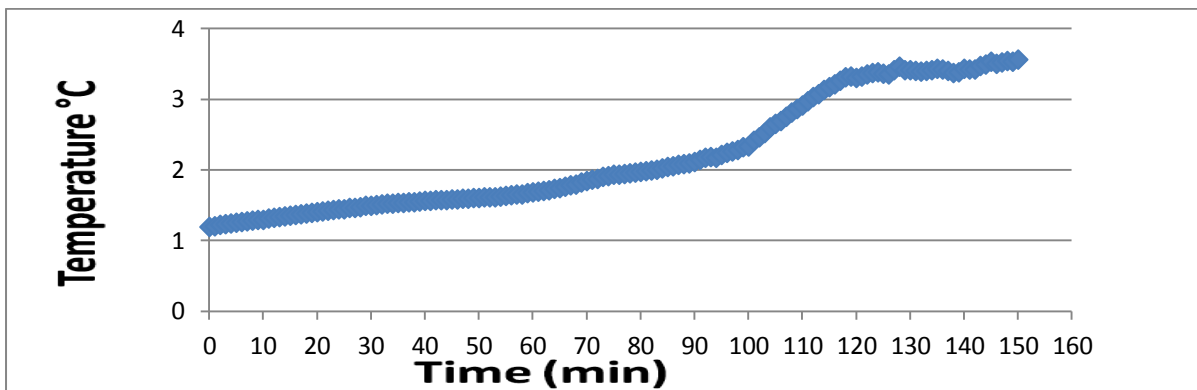
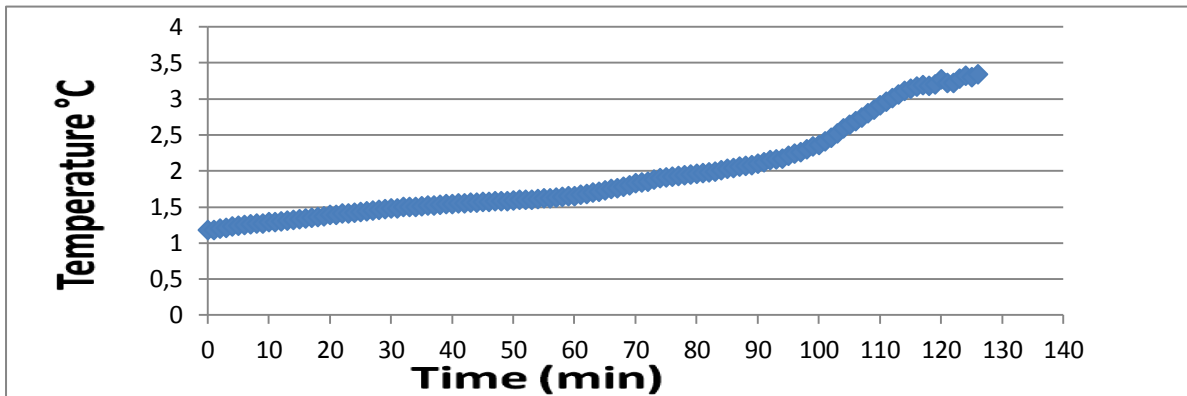
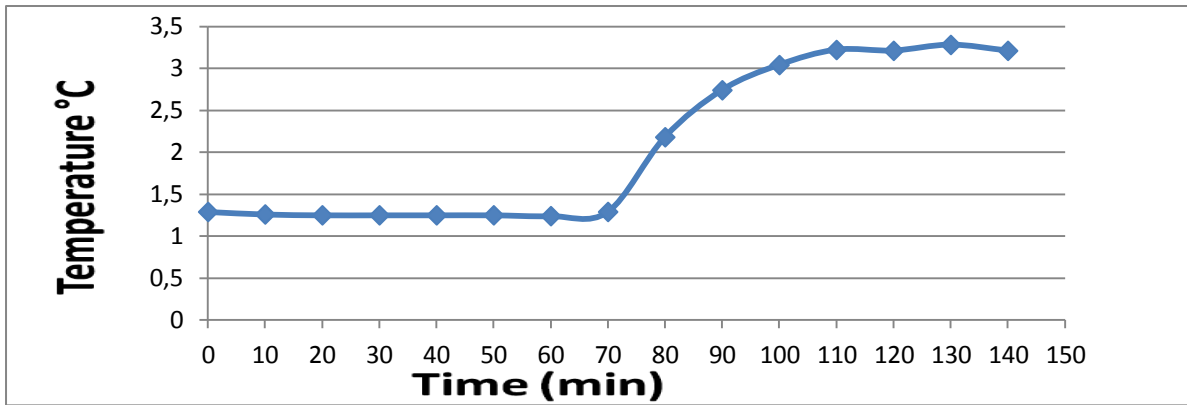


Figure A.3.2: For 1:5 Cyclopentane to water ratio



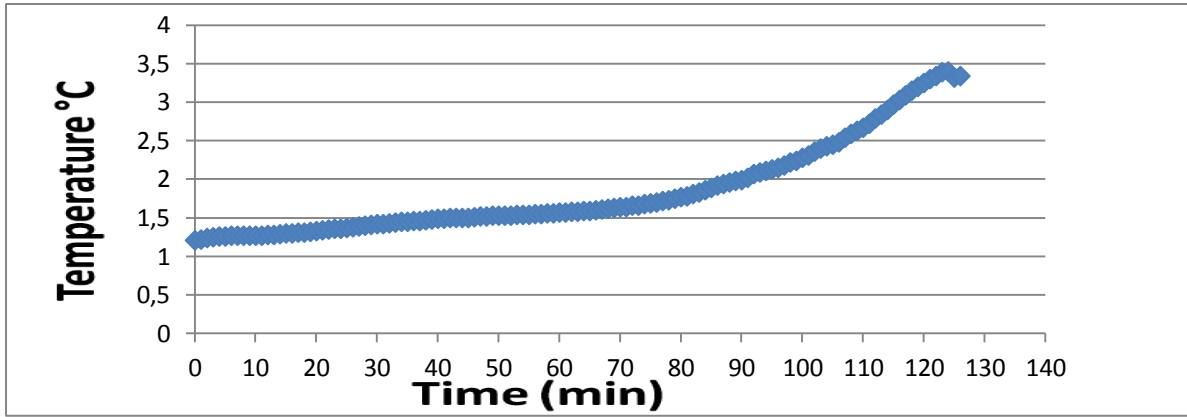
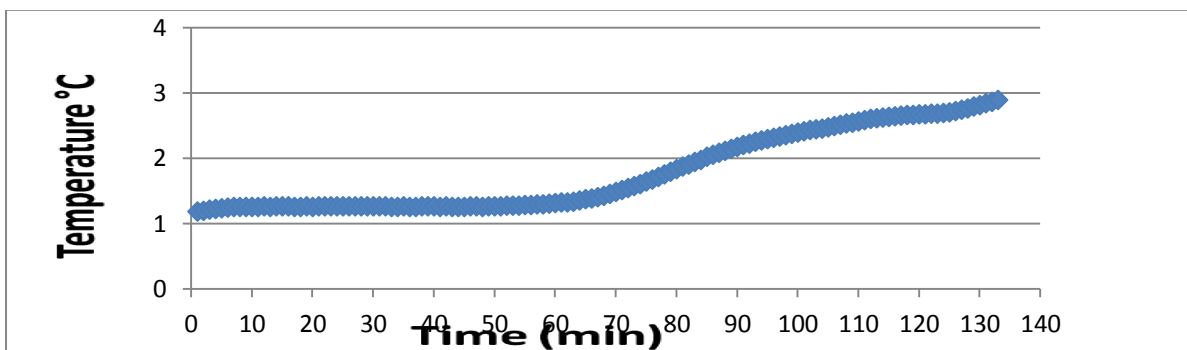
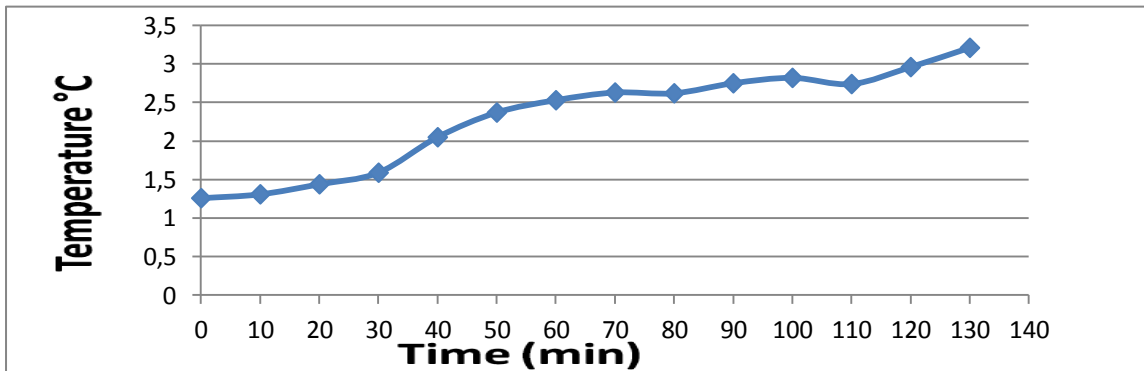
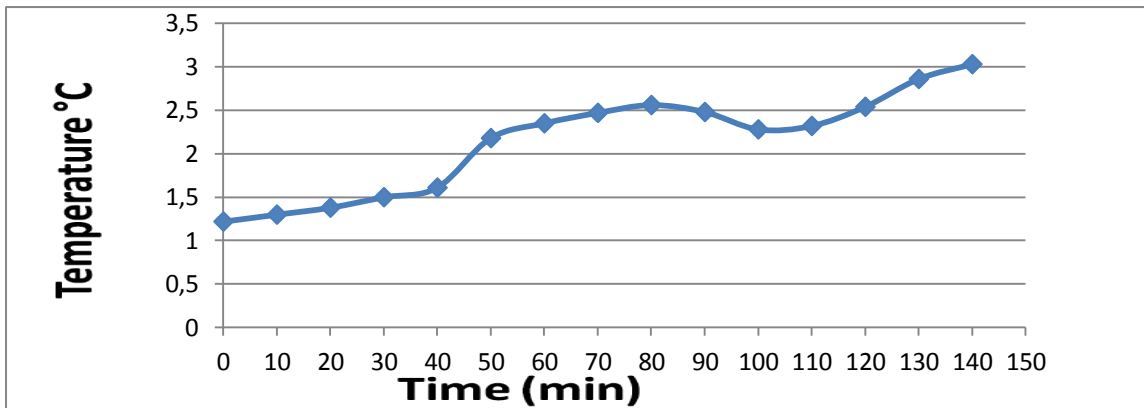


Figure A.3.3: For 1:3 span20 to water ratio.



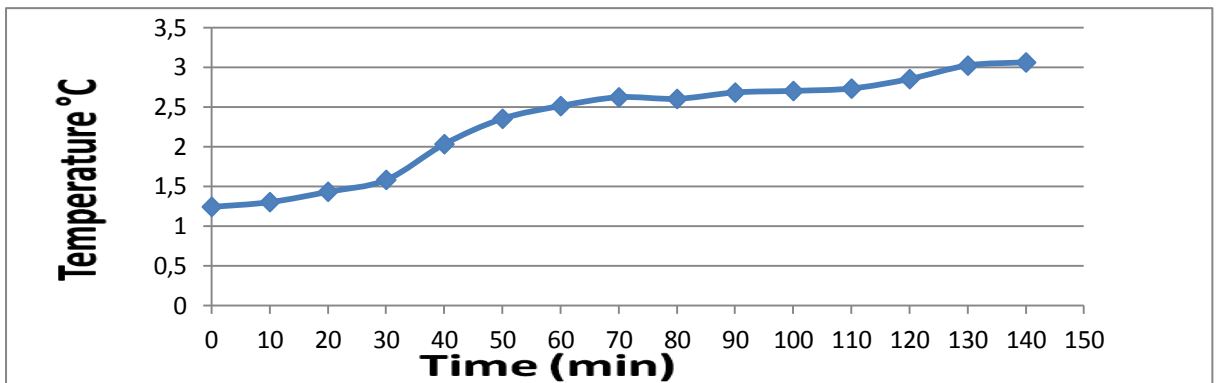
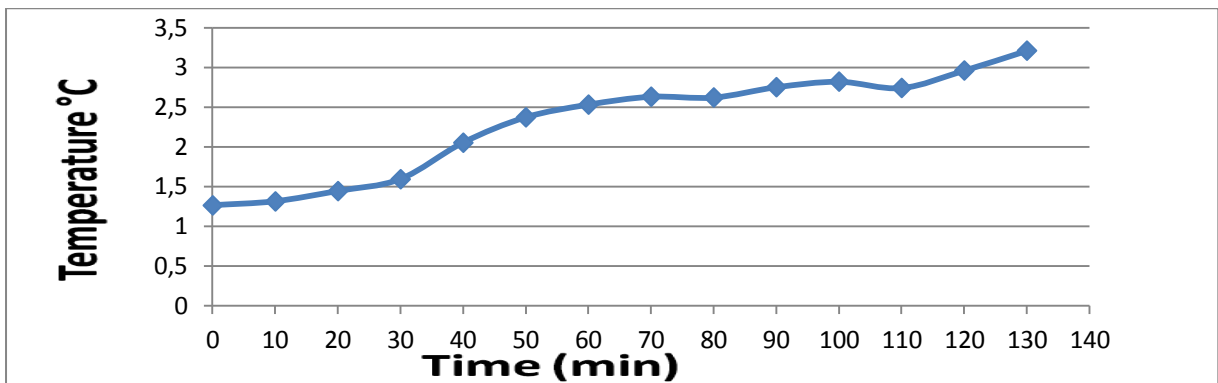
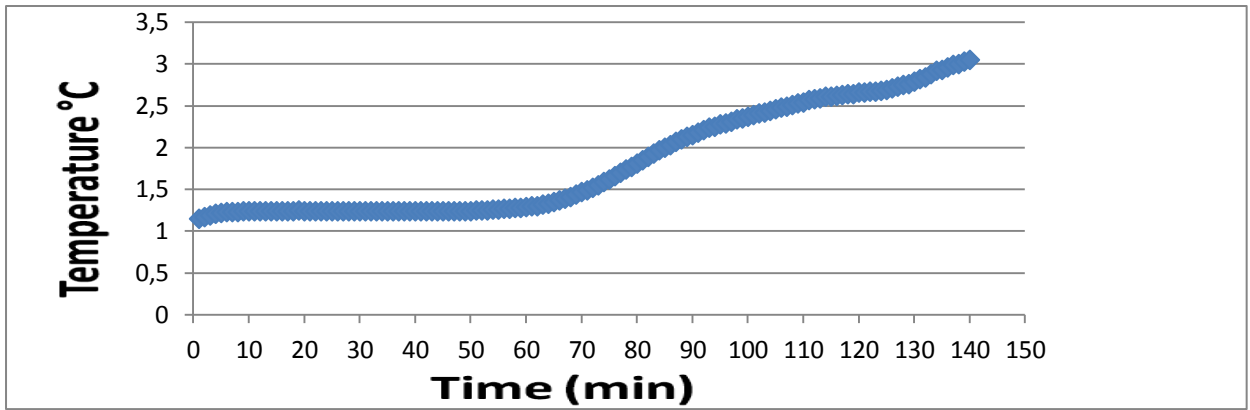


Figure A.3.4: For 1:5span20 to water ratio.

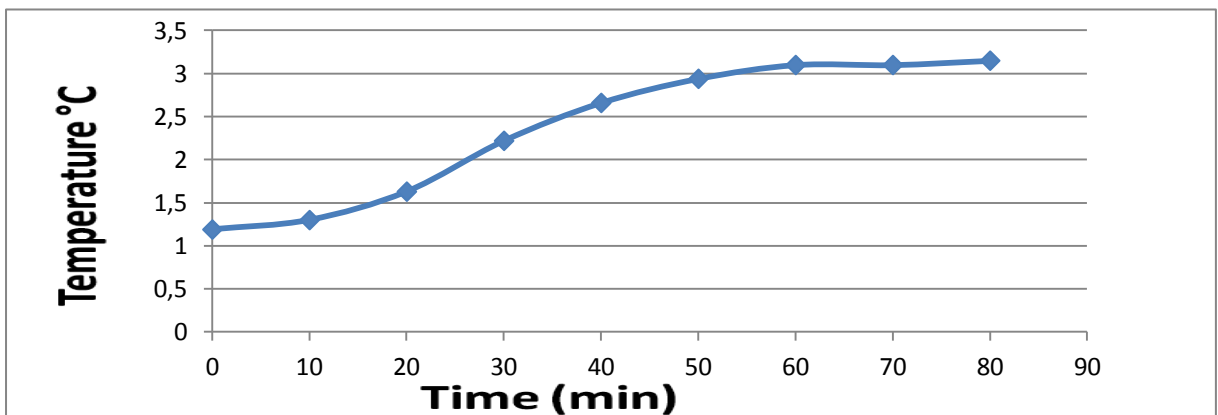
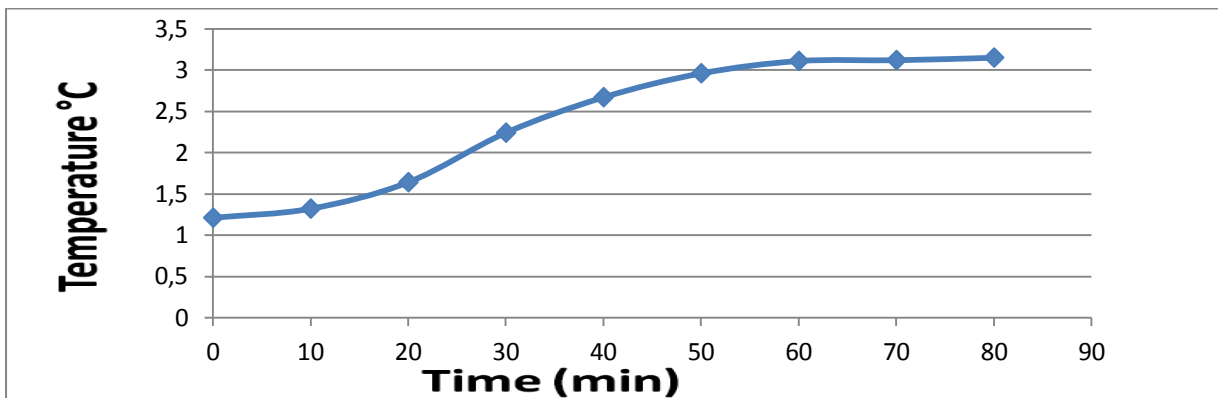
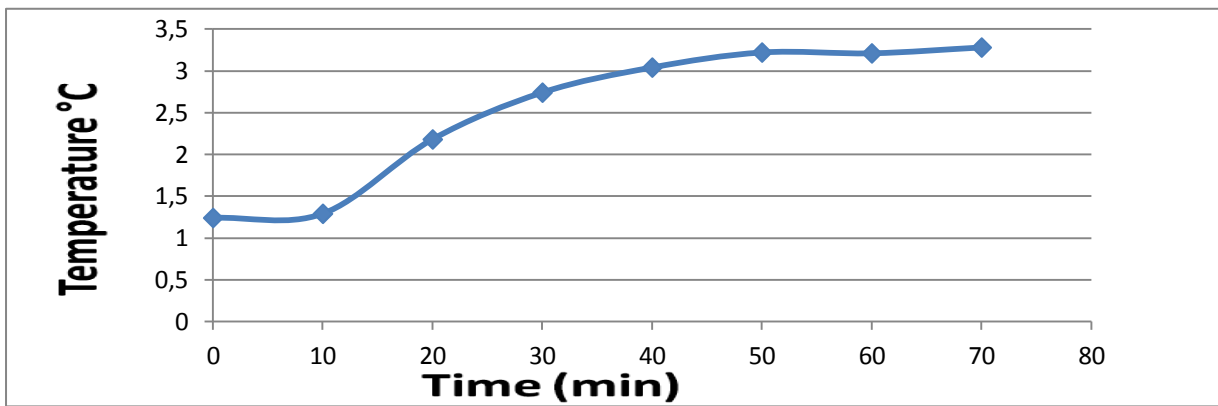
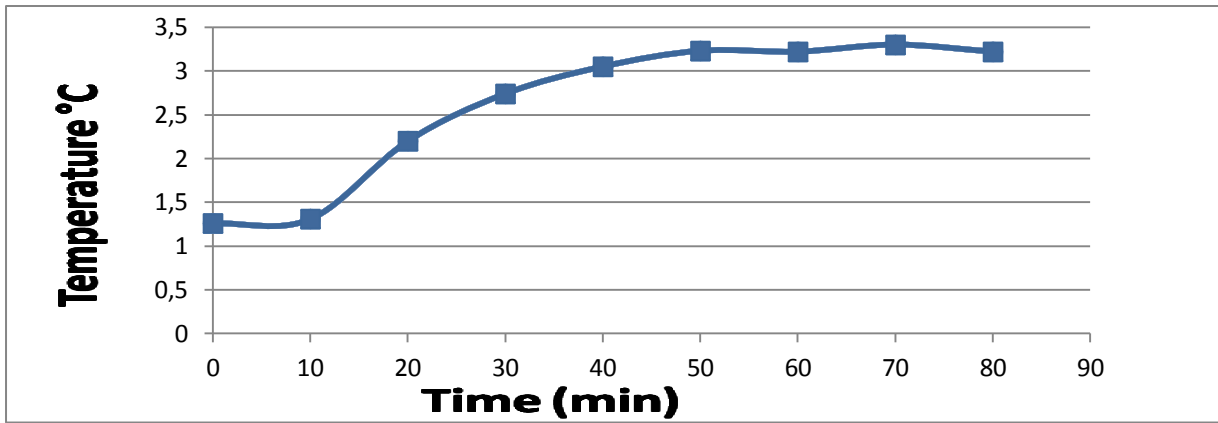


Figure A.3.5: For 1:5 Cyclopentane to tween20 ratio.

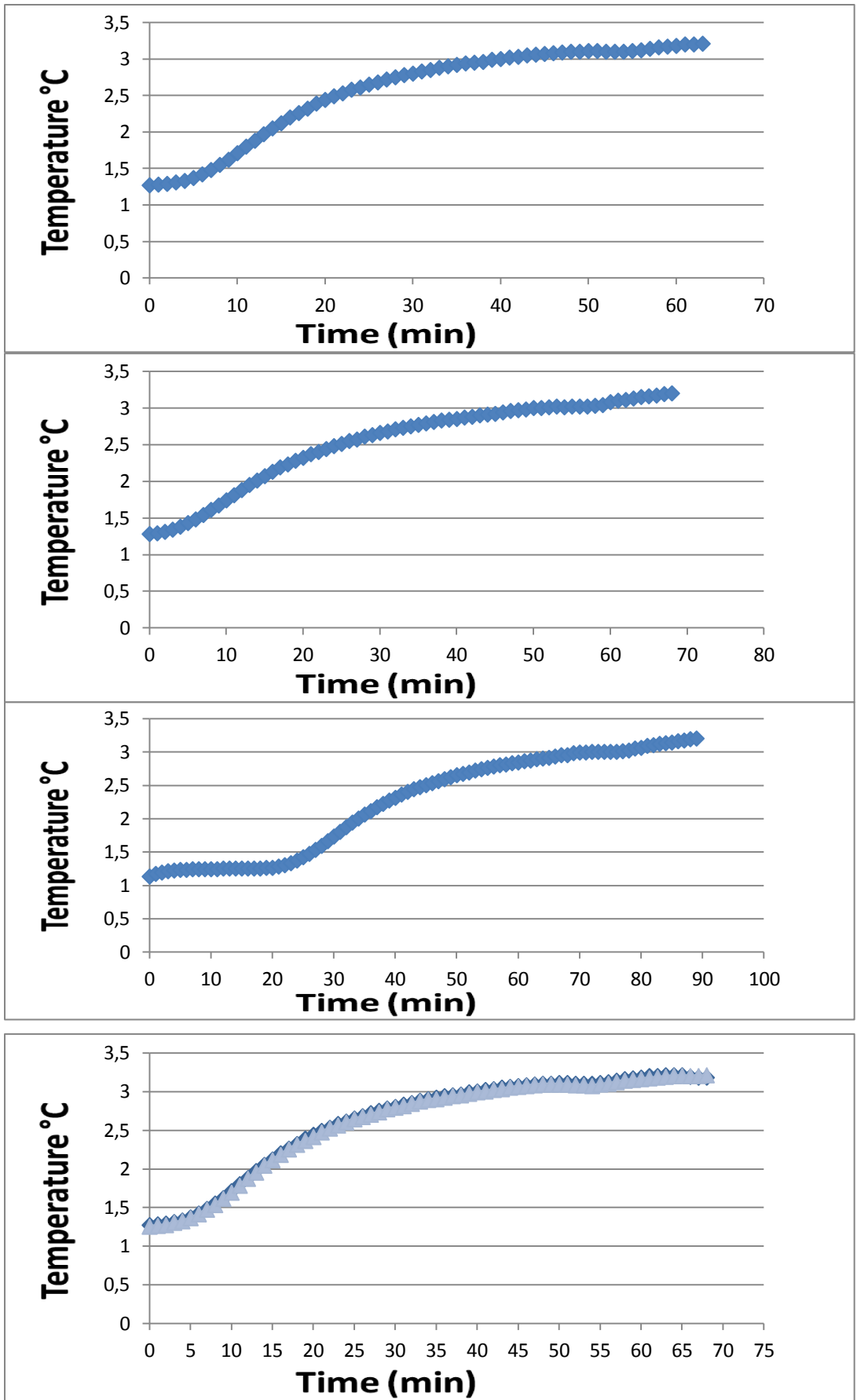


Figure A.3.6: For 1:3 Cyclopentane to Tween20 ratio.

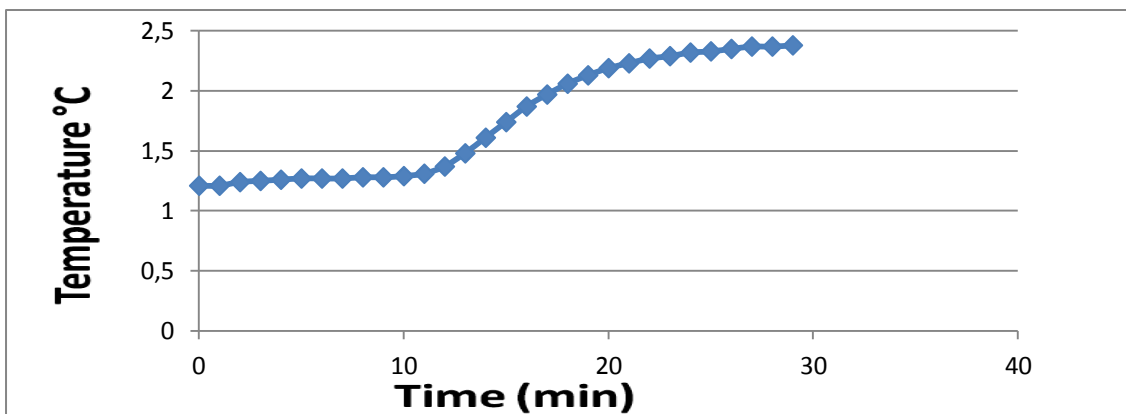


Figure A.3.7: For 1:5 Cyclopentane to THF ratio.

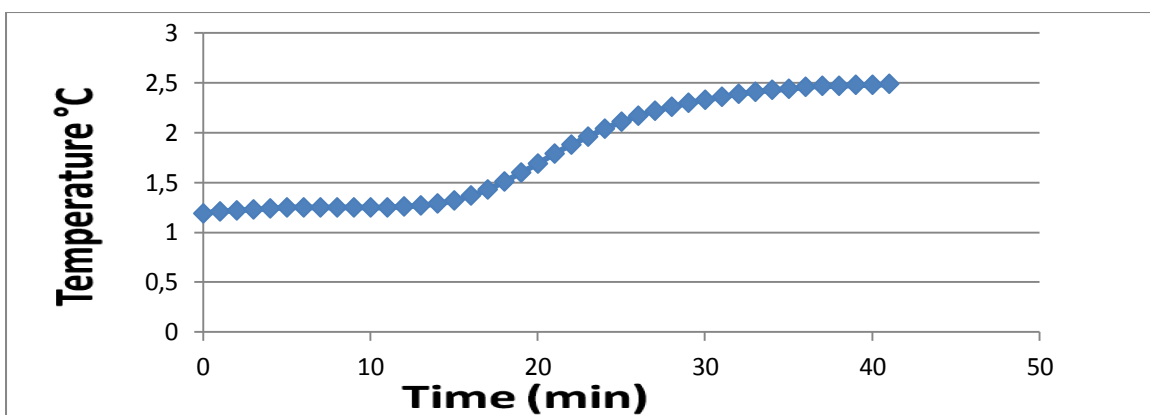


Figure A.3.8: For 1:5 span20 to water ratio.

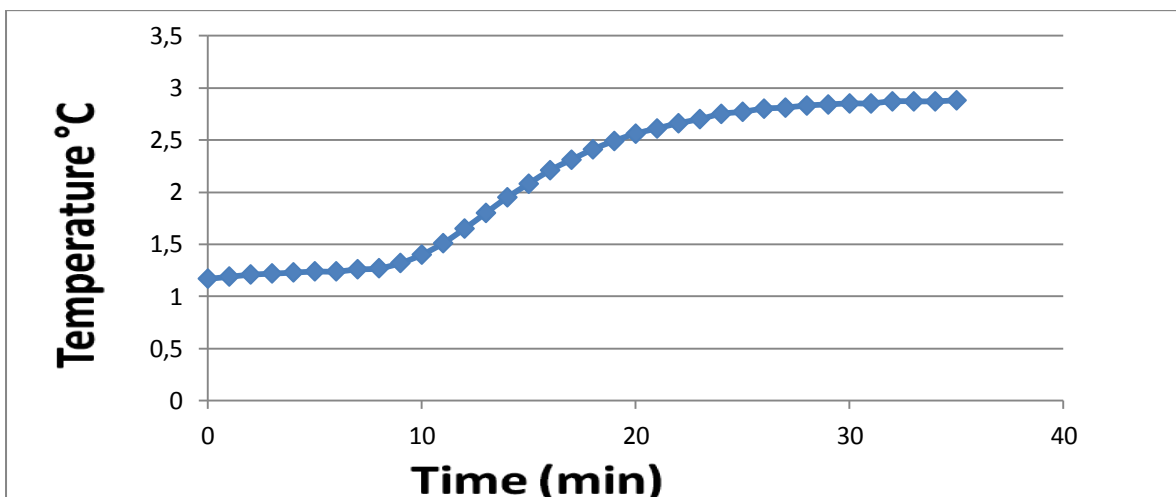


Figure A.3.9: For 1:5 cyclopentane to tween20 in THF ratio.

A.4 Determined hydration numbers

Table A.4.1: Determined hydration numbers that found using N₂ gas stream

Number of experiments	1:3CP to water	1: 5 Cp to water	1:3 Span 20 to water	1:5 span 20 to water	1:3 Cp to tween 20	1:5 Cp to tween 20	1:3 Cp to THF	1:5 span20 to THF	1:5 CP to THF in tween20
1	17.6	15.7	19.1	18.8	16.2	17.6	23.2	25.3	25.3
2	17.8	15.1	19.3	20.5	16.4	18.3	24.4	25.6	26.3
3	17.8	15.1	18.2	21	16.2	16.7		25.3	
4	18.5	15.2	18.9	20.5	15.5	16.1		26.6	
5	17.7	15.7	18.7	20.3	16.2	17.9			
6	18.3	15.6	17.5	20.9	15.9	16.6			
7	17.0	15.1	18.4	24	15.3	17			
8	17.2	15	18.6	21.9	15.2	17.7			
9	17.2	16.1	18.5	21.3	15.4	18.1			
10	16.1	15.6	18.4	19.4	15.9	19.4			
11	17.2	18.3							
12	16.8	17.2							
13	16.5	17.1							
14	17.7	16.9							
Average	17.2	15.0	18.6	20.6	16.0	17.2	23.8	25.5	23.4
Standard deviation	0.66	1.01	0.50	1.01	0.44	0.97	0.85	0.47	1.27

Table A.4.2: Determined hydration numbers that found using GC-FID

Number of experiments	1:3CP to water	1: 5 Cp to water	1:3 Span20 to water	1:5 span20 to water	1:3 Cp to tween 20	1:5 Cp to tween 20	1:3 Cp to THF	1:5 span 20 to THF	1:5 CP to THF in tween20
1	20.20	16	23.6	21.70	14.80	18.00	41.7	24.9	17.1
2	17.5	23.2	24.1	20.00	16.40	18.00	37.5	33.9	23.6
3	20.40	13.9	22.5	22.40	17.80	17.90	55.5	32.5	41
4	15.30	23	24.5		14.20		37.8		19.1
Average	18.8	19.01	23.7	21.4	15.8	17.9	43.1	30.4	25.2
Standard deviation	2.4	4.8	0.9	1.2	1.6	0.1	8.5	4.8	10.9